A THEORETICAL STUDY OF THE TRANSFERENCE OF HEAT AND MOMENTUM ACROSS TURBULENT INCOMPRESSIBLE BOUNDARY LAYERS.

by

Jose Antonio Diaz Dieguez

A thesis submitted in fulfilment of the requirement for the degree of Doctor of Philosophy.

Department of Nuclear Engineering
Queen Mary College
(University of London)

, 1977

ABSTRACT

A survey and evaluation of some models of turbulence for isothermal turbulent flows is made. Models such as mixing-length, one-equation, two-equations and three-equations are solved with the aid of a high speed computer for annular turbulent flows. The results are compared with each other and with experiment and the significance is discussed. The three-equation model (three transport equations plus the mean velocity equation) emerges as the most accurate and capable of the widest application: one set of constants only is sufficient to solve a number of turbulent flows. Also, this model does not require the prescription of any arbitrary length scale.

A study of the effect of varying the constants in the three-equation model shows that the velocity and shear stress profiles are insensitive to the variation of the constants. A variation of up to 50% in the value of the constants produces, at most, less than 2% variation in the velocity and shear stress profiles. Only the turbulence energy distribution shows some sensitivity. The position of maximum velocity for smooth annuli with different radius ratios, as well as friction factors for a number of wall conditions are calculated with the three-equation model. The comparison between predictions and experimental data shows a fairly good agreement.

Starting from this three-equation model, an extended model, capable of predicting turbulent, two-dimensional,

incompressible thermal boundary layers is developed. Three more equations are incorporated in the isothermal model, namely, (1) mean temperature equation (T), (2) convective heat flux equation ($\overline{u_y T'}$) and (3) equation for the intensity of temperature fluctuation ($\frac{1}{2}\overline{T'^2}$). Appropriate approximations are introduced and the new model of parabolic differential equations is solved simultaneously with the equations for the isothermal flow. The new five-equations model (five transport equations plus mean velocity and mean temperature equations) is applied to a number of real flows, with and without the presence of walls. Both rough and smooth walls are considered. Generally, good agreement is obtained when predicted results are compared with the available experimental data.

ACKNOWLEDGEMENTS

The author would like to take this opportunity to express his gratitude to and acknowledge

Dr. J. Wood for valuable advice and encouragement throughout this research.

Professor D.C. Leslie for help, suggestions and corrections at the various stages of this work.

The other academic staff and contemporaneous students for their many valuable opinions and discussions.

The Instituto de Energia Atomica, São Paulo, Brazil, for valuable financial support during my stay in London.

The Fundação de Amparo à Pesquiza do Estado de São Paulo, Brazil, for helping with college fees and travel expenses.

TABLE OF CONTENTS

LIST OF FIGURES

List of figures (cont'd) Page

List of figures (cont'd) Page

List of figures (cont'd) Page

List of figures (cont'd) Page

List of figures (cont'd) Page

LIST OF TABLES

NOMENCLATURE

Symbol	Meaning	Equation of first appearance
$a_k^m{}_i^{T'}$	- fourth-order tensor	(B.7)
A	- constant	(3.5)
A_j	- coefficient in the difference equation	(A.7)
A_j^*	- transformed coefficient	(A.8)
b	- constant	(4.28)
B	- constant in non-dimensional velocity profile (=1/K)	(3.15)
B_j	- coefficient in the difference equation	(A.7)
B_j^*	- transformed coefficient	(A.8)
B_r	- asymptotic value of free constant in universal velocity law for rough wall	(3.18)
$B_r(e^+)$	- free constant in a general universal law of the wall	(3.15)
$B_{rT}(e^+,Pr)$	- heat transfer roughness function	(4.54)
B_s	- asymptotic value of free constant in universal velocity law for smooth wall	(4.52)
$B_T(Pr)$	- free constant in universal temperature law for smooth wall	(4.51)

Symbol	Meaning	Equation of first appearance
C_D	- constant appearing when dissipation term of turbulence energy is modelled	(2.7)
C_e	- constant in turbulence energy equation	(2.6)
c_p	- specific heat at constant pressure	(4.1)
C_s, C_{s1}, C_{s2}	- constants in shear stress equation	(2.14)
C_{sa}	- constant appearing in the approximation of the pressure-rate term	(C.4)
C_{TT1}, C_{TT2}	- constants in intensity of temperature equation	(4.29)
C_{UT1}, C_{UT2}	- constants in heat flux equation	(4.18)
$C_\varepsilon, C_{\varepsilon 1}, C_{\varepsilon 2}$	- constants in dissipation equation	(2.13)
$\frac{d\, l_u}{dx}$	- rate of spreading of velocity field of self-preserving free shear flows	
$\frac{d\, l_T}{dx}$	- rate of spreading of thermal field of self-preserving free shear flows	
D	- pipe diameter	
De	- equivalent diameter ($=2(R_o-R_i)$)	
e	- rib height	(3.15)
e^+	- dimensionless rib height($= \frac{e.u_\tau}{\nu}$)	(3.15)
E_o	- turbulence energy ($= \frac{1}{2}\overline{u_i u_i}$)	(2.5)

Symbol	Meaning	Equation of first appearance
f	- fanning friction factor	(3.16)
f_i	- friction factor related with the internal wall in annular flow	(3.25)
f_o	- friction factor related with the external wall in annular flow	(3.25)
$G(Pr)$	- integral function, component of the free constant in universal temperature law for smooth walls	(4.52)
h	- channel width ($= R_o - R_i$)	(2.10)
$h(\xi)$	- defect function (or core similarity function)	(3.19)
$\overline{h}$	- mean value of $h(\xi)$ (volume averaged)	(3.21)
h_w	- heat transfer coefficient	
k	- thermal conductivity	(4.1)
K	- Von Karman constant	(2.4)
ℓ	- characteristic length scale of turbulence	(4.16)
l_m	- the mixing length	(2.3)
L	- length scale	(2.10)
L_d	- length scale in dissipation term of turbulence, energy equation	(2.7)

Symbol	Meaning	Equation of first appearance
L_T	- length scale in dissipation term of intensity temperature equation	(4.26)
L_μ	- length scale in viscosity term	(2.9)
$\dot{m}''$	- mass flow entering boundary	(A.2)
N	- number of grid points in numerical solution of differential equations	
Nu	- Nusselt number (= $h_w.D/k$)	(4.70)
p	- static pressure	(2.1)
p'	- fluctuating pressure	(4.13)
P	- constant in heat transfer equation proposed by Leslie and Hassid (1973)	(4.73)
Pr	- Prandtl number (= $c_p.\mu/k$)	(4.51)
Pr_t	- turbulent Prandtl number (= $\nu_T/\hat{\gamma}_T$)	(4.69)
$\dot{q}''$	- mean heat flux, normal to the wall	(4.49)
Q	- function in heat transfer equation proposed by Leslie and Hassid (1973)	(4.73)
r , R	- radial coordinate	
Re	- Reynolds number (= $\overline{U}.De.\rho/\mu$)	
R_i	- inner radius of an annulus	

Symbol	Meaning	Equation of first appearance
R_M	- radius at which mean velocity is maximum	(3.9)
R_o	- outer radius of an annulus or radius of pipe	
R_{so}	- radius of zero shear stress	
R^*	- radius ratio ($= R_i/R_o$)	(3.9)
s	- rib pitch	
St	- Stanton number ($= h_w/\rho.\bar{U}.c_p$)	(4.73)
S^*	- relation between radius defined in text	(3.9)
t	- time dimension	(2.1)
T_o	- instantaneous temperature	(4.1)
T	- time mean temperature	(4.3)
T_G	- temperature at edge of boundary layer	(4.57)
T'	- fluctuating temperature	
T_M	- maximum (or minimum) mean temperature in a cooled (or heated) fluid flow	(4.63)
T_{si}	- temperature at internal boundary	(4.62)
$\overline{\frac{1}{2} T'^2}$	- intensity of temperature fluctuation	(4.24)

Symbol	Meaning	Equation of first appearance
$\mathcal{u}$	- characteristic velocity in turbulent flow	(4.16)
u_i	- fluctuating velocity components (i=x,y,z)	(4.3)
$\overline{u_i T'}$	- convective heat flux	(4.14)
$\overline{u_y T'}$	- lateral convective heat flux	(4.22)
$\overline{u_i u_j}$	- Reynolds stresses (or shear stresses)	(4.14)
$\overline{u_x u_y}$	- Reynolds stress in x,y plane	(2.1)
u^+	- dimensionless streamwise velocity (= U/u_τ)	(3.15)
u_τ	- friction velocity (=$\sqrt{\tau_w/\rho}$)	(3.7)
U	- streamwise time mean velocity in boundary layer (x-direction)	(3.19)
$\overline{U}$	- overall bulk mean velocity	(3.16)
U_G	- time mean velocity at free edge of boundary layer	(4.59)
U_i	- time mean velocity components (i=x,y,z)	(4.3)
U_i^*	- instantaneous velocity	(4.3)
U_{MAX}	- maximum time mean velocity	(3.19)

Symbol	Meaning	Equation of first appearance
U_∞	- non-disturbed velocity in flat-plate boundary layer	
$U_{1\infty}, U_{2\infty}$	- non-disturbed velocities of each stream in plane mixing layer	
w	- rib width	
x	- cartesian coordinate, streamwise direction	(2.1)
x_i	- coordinate axes (x_i=x,y,z)	(2.2)
y	- cartesian coordinate, cross-stream direction, measured from internal boundary	(2.1)
y_ℓ	- characteristic thickness of boundary layer	(2.4)
y_{so}	- y coordinate where shear stress is zero	(2.11)
$y_{0.1}$	- cross-stream coordinate where velocity is 10% of stream velocity	
$y_{0.5}$	- cross-stream coordinate where velocity is half the stream velocity	
$y_{0.9}$	- cross-stream coordinate where velocity is 90% of stream velocity	
y^+	- dimensionless distance from wall ($= (R_o-y).u_\tau/\nu$)	(4.64)
z	- cartesian coordinate	(4.9)

Greek Symbols	Meaning	Equation of first appearance
α	- constant appearing in pressure-rate of strain term in convective heat flux equation	(4.18)
α_1 , α_2	- constants of proportionality between normal stresses and turbulence energy	(3.2)
γ	- thermal diffusivity ($= k/\rho.c_p$)	(4.11)
γ_T	- eddy diffusivity of heat	(4.68)
δ	- cross-stream distance where velocity is 0.995 of stream velocity (flat plate flow)	
δ_{ik}	- Kronecker tensor	(4.14)
ε	- rate of dissipation of turbulence energy	(2.6)
ε_T	- rate of dissipation of intensity of temperature	(4.25)
λ_1	- mixing length constant	(2.5)
λ_2	- constant in length-scale expression	(2.11)
η	- function in length-scale expression	(2.11)
μ	- molecular viscosity	(4.1)
μ_t	- turbulent viscosity	(2.9)
ν	- kinematic viscosity ($=\mu/\rho$)	(2.1)

Greek Symbols	Meaning	Equation of first appearance
ν_T	- eddy diffusivity of momentum	(4.66)
ρ	- density of fluid	(2.1)
ξ	- adimensional cross-stream variable $(=(R_o-r)/R_o)$	(3.19)
ξ_1	- value of ξ where eddy viscosity starts to be nearly constant throughout the core region in pipe flow	(3.20)
τ_w , τ	- shear stress	(3.11)
θ	- mean temperature difference $(=\lvert T(r)-T_{si}\rvert)$	(4.62)
θ_{MAX}	- maximum mean temperature difference	(4.63)
θ^+	- dimensionless temperature	(4.51)
ϕ	- a general dependent variable	(A.3)
φ	- dissipation function	(4.1)
ψ	- a stream function	(A.1)
ω	- dimensionless stream function or grid function	(2.12)
Δy	- cross-stream coordinate difference $(= y_{0.9}-y_{0.1})$	

Subscripts	Meaning
C	- Couette flow boundary
E , o	- external boundary
G	- free stream edge
I , i	- internal boundary
i,j,k,l,m	- indices denoting directions x,y,z
r , R	- denotes value at rough surface
S , w	- denotes value of quantity at wall
s	- denotes value at smooth surface
x , y	- streamwise and cross-stream directions in two-dimensional flows
1	- associated with the inner portion in Hall's transformation
2	- associated with the outer portion in Hall's transformation

Superscripts

$\overline{\quad}$	- denotes time-average of quantity in question
'	- denotes fluctuating component of quantity

CHAPTER - 1

1. Introduction.

1.1 Models of turbulence.

Turbulence always has been a major area of interest in the field of fluid mechanics: due to its importance, complexity and difficulty. Historically, Reynolds (1883) was the first to draw attention to turbulence on a qualitative-quantitative basis. Reynolds himself showed that the statistical averaging of the Navier-Stokes equations, by decomposition of the velocity field into mean and fluctuating components and time-averaging the several terms, leads to the equations of motion for turbulent flow. Because Reynolds was the first to develop such equations, these equations are often called Reynolds momentum equations. These equations involve the relation between average and fluctuating terms and describe the conservation of momentum in a turbulent flow. The Reynolds equations still remain the fundamental equations in any study of turbulence.

From the engineer's point of view, because he is interested in prediction of mean-flow quantities, his main interest focuses on the solution of the Reynolds equations, for a specified real fluid flow. A quantitative analysis of turbulence requires a realistic formulation of macroscopic behaviour of the fluid motion, therefore, it requires

equations which express the time-average requirements for the conservation of mass, momentum and energy. Whatever method is used to solve the momentum equations, it leads inevitably to a situation in which there are more unknowns than equations. Therefore, even for the simplest flow, we always have a "closure" problem. Thus, to solve a turbulence problem, we must "model" the real flow by means of arbitrary simplifications, by neglecting terms or by expressing them in convenient forms by analogy with laminar flows.

Until 1925 only simple and empirical theories of turbulence were developed. The convenient mixing-length theory, introduced by Prandtl (1925), remained as the most important and influential theory for a long time. With Taylor (1935) the idea of turbulent motion as random continuous function of position and time was introduced and, with it, the more rigorous methods of the statistical theory of turbulence. Then, more sophisticated methods begin to appear. Either by the development of new relationships with more physical meaning not implicit in the basic principles already introduced, or by the development of new relations in the form of new equations.

The vast majority of the attempts to predict turbulent motion follow the pattern of combining mathematical and physical arguments. The main weakness is that no method is complete, no model of turbulence so far generated is perfect or general, and always some empirical information must

be incorporated.

Before the advent of high-speed computers the range of turbulence problems that could be handled was very limited, mainly because of mathematical difficulties in solving the complex equations. This explains why before the 1960's only a very limited number of flows could be considered. ~~And~~ These were only solvable due to the gross simplifications introduced by integral procedures which had dominated the field until that date. The integral equation methods were developed in order to speed numerical solutions by hand calculations. This method must incorporate, implicitly or explicitly, suppositions about the global influence of turbulence in the mean flow. Global hypotheses are valid only over a very restricted range of conditions; therefore, it is difficult to extend such methods to wider classes of flows. Accuracy and width of applicability cannot be achieved without solving the partial differential equations, and to solve them, the knowledge of local properties is required.

With the advent of fast computers the use of more sophisticated numerical methods for solving the partial differential equations became feasible. From the Stanford Conference on computation of turbulent boundary layers, Kline et ali.(1969), it emerged that methods using partial differential equations are more accurate and practical than the best of the integral methods. Then, a vigorous attack in the turbulence problem, via partial differential methods,

started. An evolution from simple to more sophisticated methods, covering a very wide range of flows, followed. Launder and Spalding (1972) give a complete and detailed survey of the available turbulent models, from the simplest ones: mixing length theory and turbulent viscosity methods to the complex ones, such as, the multi-equation models. Also, very interesting and useful up to date surveys on turbulence models are presented by Bradshaw (1976), Fernholz (1976), Johnston (1976) and Reynolds and Cebeci (1976). Fernholz deals with the external, two and three-dimensional boundary layers; Johnston surveys the internal flow models and Reynolds-Cebeci are interested in the methods of calculating boundary layers in turbulent flows.

From the wide number of models proposed we see no method is absolutely general; always conditions and limitations of applicability are inherent in each model. Motivated by the desire to remove these restrictions and to achieve greater generality, a collection of work has been produced, founded on very formal and sophisticated statistical theories of turbulence. In the hope of finding a general formalism without the need for empirical assumptions, theoretical works such as Orszag (1973), Monin and Yaglom (1975) Leslie (1973) and Lumley (1970) have appeared. So far, however, rather arbitrary postulates are needed in their theories too.

It seems that the turbulence models, i.e., the partial differential equations models that lend themselves to a numerical solution, are the only practical way of treating

turbulent flows. Many individual investigations have been reported based on the idea of using a self-contained set of differential equations. Apart from the early mixing length and turbulent viscosity methods, we have models comprising one-to many equations. Among the one-equation models proposed we find the models of Glushko (1965), Bradshaw et al. (1967) and Nee and Kovasznay (1969). Glushko adopted the tactic of simulating the turbulence energy equation and assumed the turbulent viscosity proportional to the square root of the turbulence energy; Bradshaw at al., on the other hand, developed an equation directly for the shear stress; whereas, Nee and Kovasznay developed a model where the kinematic turbulent viscosity is determined from a differential equation.

All the two-equation models take the turbulence energy equation as the first equation; the distinction between models is in the second equation adopted. Ng and Spalding (1976) proposed a two-equation model where the second equation is the turbulence energy-length scale product. Among the multi-equation models, Hanjalic (1970) proposed a three-equation model, in which the equations for the turbulence energy, shear stress and dissipation are solved. With slight modifications, Hanjalic and Launder (1972b) proposed a very similar, but extended model, which refers to 7 constants. Mention may also be made of Daly and Harlow (1970) who developed a model of 5 equations, where the turbulence energy equation is substituted for the 3 normal Reynolds stresses equations. Based on the Hanjalic and Launder (1972b) model, Launder et al. (1975) developed a model also of 5 equations, similar to Daly and Harlow's model,

but with more realistic approximations, mainly in the treatment of the pressure-rate of strain term near a wall boundary. More ambitious models are those of Chou (1945), Davidov (1961) and Kolovandin and Vatutin (1969) proposing models with 17, 23 and 28 differential equations, respectively; these more complex models are also reviewed by Launder and Spalding (1972).

Naturally, a better representation of the real flow can be achieved by means of a model with more and more equations, but this would result in increasing demand for computing time which is directly proportional to the number of equations. Now, it is widely accepted that multi-equation models should become the standard method of solving turbulent flows, such is the degree of generality and precision of this technique. The principal question to be resolved is, what is the minimum necessary number of differential equations capable of representing well a wide range of turbulent flows. Computing time costs money, therefore, from the economical point of view, it is evident that models like those proposed by Chou, Davidov and Kolovandin-Vatutin are virtually unsolvable. In this work, we shall concentrate our attention on intermediate models with the purpose of selecting one, hopefully the best, that can be extended to deal with thermal boundary layers. Such a model should, ideally, contain the minimum number of equations consistent with the qualities of generality, precision and computing-economy.

1.2 Heat transfer in turbulent flows.

The transport of heat to or from fluids flowing turbulently in closed conduits, is one of the most important modes of industrial heat transfer. Engineering applications of convective heat and mass transfer are multiple and extremely varied.

By the nature of the mechanisms involved, there is an analogy between momentum and heat transfer, and a close relationship between convective heat transfer processes and fluid dynamics is observable. Thus, having established a model of turbulence that is purely hydro-dynamic, the extension to a model much more complex and general, including the transport of heat by convection, is straightforward. A survey of all studies of convective heat transfer to be found in the literature permits their classification in one of the two categories:

a) Empirical and semi-empirical methods.

b) More elaborate methods based on transport equation

1.2.1 Empirical and semi-empirical methods.

The vital question, from the engineering point of view, is to know the amount of heat transferred from the wall to the fluid or vice-versa, depending on whether the fluid is heated or cooled. For this purpose, several correlations purely empirical, based on relations between non-dimensional numbers, were developed. These relations have been modified and improved

in order to satisfy the needs of the designer of heat transfer equipment. Usually, the relationships were found from direct results of experiments on prototype equipment . These empirical expressions do not say anything fundamental about the way heat is transferred, therefore, other relations, theoretical and semi-empirical, based on a fundamental knowledge of the processes occurring, were also developed.

Reynolds (1901) was the first to predict quantitatively an 'analogy' between heat and momentum. His basic assumption was the equality of the turbulent diffusivities for momentum and heat ($\nu_T = \alpha_T$), making possible a relationship between the heat transfer coefficient and the friction factor. Since then, both simple and more elaborate methods have been proposed, for example, the works of Prandtl (1910), Colburn (1933), Martinelli (1947), Lyon (1951), Rannie (1956), Kestin and Richardson (1963), Gardner and Kestin (1963), Lawn (1969), Spalding (1961a) and, with later extensions of Kestin and Persen (1962), Spalding (1964) and Quarmby and Anand (1970). The general procedure of these workers was to establish an accurate description of the velocity profile for the turbulent flow (usually, the non-dimensional velocity u^+ vs. the non-dimensional cross-stream distance y^+), then, use any kind of 'analogy' to relate the heat transfer coefficient with the friction factor.

On the experimental side there are also many contributions, for example, Dipprey and Sabersky (1963), Kays and Leung (1963), Deissler (1955), Johnk and Hanratty (1962), Smith and Shah (1962), Edward and Sheriff (1961), Owen and

Thomson (1963), Sparrow and Hallman (1958), Kolar (1965), Gowen and Smith (1967), Bettermann (1966), Quarmby (1967), Webb et al. (1971), and others.

Although these authors, considered together, covered a very wide range of geometries, conditions and kinds of flow, their main purpose was only to make possible the calculation of the heat transfer coefficient (h_w), or, alternatively, the Nusselt or Stanton numbers. The understanding of the heat transfer mechanisms still remained slight. A better understanding of the way heat is transferred inside the fluid flow must help in the design of more efficient heat transfer equipment. But in the design of this equipment it is desirable to have a detailed knowledge of transport quantities, such as, convective heat flux, intensity of temperature fluctuation, etc., and for this it is necessary to understand the underlying heat transfer mechanisms. This is why more elaborate methods are needed.

1.2.2 More elaborate methods.

In comparison with the purely hydrodynamic or isothermal flows, very little research has been done into turbulent flows affected by a difference of temperature, by the use of higher order correlations. This is understandable because turbulent shear stresses are important 'input' to the heat transfer equations, therefore, the heat-flux models had to wait until the hydrodynamic models were satisfactorily developed.

When a turbulent flow also exchanges heat, in addition to the momentum equation, the equation of mean temperature (or thermal energy) must be solved. The averaging of the mean temperature equation gives, of course, a relation between the other mean quantities but also has a term due to turbulent effects only. This term is called convective heat flux ($\overline{u_i T'}$) and is analogous to the shear stress term in the equation for mean momentum. The knowledge of this term permits the calculation of mean temperature distributions across a turbulent flow. Therefore, a more elaborate method of predicting heat transfer must model the convective heat flux in terms of higher order correlations. Theories based on more exact analyses have been formulated only in recent years and, so far, only a small amount of work of this character has appeared.

Townsend (1958) examined the case of a stably stratified, homogeneous, non-developing free turbulent shear flow, far from walls. Using the turbulence energy equation and an equation for the mean square of temperature fluctuation, he derived a relation for the flux Richardson number (ratio of the rate at which buoyancy forces extract energy from the turbulence to the rate at which it is supplied by the shear stress), which provides a measure of the stability of the flow.

Webster (1964) and Nicholl (1970) performed two similar experimental studies of turbulence in density-stratified shear flows. Both were interested in the effects of buoyancy on the stability of the turbulent flow. They made measurements in

a wind tunnel, using air at low Reynolds numbers, measuring heat flux correlations as well as hydrodynamic correlations, in order to observe the dynamical effects caused by an increase in the temperature of the boundary.

More recently, Launder (1975) developed a model to explain the case of stably stratified shear flows, far from walls, including gravitational effects. Starting with the Reynolds shear stresses equations (for $\overline{u_i u_j}$) and the convective heat flux equation, he found non-dimensional fluctuating correlations as a function of the flux Richardson number. In his derivations, Launder neglects all convective and diffusional terms; that is, he supposes that turbulence energy production and the rate of dissipation are equal throughout the flow. In a subsequent work, Gibson and Launder (1976) extended the treatment to a more realistic situation in which the production/dissipation ratio varies. This improvement allows the consideration of jet flows as well as shear flows.

Second-order models for atmospheric entraining layers were developed by Lumley (1972), Donaldson et al. (1972) and Zeman and Lumley (1976). Lumley (1972) and Donaldson et al. (1972) utilized simple transport gradients for the third-order fluxes and produced, respectively, models of 12 and 10 differential equations. Zeman and Lumley (1976) incorporated buoyancy effects into the third-order fluxes and proposed a model with a minimum of 8 differential equations. An up-to-date and complete survey on heat and mass transport can be found in Launder (1976).

Compared with the other models, the Gibson and Launder (1976) model is an intermediate model with 4 differential equations and 2 algebraic relations, representing a compromise between physical realism and practicability of solution. Their model always approximates the transport terms, namely, convection and diffusion, in such a way that simple algebraic formulae emerge for turbulent stresses and heat fluxes. But we know that, in general, the values of the properties of turbulence are quite substantially affected by local variations, therefore, we know that transport effects are significant . Thus, to provide an entirely consistent level of closure, quantities of turbulence, such as convective heat flux , intensity of temperature fluctuation as well as shear stresses, should be found from the approximated transport differential equations. This is a deficiency in their model.

1.3 Objectives and purposes.

A study of the literature revealed that all higher-order models developed so far to predict convective heat transfer boundary layers were restricted to atmospheric or jet flows, no reference was found to flows along solid walls. Therefore, we decided to take as our main objective the development of a complete model of turbulence capable of predicting both hydrodynamic and convective boundary layers, in the presence of wall boundaries as well as free boundaries. It was also decided to pay special attention to internal turbulent flows such as pipe and annular flows which are the

most important in Nuclear Engineering.

The general philosophy of the procedure we adopt can be summarized as follows: by means of a numerical comparison, we aim to choose, from some of the existing hydrodynamic models, one that is reliable, practicable and flexible. Next, for the thermal boundary layers, we develop a set of differential equations which permits the introduction of wall effects. Three further equations are developed: (1) mean temperature equation, (2) convective heat flux equation and (3) intensity of temperature fluctuation equation, to account for the influence of heat transfer on the fluid flow. Then, the complete set of equations (hydrodynamic & heat transfer) is solved for some real flows: annular flow, pipe flow, flat-plate boundary layer, plane mixing layer and jets.

1.4 Outline of the thesis.

The thesis is divided into five chapters, of which Chapter - 1 forms an introduction. In Chapter - 2 we discuss the salient features of some existing models of turbulence for isothermal flows. By a comparison of the numerical results, these models are compared for the case of turbulent annular flow. A three-equation model emerges as the most satisfactory of those considered. Further analyses and more applications of the three-equation model are described in Chapter - 3 . In section 3.1 we study the influence of varying the constants contained in the three-equation model. The problem of the point

of maximum velocity in a smooth annulus with different radius ratios is analysed in section 3.2 . Some of the 'universal' laws for pipe flow are examined in section 3.3 . Friction factors in both smooth and rough annuli are presented in section 3.4 . Also, some methods based on Hall's (1962) transformation for comparing friction factors in asymmetric geometries, are included in that section.

The development of a thermal boundary layer model is the theme of Chapter - 4 . General equations are introduced for each one of the dependent variables. Boundary layer approximations, together with high Reynolds and local isotropy simplifications, are introduced and a final set of three differential equations is obtained. These three equations, which define the thermal model, combined with the three-equation hydrodynamic model, form a closed set of equations which is solved numerically for a group of real flows, with and without walls.

Finally, in Chapter - 5 we draw some conclusions concerning the application of the new model of turbulence to real flows. Also, discussed in this chapter are the areas in which the present work could be extended and developed by future research.

CHAPTER - 2

2. Critique of some models of turbulence.

2.1 Basic assumptions common to the models.

Since all models of turbulence originate from equations obtained from the statistical averaging of the Navier-Stokes equations, and the number of unknown terms in these equations is large, it is necessary to approximate them with sufficient accuracy to describe satisfactorily the mean flow. It is conventional in turbulence models to close the partial differential equations by using general assumptions. These basic assumptions are applicable to a fair number of practical flows. With respect to the models presented here, they are based on the following general assumptions:

a) Flows with high Reynolds numbers.

b) Fluid properties assumed constant.

c) Two-dimensional flows with a predominant direction.

d) Fluid incompressible.

The above assumptions along with the boundary layer approximations, make possible the derivation of the fundamental equation of turbulent flows which is the momentum or Reynolds equation (see, for example, Hinze (1959) or Schlichting (1968) for details of the derivation). Neglecting the external forces, the momentum equation can be written as

$$\frac{D\,U_x}{Dt} = -\frac{1}{\rho}\frac{dp}{dx} + \nu\frac{\partial^2 U_x}{\partial y^2} - \frac{\partial}{\partial y}(\overline{u_x u_y}) \qquad (2.1)$$

where,

$$\frac{D}{Dt} = \frac{\partial}{\partial t} + U_i \frac{\partial}{\partial x_i} \qquad (2.2)$$

and repeated-suffix implies summation.

The mean momentum equation (2.1) represents a relation between mean properties of the flow with the exception of the shear stress term ($\overline{u_x u_y}$) which is due to the influence of turbulence. The difference between the models we consider lies in the way that $\overline{u_x u_y}$ is related to the mean properties. In our comparison we consider the following particular models:

1) Mixing-length model.

2) One-equation model.

3) Two-equation model.

4) Three-equation model.

We now summarize the salient features of these models.

2.2 Mixing-length model.

The earliest, and simplest, attempt to close the momentum equation for turbulent flow was made by Prandtl (1925). This work is referred to as the mixing-length theory. The key assumption of this theory is the approximation

$$\overline{u_x u_y} = - l_m^2 \left| \frac{\partial U_x}{\partial y} \right| \frac{\partial U_x}{\partial y} \qquad (2.3)$$

where, l_m is the mixing-length. For flows far from walls, l_m is usually taken as uniform across the boundary layer and proportional to the thickness of the layer. In our numerical comparison of the above models we take:

$$l_m = Ky \quad \text{for} \quad 0 < y \leq \lambda_1 y_\ell / K \qquad (2.4)$$

$$l_m = \lambda_1 y_\ell \quad \text{for} \quad y > \lambda_1 y_\ell / K \ , \qquad (2.5)$$

where K is the Von Karman constant, λ_1 is also a constant (≈ 0.09) and y_ℓ is a characteristic thickness of the boundary layer. For annular flow, where there are two boundary layers, relations (2.4) and (2.5) can also be used, but when $y > h/2$ (where h is the annular gap) a new y' is defined as $y' = h - y$.

2.3 One-equation model.

With few exceptions (for example, Nee and Kovasznay's (1969)* model which uses the kinematic turbulent viscosity as the other dependent variable), the one-equation models use the turbulent energy equation (E_o) as the auxiliary equation. An appropriate equation for two-dimensional boundary layer flows was developed by Hanjalic (1970). It takes the form

$$\frac{D E_o}{Dt} = \frac{\partial}{\partial y}\left[\left(\nu + C_e \frac{E_o^2}{\varepsilon} \right) \frac{\partial E_o}{\partial y} \right] - \overline{u_x u_y} \frac{\partial U_x}{\partial y} - \varepsilon \ , \qquad (2.6)$$

where ε is called dissipation of turbulence energy and C_e is a constant. However, the set of equations (2.1) and (2.6) still do not form a closed system, $\overline{u_x u_y}$ and ε remain unknown. It can be closed by means of dimensional analysis and the use of a local isotropy concept, when the dissipation term is modelled into

$$\varepsilon = C_D \frac{E_o^{3/2}}{L_d} \ , \qquad (2.7)$$

Furthermore, by using a Prandtl-type eddy viscosity hypothesis, the Reynolds stress $\overline{u_x u_y}$ can be represented by

$$\overline{u_x u_y} = - \frac{\mu_t}{\rho} \frac{\partial U_x}{\partial y} \qquad (2.8)$$

and,

$$\mu_t = \rho E_o^{1/2} L_\mu \ , \qquad (2.9)$$

where C_D in (2.7) is a constant (≈ 0.07) and L_d, L_μ are length-scales, respectively, for dissipation and shear stress. To complete the model it is necessary to provide the length-scale variation appropriate to a particular flow. If the Reynolds numbers are high, L_d and L_μ are nearly equal, therefore, we can put $L=L_d=L_\mu$. The prescription of L is rather arbitrary and also involves empirical relationships. We test three different relations, applicable to annular flow:

a) $$L = C_D^{1/4} . Ky(1 - y/h) \qquad (2.10)$$

b) Length-scale proposed by Hanjalic (1970), taking account of the position of zero shear stress,

$$L = C_D^{1/4} . Kh \left[\eta + 0.4 \eta^2 + (A-6.4)\eta^3 \right] \qquad (2.11)$$

where,

$$\eta = \frac{y}{h} \left(1 - \frac{y}{h}\right)$$

$$A = 32 \frac{\lambda_2}{K} (1-2y_{so}/h)$$

y_{so} = y coordinate where shear stress is zero

λ_2 = constant (≈ 0.14).

c) Length-scale constant in the direction of fluid flow but varying with the grid function (ω) as

$$L = C_D^{1/4}.Kh\,\omega \qquad (\omega \leq 0.5) \qquad (2.12a)$$

$$L = C_D^{1/4}.Kh(1-\omega) \qquad (\omega > 0.5) \qquad (2.12b)$$

where, $\omega = \omega(N, R_i, R_o)$ is the grid function (see Appendix - 1 for definition), proportional to distance y from the wall, $0 \leqslant \omega \leqslant 1$

N = number of grid points.

2.4 Two-equation model.

The difficulty of finding a relationship for the length-scale, motivated the research-workers to develop new models. The next natural development was a two-equation model. Invariably, the first of these two equations is taken as the turbulence energy equation (E_o), as before. However, there is some choice of what is to be specified as the second equation. Jones and Launder (1972) and Ng and Spalding (1976) are good examples of two-equation models; the former pair chose the dissipation of turbulence energy (ϵ) as the dependent variable in the second equation, the later pair chose the product E_oL.

The procedure followed by the majority of workers was to develop an equation for ϵ and use the eddy viscosity concept to determine $\overline{u_x u_y}$. The length-scale was determined by a relation between E_o and ϵ (equal or similar to (2.7)).

For example, a dissipation equation, suitable for two-dimensional boundary layers, was proposed by Hanjalic (1970)

$$\frac{D\mathcal{E}}{Dt} = \frac{\partial}{\partial y}\left[\left(\nu + C_{\mathcal{E}}\frac{E_o^2}{\mathcal{E}}\right)\frac{\partial \mathcal{E}}{\partial y}\right] - C_{\mathcal{E}1}\mathcal{E}\frac{\overline{u_x u_y}}{E_o}\frac{\partial U_x}{\partial y} - C_{\mathcal{E}2}\frac{\mathcal{E}^2}{E_o} \quad , \quad (2.13)$$

where $C_{\mathcal{E}}$, $C_{\mathcal{E}1}$ and $C_{\mathcal{E}2}$ are constants. The predictions of the two-equation model $(E_o, \mathcal{E})$ represented by the system of equations (2.1), (2.6), (2.7), (2.8), (2.9) and (2.13) are compared in section 2.7 with experiments and with the other models.

A second two-equation model, using a shear stress equation instead of a dissipation equation, is also tested. Although this new model needs the prescription of a length-scale (in order to calculate $\mathcal{E}$), it avoids the use of the eddy viscosity hypothesis inherent in the use of equation (2.8). We take as our second equation the following equation for the shear stress derived by Hanjalic (1970)

$$\frac{D}{Dt}(\overline{u_x u_y}) = \frac{\partial}{\partial y}\left[\left(\nu + C_s\frac{E_o^2}{\mathcal{E}}\right)\frac{\partial}{\partial y}(\overline{u_x u_y})\right] - C_{s2}\left(C_{s1}E_o\frac{\partial U_x}{\partial y} + \mathcal{E}\frac{\overline{u_x u_y}}{E_o}\right), \quad (2.14)$$

where C_s, C_{s1} and C_{s2} are also constants. The two-equation model $(E_o, \overline{u_x u_y})$ given by relations (2.1), (2.6), (2.7) and (2.14), and <u>one</u> of the length-scale relationships from (2.10) to (2.12), is also compared in section 2.7 with the other models.

2.5 Three-equation model.

The desire to represent special real flows, such as flows where zero shear stress and maximum velocity do not occur at the same position, and recirculating flows, where the normal stresses are important, led to the development of multi-equation models. Among the many multi-equation models to be found in the literature, we found as amenable to a numerical approach, the following: the Hanjalic's (1970) three-equation model, the Hanjalic and Launder's (1972b) three-equation model and the Launder et al.'s (1975) five-equation model.

Hanjalic (1970) developed the three equations already presented here: the turbulence energy equation (2.6), the dissipation energy equation (2.13) and the shear stress equation (2.14). Together with the Reynolds equation (2.1)* they form a closed set of equations. No length-scale is needed, but 7 constants must be assigned numerical values. Table 2.1 gives the values assigned by Hanjalic to the constants; some of the constants he determinated from experiments in simple flows and the others he found by computer optimization.

Table 2.1 Empirical constants for the three-equation model (Hanjalic).

C_{s1}	C_{s2}	$C_{\varepsilon 1}$	$C_{\varepsilon 2}$	C_{s1}/C_e	C_{s1}/C_s	C_{s1}/C_ε
0.07	2.8	1.45	2.0	1.0	0.9	1.1

This three-equation model is also compared with the other models and with experiments in section 2.7 .

2.6 Summary of numerical method used to solve the partial differential equations.

Each one of the models represented by one, two or three equations is solved numerically for the dependent variables U_x, E_o, $\overline{u_x u_y}$ and ϵ . The solution method employed is the finite-difference procedure originated by Patankar and Spalding, where the partial differential equations are integrated in a forward-marching procedure. In Appendix - 1 a brief description of the essential features of the numerical method is given. For a full account of the numerical procedure and computer implementation, see Patankar and Spalding (1970).

One single computer program, hereafter referred to as TTBL, developed by the author, solves all 5 models of turbulence we have just described. For each model, the basic data required by the program is the geometry and flow conditions of the particular flow being considered. In order to predict asymmetric profiles which are characteristic of the annular flows, a non-uniform grid is used. The density of mesh points being greater in the vicinity of the wall. The non-uniform spacing of the grid points is of a logarithmic form and their precise distribution is made a function of the radius ratio.

At the beginning of a calculation, the computer program requires both boundary conditions and the initial profiles of the dependent variables to be specified. These initial conditions are provided by means of input data. In

practice, it is found satisfactory to assume that the initial profiles across the flow are constant. The boundary conditions are the same as those specified by Hanjalic and Launder (1972b) and Ng and Spalding (1976).

2.7 Quantitative comparison between the models.

The type of flow considered is the turbulent annular flow, and the cases of smooth annuli with two different radius ratios and annuli internally roughened, are examined. The predicted results are compared with the experiments of Lawn (1970) and Brighton and Jones (1964). A single set of constants as given in table 2.1, is used for all models tested. Von Karman's constant (K) is taken equal to 0.42 and a logarithmic grid of 60 points is used in numerical calculations.

Figure 2.1 shows the influence of length-scale on velocity, shear stress and turbulence energy profiles, using a two-equation model (E_o, $\overline{u_x u_y}$). A comparison with Lawn's (1970) experimental results shows that the length-scale expressions (2.10) and (2.11) give quite good predictions, while relation (2.12) exaggerates the asymmetry of the points of maximum velocity and zero shear stress, and therefore, is the least accurate in predicting the three profiles, the inaccuracy being mainly on the side nearer the inner wall. The 5 models are compared with the experimental results of Brighton and Jones (1964) in figure 2.2 , for the case of an annulus with a radius ratio not small. As the radius ratio is 0.562, the

asymmetry of the profiles is very small, so, as expected, all models give good predictions for velocity and shear stress profiles. However, a bigger discrepancy is observed in the turbulence energy profile.

The predicted profiles of velocity, shear stress and turbulence energy in an annulus internally roughened, are compared with experiment in figure 2.3 . As the experimental results of Lawn (1970) indicate, the maximum velocity and zero shear are shifted closer to the outer wall. The two and three-equation models predict quite well the velocity and shear profiles, while the one-equation model fails to predict the asymmetry, predicting the maximum velocity on the line of geometric symmetry of the annulus. By means of expression (2.7), length-scales for the two-equation (E_o,ε) and three-equation models are deduced. In both models E_o and ε are determined by equations. These two length-scales and the one predicted by the expression (2.10), are compared with the experimental results in figure 2.4 . As we can see, the predicted length-scale from the three-equation model (the case where $R_i/R_o=0.088$) is in better agreement with the experimental results found by Lawn (1970), except in a small region near the centre of the flow, where a depression is revealed by the experiment. Lawn justifies the presence of this depression as due to no^{ne}_{λ} production of turbulence energy in this region, and as a result, the dissipation equals the diffusion.

As can be seen from our results, all models are capable of predicting satisfactory velocity profiles. Even

the one-equation model might be capable of given good results by changing the value of some constants or/and modifying the length-scale. It is in the shear stress and turbulence energy that the major differences are exhibited. All the models, except the three-equation model and the two-equation model (E_o, ε), use some kind of length-scale. The length-scale is arbitrary and it is not, necessarily the same for all kinds of flows (and, even for the same flow, it might depend on the type of model used). It must be found by trial and error, checking against the experimental results until a 'good' length-scale is obtained. This procedure contains undesirable arbitrariness, and as a result, models using length-scale are gradually falling in disuse.

The two-equation model (E_o, ε) does not need a length-scale but uses the turbulent viscosity concept which, in some cases, fails to predict accurately the shear stress or turbulence energy profiles. As we have seen, in this particular geometry, the three-equation model gives correct predictions. This confirms the findings of Hanjalic and Launder (1972b) who tested the model in a great number of turbulent flows and also found it gave accurate results. Therefore, because of its generality and accuracy, we adopt the three-equation model in our further studies. By generality we mean that it can be applied to a variety of conditions and flows using a single set of constants.

CHAPTER - 3

3. Analysis and application of the three-equation model.

3.1 Influence of varying the constants in the three-equation model.

The three-equation model, represented by equations (2.6), (2.13) and (2.14), contains 7 adjustable constants, namely, C_{s1}, C_{s2}, $C_{\varepsilon 1}$, $C_{\varepsilon 2}$, C_e, C_ε and C_s whose values can be determinated by the application of the model to well-known simple flows, such as logarithmic flows and grid-generated turbulent flows. Several authors have recommended a set of values for these parameters. Table 3.1 summarises the values of the constants recommended. Each set of constants was optimized by fitting the theoretical results to individual experiments.

Table 3.1 Numerical values of the constants recommended by several authors.

Authors	C_{s1}	C_{s2}	$C_{\varepsilon 1}$	$C_{\varepsilon 2}$	C_e	C_ε	C_s
Hanjalic (1970)	0.07	2.8	1.45	2.0	0.07	0.064	0.078
Hanjalic and Launder (1972b)	0.07	2.8	1.45	2.0	0.064	0.065	0.08
Launder et al. (1975)	0.071	1.5	1.44	1.9	-	0.075	0.11
Jones and Launder (1973)	0.09	-	1.45	2.0	0.09	0.069	-

The values recommended by the various authors shown in table 3.1 appear to be in good agreement. This occurs not only because the models are similar, but is also due to the fact that the constants were derived by fitting the same experimental data. If the comparison between theory and experiment were to be made over a wide range of experimental data, greater differences could emerge. Therefore, in this section, we study more comprehensively the influence of varying the constants, on quantities like velocity, shear stress and turbulence energy.

By considering ideal flows we can estimate the range over which the constants should be varied. For a logarithmic flow, advection terms are zero and viscous diffusion terms are negligible. Under these conditions, the shear stress and turbulence energy equations can be even further simplified. Thus, relating the resultant terms in (2.6) and (2.14) we have

$$C_{s1} = \left[\frac{\overline{u_x u_y}}{E_o}\right]^2 \quad . \tag{3.1}$$

From the experimental data, the ratio of shear stress and turbulence energy ($\overline{u_x u_y}/E_o$) lies between 0.25 and 0.30 . Thus, C_{s1} can be assumed to vary between 0.06 and 0.09 .

The parameter C_{s2} shows greater variation among the authors. Following Rotta (1962), many workers assumed C_{s2} as

$$C_{s2} = \frac{4 + \alpha_1 - 4\alpha_2}{7\alpha_1 + 5\alpha_2 - 8} \cong 2.8 \quad , \tag{3.2}$$

where, α_1 and α_2 are constants of proportionality between normal shear stresses and turbulence energy and are given by

$$\overline{u_x^2} = \alpha_1 E_o \quad \text{and} \quad \overline{u_y^2} = \alpha_2 E_o \quad . \tag{3.3}$$

The values of α_1 and α_2 are obtained from experiments on nearly homogeneous shear flows. For example, from the experiments of Champagne et al. (1970), we found

$$\alpha_1 = 0.937 \quad \text{and} \quad \alpha_2 = 0.497 \quad . \tag{3.4}$$

Leslie (1975) pointed out that evidence is accumulating against assumption (3.3), and that the degree of anisotropy of the diagonal components varies markedly across a typical flow. Therefore, there is still some disagreement about the best value for C_{s2}, and it should be of interest to study how a change in C_{s2} affects the results given by the model. We consider the effect of varying C_{s2} in the range 1.5 to 4.0 .

In a grid-generated flow there is no production terms and the diffusion terms are negligible. This simplification permits the evaluation of $C_{\varepsilon 2}$. Applying this simplification to (2.6) and (2.13) and relating the resulting expressions for E_o and ε we obtain,

$$E_o = A\, x^{-n} \quad \text{and} \quad \varepsilon = nAU_x x^{-(n+1)} \tag{3.5}$$

where, A is a constant, x is the distance downstream of the grid, and

$$n = \frac{1}{C_{\varepsilon 2}-1} \quad . \tag{3.6}$$

The experiments of Batchelor and Townsend (1948) indicated a grid turbulence decay of the form $E_o \propto x^{-1}$ (n=1). Launder et al. (1975) suggested that n should be at least 1.1. In our analysis n is varied from 1.25 ($C_{\varepsilon 2}$=1.8), corresponding

to a high rate of decay, to 0.33 ($C_{\varepsilon 2}$=4.0), representing a low rate of decay.

Finally, imposing the condition that the dissipation equation (2.13) must also describe the logarithmic flow, it is possible to determine $C_{\varepsilon 1}$. It is well-known that for a logarithmic flow, $\partial U_x/\partial y$ and ε vary as $1/y$, or more precisely,

$$\frac{\partial U_x}{\partial y} = \frac{u_\tau}{Ky} \qquad \text{and} \qquad \varepsilon = \frac{u_\tau^3}{Ky} \quad . \tag{3.7}$$

Now, invoking (3.7) and neglecting the advection term, (2.13) becomes

$$C_{\varepsilon 1} = C_{\varepsilon 2} - C_\varepsilon K^2/C_{s1}^{3/2} \quad . \tag{3.8}$$

The proposed range of variation for $C_{\varepsilon 2}$ and C_{s1} causes $C_{\varepsilon 1}$ in (3.8) to vary from 1.15 to 3.47 . The ratios C_{s1}/C_s, C_{s1}/C_e and C_{s1}/C_ε are defined as the turbulent Prandtl Schmidt numbers for shear stress, turbulence energy and dissipation, respectively. Comparisons with experimental data show that the turbulent Prandtl-Schmidt numbers do not differ significantly from unity. Hence, we vary all 3 ratios, systematically, from 0.9 to 1.1 .

The range of values of the constants which we study is summarized for convenience in table 3.2 . The influence of varying the constants in the turbulence model is tested in a smooth annulus with small radius ratio, and the results are compared with the experimental values of Lawn (1970). The procedure for solving the three-equation model is the same as described in section 2.6 . Values of the constants are

systematically varied until all possible variations in the range are covered.

Table 3.2 Range over which the constants are varied.

C_{s1}	C_{s2}	$C_{\varepsilon 1}$	$C_{\varepsilon 2}$	$\frac{C_{s1}}{C_e}$, $\frac{C_{s1}}{C_\varepsilon}$, $\frac{C_{s1}}{C_s}$
0.06-0.09	1.5-4.0	1.15-3.47	1.8-4.0	0.9-1.1

The results are shown in figure 3.1, where velocity, shear stress and turbulence energy distributions are compared for the chosen range of the constants. As can be seen, velocity and shear stress display insensitivity to the variation of the parameters; the maximum variation of these quantities being 2%. Only the energy profile shows some sensitivity; then only C_{s1} affects the energy distribution. Roughly, an increase of 50% in C_{s1} decreases E_o by about 18%. Although the profiles of the main dependent variables are almost unaffected, some characteristic points of the flow, for example, location of maximum velocity and zero shear stress, are changed, as we shall see in the next section.

A similar study was performed by the author on jet flows, and identical pattern was observed. Profiles were nearly unchanged by variation of the constants' values, and, again, specific parameters only, for example, the rate of spreading, were greatly affected.

3.2 The position of maximum velocity in a smooth annulus.

As is well-known, fully developed annular flow involves the combination of two boundary layers, each extending from a wall to the point of maximum velocity. Each of these boundary layers may be quite different from the other, in the profiles of velocity, shear stress and other turbulence quantities. Such asymmetric distributions are substantially affected by geometrical conditions, such as annular radius ratio (R_i/R_o) or unequal roughness of walls. Here we devote some attention to the effect of varying the radius ratio and the constants, on velocity profiles in a smooth annulus. Numerical tests with the three-equation model are carried out for a range of annular radius ratios varying from 0.063 to 0.9 . The constants are varied as indicated in table 3.2 . The results are shown in figures 3.2 and 3.3 .

The velocity profiles are in figure 3.2 . A comparison with the experimental results of Brighton and Jones (1964) shows quite good agreement. Again, over the range of the constants studied, no significant change in the calculated velocity profiles is found. Both theoretical and experimental results show a flow curvature effect, that is, the points of maximum velocity and zero shear stress are shifted from the centre towards the inner wall, as the radius ratio decreases.

Kays and Leung (1963) correlated the results of various investigators, and defining

$$S^* = \frac{R_M - R_i}{R_o - R_M} \qquad \text{and} \qquad R^* = \frac{R_i}{R_o} \quad , \tag{3.9}$$

found a curve to predict the point of maximum velocity as a function of the radius ratio. They found the curve which best fits all the data to be:

$$S^* = (R^*)^{0.343} \quad . \tag{3.10}$$

A curve for symmetric shear profile (shear stress equal on both surfaces) can be derived, in order to compare with (3.10). A comparison of accurate shear stress and velocity profiles shows that the points of zero shear and maximum velocity do not coincide (the point of zero shear is nearer the inner wall than is the point of maximum velocity). But in this derivation we assume zero shear and maximum velocity occur at the same point. If we consider the balance of forces on an element of channel of length dx , we may write,

$$\tau_i = \frac{R_M^2 - R_i^2}{2R_i}\left(\frac{dp}{dx}\right) \tag{3.11}$$

$$\tau_o = \frac{R_o^2 - R_M^2}{2R_o}\left(\frac{dp}{dx}\right) \quad , \tag{3.12}$$

which gives the ratio of shear stress as

$$\frac{\tau_o}{\tau_i} = \frac{R_o^2 - R_M^2}{R_M^2 - R_i^2} \cdot \frac{R_i}{R_o} \quad . \tag{3.13}$$

If $\tau_o = \tau_i$, relation (3.13) gives $R_M = (R_i R_o)^{0.5}$ and substituting in (3.9) we find a relation to predict the point of zero shear in symmetric shear profiles, which is

$$S^* = (R^*)^{0.5} \quad . \tag{3.14}$$

The position of maximum velocity as a function of

the radius ratio is shown in figure 3.3 . Our predictions using the three-equation model are compared with the experimental results of Brighton and Jones (1964), and those referred to by Kays and Leung (1963), as well as the empirical expressions of (3.10) and (3.14). As can be seen, our predictions compare well with most of the experimental data. Although the effect on profiles is almost negligible, the point of maximum velocity is altered by the set of constants used. The influence of the variation of the constants in our predictions for S*, is also shown in figure 3.3 . We observe that the influence of C_{s1} is negligible as is also the Schmidt-Prandtl numbers. S* is mostly affected by C_{s2} and $C_{\varepsilon 2}$. An increase in C_{s2}, for a fixed $C_{\varepsilon 2}$, brings the point of maximum velocity closer to the inner wall (i.e., S* decreases). The opposite effect is observed when C_{s2} is fixed and $C_{\varepsilon 2}$ is increased. The limits of variation of S* shown in figure 3.3 are obtained with C_{s2}=4.0 and $C_{\varepsilon 2}$=1.8 for minimum S* and C_{s2}=2.0, $C_{\varepsilon 2}$=4.0 for maximum S*. The overall effect is more substantial for small radius ratios, and decreases as the radius ratio is increased.

3.3 Turbulent pipe flow.

In this section we devote some attention to the experimentally observed and so-called Laws of Similarity in fully developed turbulent flows, in the presence of rough walls. In order to verify such similarities we concentrate on the particular case of a round pipe. Numerical solutions are obtained using the three-equation model already described, and results are compared with the experiments. Three of these Laws

are well-known, namely, the law of the wall, the friction law and the velocity defect law, and some details of each are given below.

3.3.1 Law of the wall.

The law of the wall postulates the existence of a region near the wall where the non-dimensional velocity (u^+) shows a logarithmic profile of the form:

$$u^+ = B_r(e^+) + B.\ln\left(\frac{R_o-R}{e}\right) \quad , \qquad (3.15)$$

where, $e^+=eu_\tau/\nu$, e is the roughness height, (R_o-R) is the distance from the wall to the point considered, B and $B_r(e^+)$ are constants and u_τ is the friction velocity.

The velocity distribution represented by (3.15) is the logarithmic velocity profile, and the region in which is valid, namely, the outer part of the constant shear stress layer, is therefore called the logarithmic region. Many experiments confirm this relationship, and show that the constant, B=1/K, is approximately equal to 2.5 whatever the nature of the wall. The other constant, $B_r(e^+)$, depends, mainly, on the kind of wall roughness. When e^+ is large, B_r approaches an asymptotic value. Nikuradse (1950) found an asymptotic value of $B_r=8.48$ for sand-grain roughness. In the case of rib-roughened surfaces, Lawn and Hamlin (1968) pointed out a big scattering in the suggested values for B_r. The values of B_r quoted by them vary from 2.83 to 4.65. A value commonly used is $B_r=3.75$ which lies about the middle of the range of B_r values.

3.3.2 Friction Law.

Using the concept of friction factor (f), the flow through a pipe can be related to the friction it generates. It is customary to express the wall resistance in terms of a friction factor defined by

$$\tau_w = f.\frac{1}{2}\rho\overline{U}^2 \quad , \tag{3.16}$$

where, τ_w is the shear stress at the wall and $\overline{U}$ is the average mean velocity across the flow. Since the friction velocity is given by $u_\tau = (\tau_w/\rho)^{1/2}$, (3.16) can be re-written as

$$f = 2(\frac{u_\tau}{\overline{U}})^2 \quad . \tag{3.17}$$

Furthermore, we can obtain an expression for the average velocity across the whole section, which, together with (3.17) and with the Law of the wall (3.15), gives

$$\sqrt{\frac{2}{f}} = (B_r - 3.75) + B.\ln(\frac{R_o}{e}) \quad . \tag{3.18}$$

The relationship (3.18), which was proposed by Schlichting (1968), is the logarithmic friction factor formula, which predicts successfully a very large mass of experimental data.

3.3.3 Velocity defect Law.

For the outer region, or core region, of the flow, the logarithmic distribution, represented by (3.15), no longer applies since the conditions on which it is based are no longer valid. In the core region, direct viscous effects continue to

be negligible and the total stress is identified with the Reynolds stress. This implies that the velocity scale is u_τ and the length scales are R_o and r. Thus, in the core region, the velocity "defect", defined as $\frac{U_{MAX}-U(r)}{u_\tau}$, is a function of $(R_o-r)/R_o$ only. This type of similarity which holds in the core region has the form

$$\frac{U_{MAX} - U(r)}{u_\tau} = h(\xi) \quad . \tag{3.19}$$

where, U_{MAX} is the maximum velocity (in pipe flow, the velocity at the centre of the pipe), R_o is the pipe radius and $\xi = \frac{R_o-r}{R_o}$. Equation (3.19) is known as the velocity defect law, it is independent of Reynolds number and roughness height. The defect law should be regarded as an empirical relationship, although it can be shown that its form is compatible with the equations of motion.

Using the eddy viscosity formalism, Leslie (1977) developed a theoretical relation for $h(\xi)$, matching both the logarithmic and core regions. His proposed relationship is:

$$h(\xi) = B\left[\frac{(1-\xi_1)^2}{2\xi_1} + \ln\frac{\xi_1}{\xi} - (\xi_1 - \xi)\right] \quad , \xi < \xi_1$$

$$= B\,\frac{(1-\xi)^2}{2\xi_1} \quad , \xi \geqslant \xi_1 \tag{3.20}$$

where, $B=1/K$ and ξ_1 is the value of ξ where the variation of the eddy viscosity is assumed to become nearly constant for the remaining of the core region. Leslie found $\xi_1=0.16$ to be the value which results in the profile (3.20) having quite good agreement with the experimental measurements.

Spatially averaging $h(\xi)$ we obtain the mean value, $\bar{h}$, from

$$\bar{h} = \frac{1}{\pi R_o^2} \int_0^{R_o} 2\pi r h(r) dr \qquad (3.21)$$

$$= \int_0^1 2(1-\xi) h(\xi) d\xi \quad . \qquad (3.22)$$

Substituting (3.20) into (3.22) and integrating, Leslie (1977) found

$$\bar{h} = B \left(\frac{1}{4\xi_1} + \xi_1 - \frac{1}{2}\xi_1^2 + \frac{1}{12}\xi_1^3 \right) \quad . \qquad (3.23)$$

3.3.4 Comparison between experimental results and the three-equation model predictions.

The three-equation model represented by equations (2.1), (2.6), (2.13) and (2.14) is solved for a turbulent pipe flow, using the numerical technique of Patankar and Spalding (1970). The set of constants employed is the same as in table 2.1 . Reynolds numbers ranging from 5.0×10^5 to 5.0×10^6 are tested. Both sand-roughened and square-rib-roughened walls are considered, with roughness ratios (D/e) varying from 40 to 800.

The form assumed for the law of the wall (3.15) is verified in figure 3.4 . Our predictions for u^+ vs. $(R_o-R)/e$ are compared with the experimental correlations. The predicted results, for all three roughness ratios, agree quite well with the Nikuradse (1950) relation for sand-roughness (B_r=8.48). A similar good agreement is observed for square-rib-roughness. The friction factors in the turbulent rough pipe flow, as a

function of roughness ratio, are shown in figure 3.5 . As we can see, the predicted results and the experimental data, represented by (3.18), agree well for both kinds of roughness: sand-roughening with $B_r=8.48$ and square-rib-roughened wall with $B_r=3.75$.

Figure 3.6 shows the defect function $h(\xi)$, defined by (3.19), for a pipe flow with sand-roughness. The predicted results and the profile proposed by Leslie (1977) of (3.20), are very close. Also in figure 3.6 are plotted the experimental results obtained by Lawn (1970). Once again, good agreement is observed. As an alternative to (3.21), the average of the defect function ($\bar{h}$) can be defined as,

$$\bar{h} = \frac{U_{MAX}-\bar{U}}{u_\tau} = \sqrt{\frac{2}{f}}\left(\frac{U_{MAX}}{\bar{U}} - 1\right) \quad . \tag{3.24}$$

Substituting the values we find from our numerical calculations, into (3.24) we obtain $\bar{h}=4.69$; this value we find to be nearly independent of the roughness ratio and Reynolds number. But taking $\xi_1=0.16$, the relation (3.23) proposed by Leslie (1977) gives $\bar{h}=4.28$. The value $\bar{h}=4.69$ seems a little high compared to the second value of $\bar{h}$. In a similar study to that made in section 3.1 and section 3.2, that is varying the constants of table 2.1, we find that the values $C_{s2}=3.2$ and $C_{\varepsilon 2}=1.8$ decreases $\bar{h}$ to 4.32 , while the defect function remains practically unchanged. Therefore, it appears that $C_{s2}=3.2$ and $C_{\varepsilon 2}=1.8$ are better values to use in the model to predict pipe flows.

3.4 Friction factors in turbulent annular flow.

In gas-cooled reactors the basic geometry of the coolant channel is annular geometry. As a consequence, very extensive experiments have been made in annular turbulent flows (mainly with roughening and heat flux on the inner side only). In order to handle the high reactor heat fluxes, it is necessary to increase the transference of heat from the cladding to the coolant. Therefore, various geometries have been tested for this desirable characteristic . One of the most common devices used is to roughen the inner side of the channel by regularly spaced transverse square ribs. Here we examine the friction factors obtained with the three-equation model for several wall conditions and the results obtained are compared with the available experimental data. The corresponding heat transfer cofficients are discussed in section 4.4 .Three configurations are considered: (1) both walls smooth (smooth/smooth), (2) both walls rough (rough/rough) and (3) internal wall rough and external wall smooth (rough/smooth).

3.4.1 Smooth/smooth and rough/rough annuli.

To begin with, we consider the smooth/smooth annulus. Reynolds numbers varying from 1.0×10^4 to 1.1×10^6 are considered; also, the radius ratio is varied from 0.125 to 0.75 . Results predicted with the three-equation model are shown in table 3.3. These predictions are also compared in table 3.3 with the experiments of Lee and Barrow (1964), Jonsson and Sparrow (1966) Brighton and Jones (1964) and Watson (1970). As can be seen,

Table 3.3 Predicted and experimental overall friction factors in a fully developed smooth annular flow.

Reference	Re	R_i/R_o	f x100	
			Experiment	Predicted
Lee and Barrow (1964)	1.0×10^4	0.613	0.85	0.82
	4.0×10^4	0.613	0.62	0.61
	1.0×10^4	0.387	0.90	0.85
	4.0×10^4	0.387	0.64	0.61
	1.0×10^4	0.258	1.00	0.86
	4.0×10^4	0.258	0.64	0.61
Jonsson and Sparrow (1966)	5.0×10^4	0.750	0.56	0.57
	5.0×10^4	0.281	0.53	0.58
	1.0×10^5	0.281	0.47	0.49
	2.0×10^5	0.281	0.41	0.42
Brighton and Jones (1964)	1.0×10^5	0.375	0.49	0.49
	2.0×10^5	0.375	0.41	0.41
	1.0×10^5	0.125	0.47	0.48
	2.0×10^5	0.125	0.43	0.41
Watson (1970)	3.5×10^5	0.513	0.40	0.39
	5.1×10^5	0.513	0.36	0.36
	7.7×10^5	0.513	0.34	0.34
	9.5×10^5	0.513	0.34	0.34

the overall agreement is good, especially for high Reynolds numbers.

The variation of the friction factor in a rough/rough annulus, as a function of Reynolds number, is shown in figure 3.7 . The roughening on both sides is achieved by square ribs. From figure 3.7 we see that the overall friction factor has a nearly constant value and is in excellent agreement with the experimental data of Lawn and Hamlin (1969). Also in figure 3.7 we plot the friction factors for the internal and external surfaces, f_i and f_o, respectively . A slight disagreement between prediction and experiment is observed. We suggest that this discrepancy is due to the definitions of f_i and f_o. We define our f_i and f_o by a relation similar to (3.16), using the same average mean velocity $\overline{U}$ to calculate both factors. While Lawn and Hamlin define,

$$f_i = \frac{\tau_i}{\frac{1}{2}\rho \overline{U}_i^2} \qquad \text{and} \qquad f_o = \frac{\tau_o}{\frac{1}{2}\rho \overline{U}_o^2} \quad , \qquad (3.25)$$

where, $\overline{U}_i$ is the average mean velocity for the portion of flow between the inner wall and the point of zero shear stress, and $\overline{U}_o$ is the average mean velocity for the outer portion.

The influence of the radius ratio (R*) on friction factors in smooth/smooth and rough/rough annular flow is shown in figure 3.8 . The experimental data is that cited by Watson (1970) and shows that the effect of radius ratio is significant only for small and moderate Reynolds numbers ($Re < 10^5$). This effect is observed also in our predictions as shown by figure 3.8 . The smooth/smooth and the rough/rough annuli (sand-

roughened, B_r=8.48) are independent of radius ratio. The radius ratio seems to show some effect only on square-rib roughened annuli (with B_r=3.75), when $R^* \leq 0.4$. For example, when R* is decreased from 0.4 to 0.2, the overall friction factor increases by 16%.

3.4.2 Annulus internally roughened.

3.4.2.1 Overall friction factors.

Numerical calculations with our three-equation model are carried out for an annular turbulent flow having the internal wall roughened and the external wall smooth. Several Reynolds numbers and radius ratios, as well as different kinds of roughness, are considered. Predicted overall friction factors with $Re=5.0 \times 10^5$ and R*=0.5 as functions of roughness ratio (De/e) and kind of roughness (B_r), are shown in figure 3.9 . In order to check our predictions, we compare our results with the experimental data of Lee (1972) and Wilkie (1966) in figure 3.10 . Although both authors used the same kind of roughness (i.e. square ribs), we observe a scattering in the experimental values. This is due to different geometrical conditions, i.e., different radius ratios, ribs pitch ratio (s/e) and ribs width ratio (e/w), being used by the two workers. In figure 3.10 we show predictions with two values of B_r, namely, 3.75 and 3.0 . As we can see, an acceptable agreement is obtained with the value B_r=3.75, this curve being the best fit to experimental data.

3.4.2.2 Hall's transformation.

In order to enable a comparison of friction factors and heat transfer coefficients in channels with different cross-sections, or different kinds of roughness at each wall, or even different proportions of heated and unheated surfaces, Hall (1962) devised a transformation method. The key feature of the method he proposed lies in the isolation of the effect of each wall. For example, in an annulus internally roughened, the assumption is made that the distribution of the fully developed flow is largely determined by the geometry of the flow area between the rough surface and the surface of zero shear stress, and is little affected by the smooth surface opposite. Then, we can define a separate friction factor for the system associated with the rough surface (and a friction factor to be associated with the system of smooth surface). The assumption is then made of equivalent diameter, defined by the flow area between the zero shear stress and the rough surfaces and by the rough surface perimeter. Finally, a further assumption is made that the resulting friction factor and Reynolds number will be the same as would exist for a circular passage having the same relative roughness and the same equivalent diameter.

In its original form, Hall's method requires the measurement of the velocity and temperature distributions in the channel. It is assumed that the position of zero shear stress is coincident with that of maximum velocity. By applying a force balance on the two regions of the annular passage,

namely, rough/zero shear surfaces and smooth/zero shear surfaces, Hall (1962) found:

$$\tau_i = \frac{R_M^2 - R_i^2}{2R_i} \cdot \frac{dp}{dx} = \frac{1}{4} \frac{dp}{dx} De_1 = f_1 \frac{\bar{\rho}_1 \bar{U}_1^2}{2} \tag{3.26}$$

$$\tau_o = \frac{R_o^2 - R_M^2}{2R_o} \cdot \frac{dp}{dx} = \frac{1}{4} \frac{dp}{dx} De_2 = f_2 \frac{\bar{\rho}_2 \bar{U}_2^2}{2} \tag{3.27}$$

where, the equivalent diameters De_1 and De_2, associated with the rough and smooth portions, are defined as,

$$De_1 = \frac{4\pi(R_M^2 - R_i^2)}{2\pi R_i} \tag{3.28}$$

$$De_2 = \frac{4\pi(R_o^2 - R_M^2)}{2\pi R_o} \tag{3.29}$$

The overall friction factor is given by the Fanning equation:

$$f = \frac{De}{2\bar{\rho}\bar{U}^2} \cdot \frac{dp}{dx} \tag{3.30}$$

where, De, $\bar{\rho}$ and $\bar{U}$ now refer to the whole of the annular passage and, also,

$$De = 2(R_o - R_i) \quad . \tag{3.31}$$

Now, relating (3.26), (3.27) and (3.30) it follows

$$\frac{f_1}{f} = \frac{\bar{\rho}\bar{U}^2}{\bar{\rho}_1 \bar{U}_1^2} \frac{De_1}{De} \quad , \tag{3.32}$$

and

$$\frac{f_2}{f} = \frac{\overline{\rho}\overline{U}^2}{\overline{\rho}_2\overline{U}_2^2} \frac{De_2}{De} \quad . \tag{3.33}$$

By analogy with the Reynolds number for the whole passage, the Reynolds number for each section is defined as,

$$Re_1 = \frac{\overline{U}_1 De_1 \overline{\rho}_1}{\mu_1} \qquad \text{and} \qquad Re_2 = \frac{\overline{U}_2 De_2 \overline{\rho}_2}{\mu_2} \quad . \tag{3.34}$$

(i) Iterative methods based on Hall's transformation.

In an attempt to avoid the measurement of velocity distribution as proposed by Hall (1962), a number of simplified methods of transformation have been proposed. One of the most popular is the method developed by Wilkie (1966), in which the shear stress on the smooth wall is obtained by a correlation, and related to the rough wall by means of three parameters K_1, K_2 and K_3, obtained from the analysis of a large number of experiments. Wilkie developed a system of 3 equations which can be solved iteratively for the unknowns f_1 and De_1. This method still assumes that the surface of zero shear and maximum velocity are coincident.

We now propose an even simpler method based on well known empirical correlations, which gives results which do not differ significantly from the Wilkie method. Since the average mean velocity in each of the two sections does not differ too much from the average mean velocity of the whole annulus, then we can assume $\overline{U} = \overline{U}_1 = \overline{U}_2$. Now, relating (3.32) and (3.33) we

obtain,

$$\frac{f_1}{f_2} = \frac{De_1}{De_2} \quad . \tag{3.35}$$

The friction factors f_1 and f_2 in each section can be derived from pipe correlations, provided that equivalent diameters De_1 and De_2 are used. We use two well-known correlations which summarize most of the experimental data in pipes. For the inner (rough) section we adopt the relation proposed by Schlichting (1968). This relationship was introduced earlier in (3.18) but is reproduced here for convenience:

$$\sqrt{\frac{2}{f_1}} = (B_r - 3.75) + 2.5 \ln\left(\frac{De_1}{2e}\right) \quad .$$

The friction factor for the outer (smooth) section is well predicted by the Blasius formula,

$$f_2 = 0.046 Re_2^{-0.2} \quad . \tag{3.36}$$

Thus, for a given geometry (i.e., R_i, R_o, Re and e known), the set of equations (3.28), (3.29), (3.34), (3.35), (3.18) and (3.36) can be solved iteratively. An initial guess for R_M is required; a reasonable starting value is $R_M=(R_i R_o)^{1/2}$. The overall friction factor for the whole channel is then calculated by

$$f = f_1 \frac{De}{De_1} \quad . \tag{3.37}$$

Using this method we calculate the overall friction factors in annuli with radius ratio equal to 0.5 and Reynolds number equal to 5.0×10^5. Parameters B_r and e, which characterize the kind of roughness on the inner wall, are varied in the range:

$$2.0 \leqslant B_r \leqslant 8.48 \qquad \text{and} \qquad 40 \leqslant \frac{De}{e} \leqslant 800 \quad .$$

Results are compared in figure 3.11 with those obtained by the three-equation model, under the same geometrical conditions. As we can see, this method gives results about 10-15% lower than the three-equation model for the same value of B_r. Results of this method with other values of B_r are also shown in figure 3.11. Roughly, the same friction factors are obtained with this method if one uses a B_r value which is 1 less than the B_r value used in the three-equation model. Therefore, this method gives good predictions provided that we use a B_r=7.48 for sand roughness and a B_r=2.75 for square-rib-roughening.

(ii) Methods using the true position of zero shear stress.

The previous methods are based on the assumption that the surfaces of zero shear and maximum velocity are coincident. Direct measurements by Hanjalic and Launder (1972a) in a rectangular channel and Lawn (1970) in an annulus have shown that, where there is an asymmetric velocity profile, the positions of zero shear and zero velocity gradient differ by quite large amounts. This led Nathan and Pirie (1970) to develop a transformation based on the actual position of the surface of zero shear. In fact, their method is an extension of Wilkie's (1966) method, and the functions K_1, K_2 and K_3 are modified to allow for the difference between the positions of zero shear and maximum velocity.

We also propose a method for calculating friction factors in annuli, based in Hall's formulation and pipe correlations, using the actual position of zero shear stress, R_{so}. Using R_{so} instead of R_M, from (3.28) it is possible to calculate De_1. Then, from (3.18) we can find f_1 and, finally, the overall friction factor is calculated by means of (3.32). The values of R_{so} are determined by applying the three-equation model to an annulus internally roughened with $R^*=0.5$ and $Re=5.0x10^5$. Since the three-equation model gives velocity and shear profiles, it is simple matter to obtain R_{so} from those distributions. Overall friction factors are obtained with this method and results are shown in figure 3.12 . These results are compared with the three-equation model and with the results from the previous iterative method. As expected, the new method gives better agreement with the three-equation model (for the same B_r) than does the iterative method. As can be seen in figure 3.12, this method using the true position of zero shear gives the same friction factors as the three-equation model, if we use a B_r value which is, roughly, 0.5 less than the B_r used in the three-equation model.

(iii) Transformed friction factors.

The two methods just developed illustrate clearly the difficulty of choosing which value of B_r is the most apposite. To avoid this problem, a similar method to the iterative method (but without the iterative process) can be introduced. This is obtained by working with the relations on the smooth side of the annulus. The friction factor on the outer side (smooth wall)

is given by (3.36) as

$$f_2 = 0.046Re_2^{-0.2} = 0.046Re^{-0.2}\left[\frac{De_2}{De}\right]^{-0.2} = \frac{De_2}{De}\cdot f \ ,$$

thus,

$$\frac{De_2}{De} = \left[\frac{0.046Re^{-0.2}}{f}\right]^{5/6} \ . \qquad (3.38)$$

Once Re and f for the whole channel are known, from (3.38) and (3.29) it is possible to calculate R_M. Then, De_1 is obtained from (3.28) and, finally, (3.37) gives the transformed friction factor f_1.

Overall friction factors in annuli with square-rib roughening on the inner side are calculated using the three-equation model. The geometry parameters used are $R^*=0.5$; $Re=5.0\times10^5$ and $20 \leq De/e \leq 800$. Results are transformed in terms of f_1 vs. e/De_1, by using the simple method just described. Predictions and experimental data are compared in figure 3.13. As can be seen, our predicted results agree quite well with the experimental data of Watson (1970). Also a good agreement is observed with the results from the transformations of Wilkie (1966) and Nathan and Pirie (1970). Included in figure 3.13 is the Schlichting's (1968) correlation, (3.18), with $B_r=3.0$ and $B_r=3.75$. The line with $B_r=3.0$ matches fairly well our predictions. Based on his own experiments, Wilkie (see Leslie (1976)) proposed, for annular flow or cluster configurations, that the transformed friction factor is given by,

$$f_1 = 0.0098 + 1.92\,\frac{e}{De_1} \ . \qquad (3.39)$$

Therefore, in figure 3.13 we also plot Wilkie's correlation (3.39). Wilkie's expression predicts greater

friction factors than any of the other methods. For small transformed roughness ratios (i.e. small e/De_1) the difference is slight and may be acceptable. The experimental results of Wilkie (1966) were obtained for roughness ratios less than 0.011 (roughly, $e/De_1 \leq 0.06$). Thus we regard $e/De_1 \cong 0.01$ as the upper limit of the validity of (3.39). Therefore, the application of relation (3.39) must be restricted to within that range of validity.

CHAPTER - 4

4. Thermal boundary layers.

4.1 Equations for thermal boundary layers in turbulent flow.

Having selected a versatile model of turbulence, which can be solved in a reasonable amount of computing time, and which is capable of solving purely hydrodynamic boundary layers, we can devote our attention to the thermal boundary layers. As we remarked in section 1.2, the hydrodynamic model can be extended to a new and complete model which combines the effects of heat and momentum transfer. Three equations, namely, (1) mean temperature equation, (2) convective heat flux equation and (3) intensity of temperature fluctuation equation, are sufficient to describe the influence of heat transfer on the turbulent fluid flow. Thus, the new model, in addition to the three-equation model (3 transport equations, $\overline{u_x u_y}$, E_o and ε plus the momentum equation), will have 2 transport equations more, plus the mean temperature equation. Therefore, for consistency of nomenclature, we call this new model the five-equation model. Although we propose the simultaneous solution of 7 differential equations, this new model still can be considered as an intermediate model when compared with the ten-equation model proposed by Donaldson et al. (1972) and the twelve-equation model proposed by Lumley (1972). Also, as we shall see, it is uncomplicated, numerically amenable and accurate.

As was mentioned in the Introduction, the system of thermal equations, even after the boundary layer simplifications, has more unknown quantities than equations; therefore, a closure procedure is needed. The following sections contain the development and closure of the thermal boundary layer equations. In order to make possible these simplifications, we will ~~assume~~ make the same general assumptions specified in section 2.1 . Differences of temperature between fluid and boundary must be assumed small, in order to make acceptable the assumption of constant fluid properties. If it transpires that some other assumptions are needed, they will be stated as they occur.

4.1.1 Equation for the mean temperature.

The basic equation for the conservation of energy in a laminar incompressible fluid, neglecting the potential energy, is

$$\rho c_p \cdot \frac{DT_o}{Dt} = \frac{\partial}{\partial x_m}\left(k \frac{\partial T_o}{\partial x_m}\right) + \mu \varphi \qquad (4.1)$$

where,

$$\varphi = \left(\frac{\partial U_i^*}{\partial x_j} + \frac{\partial U_j^*}{\partial x_i} \right) \frac{\partial U_i^*}{\partial x_j} \quad . \qquad (4.2)$$

T_o and U_k^* are the instant values of temperature and velocity. In turbulent flows, variables like velocity, pressure temperature, etc., do not remain constant with time at a fixed point, they perform very irregular fluctuations. Thus, using the concept of "time average", we can assume each dependent variable is the sum of a mean value plus a

fluctuating value. Therefore, we specify the variables as

$$T_o = T + T' \qquad (4.3)$$
$$U_i^* = U_i + u_i \quad .$$

In these relations, T and U_i are the mean temperature and mean velocity, while, T' and u_i are the respective turbulent fluctuations. By definition, the time average of a fluctuating component is zero, thus

$$\overline{T'} = 0 \qquad \text{and} \qquad \overline{u_i} = 0 \qquad (4.4)$$

Substituting (4.3) and (4.2) in (4.1) and averaging we find

$$\rho c_p\left[\overline{\frac{\partial}{\partial t}(T+T')} + \overline{(U_i+u_i)\frac{\partial}{\partial x_i}(T+T')}\right] = \frac{\partial}{\partial x_m}\overline{\left(k\,\frac{\partial}{\partial x_m}(T+T')\right)} +$$
$$\mu\overline{\left[\left(\frac{\partial}{\partial x_j}(U_i+u_i) + \frac{\partial}{\partial x_i}(U_j+u_j)\right)\right]\cdot\frac{\partial}{\partial x_j}(U_i+u_i)}\,. \qquad (4.5)$$

Considering separately each term of (4.5) and using the continuity equations

$$\frac{\partial U_i}{\partial x_i} = 0 \qquad \text{and} \qquad \frac{\partial u_i}{\partial x_i} = 0 \quad , \qquad (4.6)$$

plus relations (4.4), we obtain

$$\frac{DT}{Dt} = \frac{k}{\rho c_p}\frac{\partial^2 T}{\partial x_i \partial x_i} + \frac{\mu}{\rho c_p}\left(\frac{\partial U_i}{\partial x_j} + \frac{\partial U_j}{\partial x_i}\right)\frac{\partial U_i}{\partial x_j} +$$
$$+ \frac{\mu}{\rho c_p}\overline{\left(\frac{\partial u_i}{\partial x_j} + \frac{\partial u_j}{\partial x_i}\right)\frac{\partial u_i}{\partial x_j}} - \frac{\partial}{\partial x_i}\left(\overline{u_i T'}\right) \quad . \qquad (4.7)$$

Equation (4.7) is the general equation for the mean temperature in an incompressible turbulent flow. Reynolds(1974)

shows that the dissipation in the turbulent field, represented by the term

$$\frac{\mu}{\rho c_p}\,\overline{\left(\frac{\partial u_i}{\partial x_j}+\frac{\partial u_j}{\partial x_i}\right)\frac{\partial u_i}{\partial x_j}}\quad ,$$

varies slowly along the channel. This term is negligible, in comparison with the other terms of (4.7), for the majority of flows. It is of significance only when the flow is nearly adiabatic, or when the velocity is very high (i.e., comparable with the speed of the sound). Since these two conditions are beyond the range of our consideration, we will neglect this term in (4.7). For incompressible flow, the effects of viscous dissipation in the mean flow can be ignored too. Therefore, we assume

$$\frac{\mu}{\rho c_p}\left(\frac{\partial U_i}{\partial x_j}+\frac{\partial U_j}{\partial x_i}\right)\frac{\partial U_i}{\partial x_j}\cong 0 \qquad (4.10)$$

Now, with the two simplifications above and introducing the boundary layer approximations

$$\text{a)}\ \frac{\partial}{\partial x}(\ )_x \ll \frac{\partial}{\partial y}(\ )_x \quad ; \quad \frac{\partial}{\partial y}(\ )_y \ll \frac{\partial}{\partial y}(\ )_x \qquad (4.8)$$

$$\text{b)}\ \frac{\partial}{\partial z}(\ )_{x,y} = 0 \quad \text{(symmetric or two-dimensional flow)} \qquad (4.9)$$

the equation of mean temperature (4.7) becomes

$$\frac{DT}{Dt} = \gamma\frac{\partial^2 T}{\partial y^2} - \frac{\partial}{\partial y}\overline{(u_y T')} \quad , \qquad (4.12)$$

where $\gamma = \dfrac{k}{\rho \cdot c_p}$ is the thermal diffusivity. (4.11)

Equation (4.12) is the final form of the mean temperature equation for two-dimensional incompressible turbulent flow. Comparing (4.12) with the corresponding equation for laminar boundary flow, the only difference is the presence of the term $\frac{\partial}{\partial y}(\overline{u_y T'})$ which represents the effect of turbulent transport of heat and is analogous to the Reynolds stress term in the equation of mean momentum (2.1).

4.1.2 Equation for the convective heat flux.

An equation for the convective heat flux $(\overline{u_i T'})$ can be derived from the Navier-Stokes equation and the equation for conservation of thermal energy (4.1). Neglecting external forces and buoyancy effects, the Navier-Stokes equation for turbulent flow is

$$\frac{\partial}{\partial t}(U_i+u_i) + (U_k+u_k)\frac{\partial}{\partial x_k}(U_i+u_i) = \nu \frac{\partial^2}{\partial x_m \partial x_m}(U_i+u_i) - \frac{1}{\rho}\frac{\partial}{\partial x_i}(p+p') \quad . \qquad (4.13)$$

Multiplying (4.1) by u_i, (4.13) by T', making use of relations (4.4), averaging and summing the two resultant equations, we obtain

$$\frac{D}{Dt}(\overline{u_i T'}) = \underbrace{-\left(\overline{u_i u_k}\frac{\partial T}{\partial x_k} + \overline{u_k T'}\frac{\partial U_i}{\partial x_k}\right)}_{(I)} \underbrace{- (\nu+\gamma)\overline{\frac{\partial T'}{\partial x_k}\cdot\frac{\partial u_i}{\partial x_k}}}_{(II)} + \underbrace{\overline{\frac{p'}{\rho}\cdot\frac{\partial T'}{\partial x_i}}}_{(III)} - \underbrace{\frac{\partial}{\partial x_k}\left(\overline{u_i T' u_k} + \delta_{ik}\overline{\frac{p'T'}{\rho}}\right)}_{(IV)} \quad , \qquad (4.14)$$

$$(V)$$

where δ_{ik} is the Kronecker delta, i.e.,

$$\delta_{ik} = 1 \quad \text{when} \quad i = k$$

$$= 0 \quad \text{when} \quad i \neq k$$

Terms in (4.14) have the following physical interpretation:

Term I - Advection (or convection), represents the rate of change of convective heat flux.

Term II - Production from the mean flow.

Term III- Viscous and conductive molecular dissipation.

Term IV - "Pressure-rate of strain".*

Term V - Turbulent diffusion.

The above equation for convective heat flux contains a number of unknown correlations of fluctuating quantities. Therefore, in its present form, of course, it is not immediately employable in a model of turbulent motion. Thus, (4.14) must be closed, i.e., the unknown quantities need to be approximated in terms of the main dependent variables. The following sections describe the approximations and assumptions made, in order to simplify the convective heat flux equation (4.14) .

* In fact, term IV is a pressure-temperature gradient correlation but, as this term is the counterpart of the pressure-strain correlation in the stress equations, throughout this thesis we call it "pressure-rate of strain" term.

4.1.2.1 Viscous and conductive dissipation terms.

The first terms to receive attention are the dissipation terms III, which are

$$\nu \overline{\frac{\partial T'}{\partial x_k} \cdot \frac{\partial u_i}{\partial x_k}} \qquad (4.15)$$

and

$$\gamma \overline{\frac{\partial T'}{\partial x_k} \cdot \frac{\partial u_i}{\partial x_k}} \quad . \qquad (4.16)$$

The dissipative correlations (4.15) and (4.16) are zero in isotropic turbulence and will be negligible also in non-isotropic turbulence provided that, as we assume here, the turbulence Reynolds number is high. Thus, we can make

$$(\nu + \gamma) \overline{\frac{\partial T'}{\partial x_k} \cdot \frac{\partial u_i}{\partial x_k}} \cong 0 \quad . \qquad (4.17)$$

4.1.2.2 "Pressure-rate of strain" term.

As shown in Appendix - 2, the "pressure-rate of strain" term, IV, can be approximated by the sum of two terms: the first due only to turbulent effects and the second due to mean motion effects. Therefore, from Appendix - 2, we have

$$\overline{\frac{p'}{\rho} \cdot \frac{\partial T'}{\partial x_i}} = - C_{UT1} \frac{\varepsilon}{E_o} \overline{u_i T'} + \alpha \overline{u_m T'} \frac{\partial U_i}{\partial x_m} \quad , \qquad (4.18)$$

where C_{UT1} and α are constants.

4.1.2.3 Turbulent diffusion term.

Tennekes and Lumley (1973) pointed out that nearly all previous authors have neglected the pressure-work term $\frac{\partial}{\partial x_k}\left(\delta_{ik}\frac{\overline{u_k p'}}{\rho}\right)$ which appears in the shear stress equation. Those who neglected the term justified its omission on the grounds of a poor correlation existing between p' and u_k. Now, the quantity $\frac{\partial}{\partial x_k}\left(\delta_{ik}\frac{\overline{T'p'}}{\rho}\right)$, which occurs in the turbulent diffusion term V, corresponds to the pressure-work term of the shear stress equation. Thus, by analogy, we assume that a poor correlation exists between p' and T', and so the average product $\overline{p'T'}$ may be neglected. Zeman and Lumley (1976) and Launder (1975) also closed the convective heat flux equation by neglecting this term. Therefore, the pressure effect on the diffusion term V is assumed zero, i.e.

$$\frac{\partial}{\partial x_k}\left(\delta_{ik}\frac{\overline{T'p'}}{\rho}\right) = 0 \quad . \tag{4.19}$$

The triple correlation $\overline{u_i T' u_k}$ is also a component of the turbulent diffusion term V. Triple correlations are neglected by some workers. But we ourselves do not follow this practice because these terms have order of magnitude of the production terms II, and therefore, they should be included. Following the procedures proposed by Chou (1945) and Hanjalic and Launder (1972b), we find, after some approximations and further assumptions, an algebraic relation to simulate the triple correlation terms as a function of second-order correlations. The detailed derivation is described in Appendix - 3. There, it is shown that we may write

$$\overline{u_i T' u_k} = - C_{UT2} \frac{E_o}{\varepsilon} \left(\overline{u_i u_m} \frac{\partial}{\partial x_m} \overline{u_k T'} + \overline{u_m T'} \frac{\partial}{\partial x_m} \overline{u_i u_k} + \overline{u_k u_m} \frac{\partial}{\partial x_m} \overline{u_i T'} \right) \tag{4.20}$$

where, C_{UT2} is a constant.

4.1.2.4 Approximate equation for two-dimensional convective heat flux.

Substituting relations (4.17), (4.18), (4.19) and (4.20) in (4.14) we obtain

$$\frac{D}{Dt}(\overline{u_i T'}) = - \left(\overline{u_i u_k} \frac{\partial T}{\partial x_k} + \overline{u_k T'} \frac{\partial U_i}{\partial x_k} \right) - C_{UT1} \frac{\varepsilon}{E_o} \overline{u_i T'} + \alpha \left(\overline{u_m T'} \frac{\partial U_i}{\partial x_m} \right.$$
$$\left. + \frac{\partial}{\partial x_k} \left[C_{UT2} \frac{E_o}{\varepsilon} \left(\overline{u_i u_m} \frac{\partial}{\partial x_m} \overline{u_k T'} + \overline{u_m T'} \frac{\partial}{\partial x_m} \overline{u_i u_k} + \overline{u_k u_m} \frac{\partial}{\partial x_m} \overline{u_i T'} \right) \right] \right), \tag{4.21}$$

It is interesting to note that neglecting both terms the convection and second-order products and introducing the buoyancy effects, (4.21) reduces to the equation proposed by Launder (1975) in his study of free shear flows under gravitational effects. Zeman and Lumley (1976) when modelling buoyancy driven mixed layers also found a similar equation to (4.21). In their approach Zeman and Lumley neglected the convection term and included buoyancy effects in the triple correlations; buoyancy effects being a major considering in atmospheric flows which were their particular concern.

When we introduce the boundary layer approximations (4.8) and (4.9), a further simplification of (4.21) for two-dimensional flows is obtained, namely,

$$\frac{D}{Dt}(\overline{u_y T'}) = -\overline{u_y^2}\frac{\partial T}{\partial y} - C_{UT1}\frac{\varepsilon}{E_o}\overline{u_y T'} + \frac{\partial}{\partial y}\left(C_{UT2}\frac{E_o}{\varepsilon}2\overline{u_y^2}\frac{\partial}{\partial y}\overline{u_y T'}\right) . \tag{4.22}$$

Obviously, as we are interested only in the convective heat flux component $\overline{u_y T'}$, terms containing α do not appear in (4.22), because the relation $\frac{\partial U_y}{\partial x_m}$ is negligible in boundary layer approximations. Terms containing α will appear when the equation for $\overline{u_x T'}$ is derived (this is the case, for example, in shear flows with buoyancy effects where the term $\overline{u_x T'}$ is important).

As was previously mentioned, nearly all experimental work suggests a linear relationship between normal shear stresses and turbulence energy. This was expressed in (3.3) and takes the form

$$\overline{u_y^2} = \alpha_2 E_o \quad . \tag{3.3}$$

Finally, substituting (3.3) in (4.22) and rearranging the terms one finds

$$\frac{D}{Dt}(\overline{u_y T'}) = \frac{\partial}{\partial y}\left(C_{UT2}\frac{E_o^2}{\varepsilon}\frac{\partial}{\partial y}(\overline{u_y T'})\right) - C_{UT1}\frac{\varepsilon}{E_o}\overline{u_y T'} - \alpha_2 E_o \frac{\partial T}{\partial y} . \tag{4.23}$$

Equation (4.23) is an approximate, differential equation for the convective heat flux as a function of known dependent variables and with 3 constants C_{UT1}, C_{UT2} and α_2. The constants will be evaluated later.

4.1.3 Equation for the intensity of temperature fluctuation.

Although (4.12) and (4.23), together with the purely hydrodynamic equations form a closed system, we also introduce and solve the equation for the intensity of temperature fluctuation ($\frac{1}{2}\overline{T'^2}$). A knowledge of this term, which is very similar to the turbulence energy, permits the determination of important correlations between heat and momentum. Also, this term may be needed for future developments of the model, for example, in the study of shear flows with buoyancy effects. In the later, the convective heat flux equation contains the term $\frac{1}{2}\overline{T'^2}$, thus, a transport equation for the intensity of temperature fluctuation will be needed.

An equation for $\frac{1}{2}\overline{T'^2}$ is easily obtained by multiplying the equation for conservation of thermal energy (4.1) (neglecting the dissipation term) by the temperature fluctuation T', and averaging. This yields

$$\underset{(I)}{\frac{D}{Dt}\left(\overline{\tfrac{1}{2}T'^2}\right)} = \underset{(II)}{\gamma\frac{\partial^2}{\partial x_i \partial x_i}\left(\overline{\tfrac{1}{2}T'^2}\right)} - \underset{(III)}{\overline{u_k T'}\frac{\partial T}{\partial x_k}} - \underset{(IV)}{\frac{\partial}{\partial x_k}\left(\overline{\tfrac{1}{2}T'^2 u_k}\right)} \underset{(V)}{-\gamma\left(\overline{\frac{\partial T'}{\partial x_k}}\right)^2}. \tag{4.24}$$

Terms in (4.24) have a similar meaning to the terms in the turbulence energy equation, specifically,

Term I - Advection (or convection), represents the rate of change in the intensity of temperature fluctuation.

Term II+V- Dissipation of fluctuating intensity by heat conduction (molecular dissipation).

Term III - Production of fluctuating intensity of temperature by turbulent flux of heat along the gradient of mean temperature.

Term IV - Turbulent diffusion of fluctuating intensity of temperature.

Equation (4.24) has only two terms which are not functions of any of the main dependent variables. These are terms IV and V, therefore, only these two need be approximated.

4.1.3.1 Dissipation of fluctuating intensity, term V.

Let ε_T represent the dissipation term in (4.24). Thus,

$$\varepsilon_T = \gamma \overline{\left(\frac{\partial T'}{\partial x_k} \right)^2} \qquad (4.25)$$

is the rate of dissipation of temperature intensity fluctuation and, in the subject of heat fluctuations, plays the same role as ε does for velocity fluctuations. Townsend (1976) proposed that the dissipation rate ε_T should be proportional to $\overline{T'^2}$ and $E_o^{1/2}$, thus, we may assume

$$\varepsilon_T = \overline{T'^2} \cdot \frac{E_o^{1/2}}{L_T} \quad , \qquad (4.26)$$

where, L_T is a length-scale determined by the large-scale properties and is similar in magnitude to the dissipation length-scale L_d defined in expression (2.7). Following Townsend (1976), we assume,

$$L_T = b.L_d \qquad (4.27)$$

where, b is a constant. Now, using the relationships (4.26), (4.27) and (2.7), the dissipation rate of temperature intensity fluctuation becomes

$$\varepsilon_T = C_{TT1} \frac{\varepsilon}{E_o} \left(\overline{\tfrac{1}{2}T'^2}\right) \quad , \tag{4.28}$$

where, C_{TT1} is a new constant given by

$$C_{TT1} = \frac{2}{b.C_D} \quad . \tag{4.29}$$

4.1.3.2 Turbulent convection, term IV.

The other term in (4.24) needing approximation is the turbulent diffusion term $\frac{\partial}{\partial x_k}\left(\overline{\tfrac{1}{2}T'^2 u_k}\right)$. We will assume that $\overline{\tfrac{1}{2}T'^2 u_k}$ is proportional to the gradient of the fluctuating intensity of temperature, i.e.

$$\overline{\tfrac{1}{2}T'^2 u_k} \propto \frac{\partial}{\partial x_k}\left(\overline{\tfrac{1}{2}T'^2}\right) \quad . \tag{4.30}$$

Then, by purely dimensional analysis, (4.30) becomes

$$\overline{\tfrac{1}{2}T'^2 u_k} = - C_{TT2} \frac{E_o^2}{\varepsilon} \frac{\partial}{\partial x_k}\left(\overline{\tfrac{1}{2}T'^2}\right) \quad , \tag{4.31}$$

where, C_{TT2} is a constant and E_o^2/ε may be interpreted as the product of a velocity-scale and a length-scale.

4.1.3.3 Approximate equation for two-dimensional intensity of temperature fluctuation.

Introducing the approximations represented by (4.28), (4.31) and rearranging the terms, (4.24) becomes

$$\frac{D}{Dt}\overline{(\tfrac{1}{2}T'^2)} = \frac{\partial}{\partial x_i}\left[(\gamma + C_{TT2}\frac{E_o^2}{\varepsilon})\frac{\partial}{\partial x_i}\overline{(\tfrac{1}{2}T'^2)}\right] - \overline{u_k T'}\frac{\partial T}{\partial x_k} - C_{TT1}\frac{\varepsilon}{E_o}\overline{(\tfrac{1}{2}T'^2)} \quad . \tag{4.32}$$

If we neglect convection and diffusion terms, the equation (4.32) becomes

$$\overline{T'^2} = -\frac{2}{C_{TT1}}\cdot\frac{E_o}{\varepsilon}\overline{u_k T'}\frac{\partial T}{\partial x_k} \quad , \tag{4.33}$$

which is the relation proposed by Launder (1975). Also, if we use the dissipation term (ε_T) in its original form (4.25), neglect the convection term and also neglect the molecular effect on the diffusion, (4.32) becomes the equation proposed by Zeman and Lumley (1976).

In their model, Zeman and Lumley (1976) developed a transport equation for ε_T, instead of using an approximation similar to (4.28). Naturally, their procedure increases the computing time. Also, the closure of a transport equation for ε_T is achieved by using such crude approximations that its contribution to increasing the accuracy in predicting $\overline{\frac{1}{2}T'^2}$ is very small. Therefore, we regard approximation (4.28) as the most suitable for our calculations.

For a two-dimensional flow with movement predominantly in the x-direction, the boundary layer approximations (4.8) and (4.9) are applicable. As a consequence, (4.32) becomes

$$\frac{D}{Dt}\overline{(\tfrac{1}{2}T'^2)} = \frac{\partial}{\partial y}\left[(\gamma + C_{TT2}\frac{E_o^2}{\varepsilon})\frac{\partial}{\partial y}\overline{(\tfrac{1}{2}T'^2)}\right] - \overline{u_y T'}\frac{\partial T}{\partial y} - C_{TT1}\frac{\varepsilon}{E_o}\overline{(\tfrac{1}{2}T'^2)}. \tag{4.34}$$

A final comment about the inclusion of the molecular diffusion term $\gamma \frac{\partial^2}{\partial y^2}(\overline{\frac{1}{2}T'^2})$ seems in order. We recognize the small influence of this term and, like many other molecular effects, it should perhaps be ignored, but as we retain similar terms in the equations for turbulence energy, shear stress and dissipation, in order to maintain the same level of closure, it seems appropriate also to retain this term in the intensity of temperature fluctuation equation.

4.1.4 The final form of the turbulent model.

The thermal set of equations just developed, together with the three-equation model, form the new five-equation model of turbulence. Thus, summarizing, the equations which represent the new model of turbulence are:

1) Mean momentum equation

$$\frac{D}{Dt}U_x = \frac{\partial}{\partial y}(\nu\frac{\partial U_x}{\partial y} - \overline{u_x u_y}) - \frac{1}{\rho}\frac{dp}{dx} \qquad (2.1)$$

2) Turbulence energy equation

$$\frac{D}{Dt}E_o = \frac{\partial}{\partial y}\left[(\nu + C_e\frac{E_o^2}{\epsilon})\frac{\partial E_o}{\partial y}\right] - \overline{u_x u_y}\frac{\partial U_x}{\partial y} - \epsilon \qquad (2.6)$$

3) Shear stress equation

$$\frac{D}{Dt}(\overline{u_x u_y}) = \frac{\partial}{\partial y}\left[(\nu + C_s\frac{E_o^2}{\epsilon})\frac{\partial}{\partial y}(\overline{u_x u_y})\right] - C_{s2}(C_{s1}E_o\frac{\partial U_x}{\partial y} + \epsilon\frac{\overline{u_x u_y}}{E_o}) \qquad (2.14)$$

4) Dissipation of turbulence energy equation

$$\frac{D}{Dt}\varepsilon = \frac{\partial}{\partial y}\left[\left(\nu + C_\varepsilon \frac{E_o^2}{\varepsilon}\right)\frac{\partial \varepsilon}{\partial y}\right] - C_{\varepsilon 1}\varepsilon\frac{\overline{u_x u_y}}{E_o}\cdot\frac{\partial U_x}{\partial y} - C_{\varepsilon 2}\frac{\varepsilon^2}{E_o} \quad (2.13)$$

5) Mean temperature equation

$$\frac{D}{Dt}T = \frac{\partial}{\partial y}\left(\gamma\frac{\partial T}{\partial y} - \overline{u_y T'}\right) \quad (4.12)$$

6) Convective heat flux equation

$$\frac{D}{Dt}(\overline{u_y T'}) = \frac{\partial}{\partial y}\left(C_{UT2}\frac{E_o^2}{\varepsilon}\frac{\partial}{\partial y}(\overline{u_y T'})\right) - C_{UT1}\frac{\varepsilon}{E_o}\overline{u_y T'} - \alpha_2 E_o \frac{\partial T}{\partial y} \quad (4.23)$$

7) Intensity of temperature fluctuation equation

$$\frac{D}{Dt}(\overline{\tfrac{1}{2}T'^2}) = \frac{\partial}{\partial y}\left[\left(\gamma^* + C_{TT2}\frac{E_o^2}{\varepsilon}\right)\frac{\partial}{\partial y}(\overline{\tfrac{1}{2}T'^2})\right] - \overline{u_y T'}\frac{\partial T}{\partial y} - C_{TT1}\frac{\varepsilon}{E_o}(\overline{\tfrac{1}{2}T'^2}) \quad (4.34)$$

Hanjalic (1970) and Hanjalic and Launder (1972b) give suitable values for constants C_s, C_{s1}, C_{s2}, C_e, C_ε, $C_{\varepsilon 1}$ and $C_{\varepsilon 2}$ as shown in table 2.1 . Also, a comprehensive study on the influence of varying these constants was made in section 3.1 . Our next step is to determine the constants C_{UT1}, C_{UT2}, C_{TT1}, C_{TT2} and α_2 which appear in the thermal equations.

4.2 Evaluation of constants in the convective heat flux and intensity of temperature equations.

4.2.1 The constants C_{UT1}, C_{TT1} and α_2.

The constants C_{UT1}, C_{TT1} and α_2 can be found to

within narrow limits, provided that the set of equations summarized in section 4.1.4 satisfies the experimental data for simple turbulent flows. In this evaluation we use a similar process to that adopted by Launder (1975).

Firstly, C_{TT1} is determined by considering a grid-generated turbulent flow. In this kind of flow, the production term is zero and the diffusion terms are negligible. Thus, the turbulence energy equation (2.6) and the intensity of temperature fluctuation (4.34) become, respectively,

$$\frac{D}{Dt}E_o = U_x \frac{dE_o}{dx} = -\varepsilon \qquad (4.35)$$

and,

$$\frac{D}{Dt}(\overline{\tfrac{1}{2}T'^2}) = U_x \frac{d}{dx}(\overline{\tfrac{1}{2}T'^2}) = -C_{TT1}\frac{\varepsilon}{E_o}(\overline{\tfrac{1}{2}T'^2}) \quad . \qquad (4.36)$$

Substituting (4.35) in (4.36) and rearranging the terms, we have

$$\frac{1}{(\overline{\tfrac{1}{2}T'^2})} \cdot \frac{d}{dx}(\overline{\tfrac{1}{2}T'^2}) = C_{TT1}\frac{1}{E_o} \cdot \frac{dE_o}{dx} \quad . \qquad (4.37)$$

Following the work of Gibson and Schwarz (1963), Launder (1975) assumed that $\overline{T'^2}$ varies inversely as the power 1.5 of distance behind the grid, i.e.,

$$\overline{\tfrac{1}{2}T'^2} = A.x^{-1.5} \quad , \qquad (4.38)$$

where, A is a constant. Leslie (1975) recommends that the grid turbulence energy decays like $x^{-1.0}$, i.e.,

$$E_o = B.x^{-1.0} \quad , \qquad (4.39)$$

where, B is a constant. Relations (4.38) and (4.39) yield, respectively,

$$\frac{1}{\frac{1}{2}\overline{T'^2}} \cdot \frac{d}{dx}\left(\frac{1}{2}\overline{T'^2}\right) = -1.5\ x^{-1} \qquad (4.40)$$

and,

$$\frac{1}{E_o} \cdot \frac{dE_o}{dx} = -\ 1.0\ x^{-1} \quad . \qquad (4.41)$$

Thus, substituting (4.40) and (4.41) in (4.37) we obtain

$$C_{TT1} = 1.5 \quad . \qquad (4.42)$$

The values for the other constants C_{UT1} and α_2 are found using the experimental data for nearly homogeneous shear flows, in connection with the equations for convective heat flux and intensity of temperature fluctuation. For nearly homogeneous flow, both equations have the convection and diffusion terms very small and they can be neglected. Thus, from (4.23) and (4.34) we have, respectively,

$$C_{UT1}\ \frac{\epsilon}{E_o}\ \overline{u_y T'} = -\ \alpha_2 E_o\ \frac{\partial T}{\partial y} = -\ \overline{u_y^2}\ \frac{\partial T}{\partial y} \qquad (4.43)$$

and,

$$\overline{u_y T'}\ \frac{\partial T}{\partial y} = -\ C_{TT1}\ \frac{\epsilon}{E_o}\left(\frac{1}{2}\overline{T'^2}\right) \quad . \qquad (4.44)$$

Substituting the mean temperature gradient $\frac{\partial T}{\partial y}$ from (4.44) into (4.43) and rearranging the terms, we have

$$C_{UT1} = \frac{1}{2} \cdot C_{TT1}\ \frac{(\overline{u_y^2})(\overline{T'^2})}{(\overline{u_y T'})^2} \quad . \qquad (4.45)$$

From the experimental data of Webster (1964), the correlation between fluctuating quantities $(\overline{u_y T'})^2/((\overline{u_y^2})(\overline{T'^2}))$ is, approximately, 0.2 . Introducing this value and the value

suggested for C_{TT1} into (4.45), we obtain

$$C_{UT1} = 3.75 \quad . \tag{4.46}$$

The constant α_2, defined in (3.3), is also evaluated from the experiments in nearly homogeneous shear flows. Champagne et al. (1970) found $\alpha_2 \cong 0.49$. Webster (1964), with a similar kind of flow, but with temperature variation, found α_2 varying from 0.4 to 0.6, depending on the Richardson number. Here we will adopt the mean of the values, that is

$$\alpha_2 = 0.5 \, . \tag{4.47}$$

4.2.2 The constants C_{UT2} and C_{TT2}.

For nearly homogeneous shear flows, the diffusion and convection terms appearing in the shear stress equation (2.14) can be neglected, thus

$$C_{s1} E_o \frac{\partial}{\partial y} U_x = - \frac{\varepsilon}{E_o} \overline{u_x u_y}$$

or, what is equivalent,

$$\frac{\overline{u_x u_y}}{\frac{\partial U_x}{\partial y}} = - C_{s1} \frac{E_o^2}{\varepsilon} \quad . \tag{4.48}$$

The inspection of equations (4.23) for $\overline{u_y T'}$ and (4.34) for $\frac{1}{2}\overline{T'^2}$ shows that the coefficients of the diffusion terms, C_{UT2} and C_{TT2}, are proportional to E_o^2/ε . So, according to (4.48), the diffusion constants C_{UT2} and C_{TT2} are proportional to C_{s1}, too. Ratios C_{s1}/C_{UT2} and C_{s1}/C_{TT2} are

identified as the effective Prandtl-Schmidt numbers. As Patankar and Spalding (1970) reported, effective Prandtl-Schmidt numbers are around unity for most of the confined flows. For free turbulent flows it seems that these numbers are lower (~ 0.07). In our computations we use ratios $C_{sl}/C_{UT2} = 1$ and $C_{sl}/C_{TT2} = 1$. Table 4.1 summarizes the values assigned to the constants in the thermal model.

Table 4.1 Empirical constants used in thermal model.

C_{UT1}	C_{TT1}	α_2	C_{sl}	$\frac{C_{sl}}{C_{UT2}}$	$\frac{C_{sl}}{C_{TT2}}$
3.75	1.5	0.5	0.07	1	1

4.3 Flows studied and description of the solution procedure used.

4.3.1 Flows studied.

For the purpose of testing the complete model of turbulence just described, as well as for showing the capability and universality of the model, several types of turbulent flows are considered:

a) Annular turbulent flow.

b) Pipe turbulent flow.

c) Boundary layer on a flat-plate.

d) Plane mixing layer (with and without stagnant surroundings).

e) Plane jet in stagnant surroundings.

For each type of flow, the set of 7 simultaneous equations, (2.1), (2.6), (2.14), (2.13), (4.12), (4.23) and (4.34), is solved numerically. The complexity of the calculations is such that, of course, the aid of a high-speed computer is essential.

4.3.2 Solution procedure.

The solution method employed is based on the finite-difference procedure developed by Patankar and Spalding (1970), already referred to in section 2.6 . The method is summarized in Appendix - 3. The computer program developed by the author to solve the three-equation model (and the other models developed in Chapter - 2) is expanded in order to solve the additional equations of the thermal model. One single program solves all the 5 flows listed in section 4.3.1 . Each type of flow is specified by a series of geometrical parameters and indices in the input data to the program. Initial profiles of the dependent variables and the specification of boundary conditions are described in the following section.

4.3.2.1 Boundary conditions for dependent variables.

The flows considered are a combination of two of the

following boundaries:

(i) Wall boundary.

(ii) Free stream boundary.

(iii) Symmetric boundary.

Boundary conditions for the variables U_x, E_o, ϵ and $\overline{u_x u_y}$ are the same as specified by Hanjalic and Launder (1972). The boundary conditions for the heat transfer variables T, $\overline{u_y T'}$ and $\frac{1}{2}\overline{T'^2}$, for each one of the boundary types, are specified below.

(i) Wall boundary.

Boundary conditions for mean temperature, convective heat flux and intensity of temperature fluctuation, in a region near a wall can be deduced by using the approximations of one-dimensional Couette flow. The boundary condition for $\overline{u_y T'}$ is given by the mean temperature equation applied to Couette flow, which is

$$\left[\overline{u_y T'}\right]_C = - \frac{\dot{q}''}{\rho c_p} \qquad (4.49)$$

where, subscript C denotes the condition at the edge of the viscous sublayer where the Couette flow approximation is still valid. Consequently, for wall boundary layers, the conditions are actually applied "near" the wall.

Boundary conditions for the intensity of temperature fluctuation follow directly from the intensity equation (4.34), after neglecting convection terms and diffusion terms, thus we

can write,

$$\left[\overline{\tfrac{1}{2}T'^2}\right]_C = -\frac{1}{C_{TT1}}\left[\frac{E_o}{\varepsilon}\,\overline{u_y T'}\,\frac{\partial T}{\partial y}\right]_C \quad . \tag{4.50}$$

The boundary condition for the temperature "near" the wall can be established by using well-known empirical functions. The logarithmic law (or law of the wall) for the temperature profiles provides the means for fixing the mean temperature at the edge of the viscous sublayer. The temperature logarithmic law, for smooth walls, at the edge of the viscous sublayer is represented by

$$\theta^+ = \frac{c_p(T_C - T_S)\rho\, u_\tau}{\dot{q}''} = B_T(Pr) + B\,\ln\left(\frac{y_C\, u_\tau}{\nu}\right) \tag{4.51}$$

where, subscript S denotes conditions at wall, y_C is the distance from the wall to the edge of the viscous sublayer, $B_T(Pr)$ and B are constants which depend on the type and thermal condition of wall surface.

Spalding (1964) surveyed the experimental data and recommended for smooth walls $B_T(Pr) = 3.3$ and $B = 2.22$. In order to better specify the condition of the fluid and type of wall, most workers have preferred to resolve $B_T(Pr)$ as

$$B_T(Pr) = B_s + G(Pr) \quad . \tag{4.52}$$

Where, B_s is a constant accounting for the type of wall and G(Pr) is a function which accounts for the condition of the fluid. For smooth walls B_s is usually taken equal to 5.5 . Many relations for G(Pr) have been proposed, for example, Leslie and Hassid (1973) used a correction in the von Karman

analogy and computed the function G(Pr). Their results are tabulated as a function of the Prandtl number. Another proposed form for G(Pr), also based on the von Karman analogy, is

$$G(Pr) = 5(Pr - 1) + 5\cdot\ln\left[1 + \frac{5}{6}(Pr - 1)\right] \quad . \qquad (4.53)$$

Our calculations are performed for a fluid with $Pr=0.7$. This value of Pr introduced in (4.53) and (4.52) gives $B_T(Pr)=2.56$. Introducing Leslie and Hassid (1973) results in (4.52) the value $B_T(Pr)=2.63$ is obtained. We adopt $B_T(Pr)=2.9$ which gives the most accurate predictions in our numerical calculations. The other constant, B, which appears in (4.51) is taken equal to 2.5 , following most other authors.

For rough walls, the temperature law of the wall is conventionally represented as

$$\theta^+ = B_{rT}(e^+,Pr) + B\cdot\ln(\frac{y_C}{e}) \quad . \qquad (4.54)$$

Where, $B_{rT}(e^+,Pr)$ is a function which describes the conditions of the wall. This function is not so easily found as $B_T(Pr)$ since there is greater disagreement between the experimental data. Several relations for $B_{rT}(e^+,Pr)$ have been proposed. The one considered the best is that due to Dipprey and Sabersky (1963) who found experimentally the relationship (valid in the 'fully rough' region ($e^+ \geq 70$)).

$$B_{rT}(e^+,Pr) = 5.19(e^+)^{0.2}Pr^{0.44} \quad , \qquad (4.55)$$

where, $$e^+ = Re\cdot(\frac{f}{2})^{\frac{1}{2}}\cdot\frac{e}{De} \quad . \qquad (4.56)$$

(ii) Free boundary.

At the free-stream edge, the boundary condition must be the same as the undisturbed surrounding flow condition, that is,

$$T = T_G \tag{4.57}$$

and

$$\left[\overline{u_y T'}\right]_G = 0 \quad . \tag{4.58}$$

Where, subscript G denotes evaluation of variables at the edge of the free boundary. The condition for the intensity of temperature fluctuation is established by the degenerate form of the intensity of temperature equation (4.34), which is

$$U_G \frac{d}{dx}\left(\overline{\tfrac{1}{2}T'^2}\right)_G = - C_{TT1} \frac{\varepsilon_G}{E_{oG}} \left(\overline{\tfrac{1}{2}T'^2}\right)_G \quad . \tag{4.59}$$

(iii) Symmetry axis.

When the boundary layer is a symmetric axis, the boundary conditions for the convective heat flux and intensity of temperature fluctuation are, respectively,

$$\overline{u_y T'} = 0 \tag{4.60}$$

and

$$\frac{\partial}{\partial y}\left(\overline{\tfrac{1}{2}T'^2}\right) = 0 \quad . \tag{4.61}$$

4.3.2.2 Initial profiles of dependent variables.

In addition to the boundary conditions, profiles for dependent variables at the beginning of the step by step procedure are also needed. At the starting point, the mean

temperature is assumed constant, the intensity of temperature fluctuation is assumed uniform and proportional to the mean temperature and, finally, the convective heat flux is set equal to zero. It is perhaps worth emphasizing here that the types of flow considered in this chapter are self-preserving or equilibrium flows, and the initial profiles do not have a significant effect on the flow downstream.

4.4 Discussion of results.

4.4.1 Turbulent annular flow.

The complete model of turbulence, combining hydrodynamic and thermal effects (from now on called five-equation model), is applied to an annular flow under a number of wall conditions. We will give only the results for the case of smooth annuli heated (or cooled) on the inner side while the outer side is insulated. The fluid used is air with a Prandtl number equal to 0.7 , and the maximum temperature difference inside the channel (θ_{MAX}) is 30 ^{o}C. Numerical calculations are performed using a non-uniform grid with 60 points. The dynamical equations are solved using the set of constants given in table 2.1 . In order to verify the sensitivity of the thermal quantities to changes in the constants, the constants C_{UT1} and C_{TT1} were varied in a range of values around the calculated values shown in table 4.1 . C_{UT1} and C_{TT1} were varied from 2.5 to 4.0 and from 1.0 to 2.0, respectively. Very small differences were observed in the results, therefore, the values

of the constants assigned in table 4.1 are retained. Results for smooth annuli are shown in figures 4.1 to 4.12 .

Temperature (θ/θ_{MAX}) and velocity (U/U_{MAX}) profiles are plotted in figure 4.1 . Here, θ stands for the difference between the temperature at the internal wall and the temperature at a given point in the fluid,

i.e. $$\theta = \left| T_{si} - T(r) \right| \quad . \tag{4.62}$$

And therefore,

$$\theta_{MAX} = \left| T_{si} - T_M \right| \tag{4.63}$$

where, T_{si} is the temperature at the internal wall and T_M is the minimum (or maximum) fluid temperature when the fluid is heated (or cooled). The velocity profile shown in figure 4.1 is compared with the experimental results of Lawn (1970), and our predictions agree very well. Since we use a fluid with Pr=0.7, the temperature distribution should lie below the velocity distribution, although they should be close to one another. As can be seen in figure 4.1, when the internal wall is cooled (or heated), the velocity and temperature profiles are not too close; this is because the velocity is much more sensitive to the influence of the small radius ratio, while the temperature is almost unaffected by the radius ratio, although as we will see later, the heat transfer coefficient is slightly affected by the radius ratio. But, when the conditions of heating are changed, i.e., when the internal wall is insulated and the external wall cooled (or heated), velocity and temperature show a much closer agreement, as is also shown in figure 4.1 .

Temperature and velocity profiles in the non-dimensional forms θ^+ and u^+ are plotted in figure 4.3 . All results are referred to the internal wall. Velocity profile is compared with the experimental results of Knudsen and Katz (1958) for annuli with small radius ratio. As can be seen, our results are well inside the range of Knudsen and Katz annular measurements. The temperature profile is compared with two relationships: one proposed by Spalding (1964) and the other is deduced from the results of Leslie and Hassid (1973). The relationship proposed by Spalding (1964) is based on the results of a number of experiments. He proposes the relation

$$\theta_i^+ = 3.3 + 2.22 \ln y_i^+ \quad . \tag{4.64}$$

Using the results obtained by Leslie and Hassid (1973) we can find a new relation for θ_i^+. For a smooth wall $B_s=5.5$ and from Leslie and Hassid with $Pr=0.7$ we get $G(Pr)=-2.87$, thus (4.52) gives $B_T(Pr)=2.63$. Hence, with $B=2.5$, (4.51) becomes

$$\theta_i^+ = 2.63 + 2.5 \ln y_i^+ \quad . \tag{4.65}$$

Relations (4.64) and (4.65) are also plotted in figure 4.3 . As we can see, our results compare well with both relationships.

The shear stress and convective heat flux profiles are shown in figure 4.2 . The shear stress distribution is in good agreement with the Lawn (1970) experimental results. The extreme difficulty of measuring fluctuating temperature correlations is the responsible for the lack of experimental results in this field of study. Thus our predictions cannot be compared with experimental data. Nevertheless, we can see in

figure 4.2 the similarity between shear stress and convective heat flux profiles, which confirms the assumption at the heart of all analogies between momentum and heat transfer.

The distributions of turbulence energy and intensity of temperature fluctuation are shown in figure 4.4 . The ratios shear stress/turbulence energy and convective heat flux/(intensity of temperature fluctuation x turbulence energy) are plotted in figure 4.5 . In both figures, the exclusively dynamic correlations are in good agreement with the Lawn (1970) experimental results for smooth annulus. Although there is no available experimental data to corroborate our theoretical results for the heat transfer correlations shown in figures 4.4 and 4.5 , it seems that our distributions represent well the physical behaviour of the intensity of temperature fluctuation and convective heat flux ratio.

The balances of turbulence energy and intensity of temperature fluctuation, in terms of each component (production, dissipation and diffusion), are plotted in figures 4.6 and 4.7 , respectively. The turbulence energy terms agree well with the measured values of Lawn (1970). In figure 4.7 , the same kind of behaviour,as shown in figure 4.6 for the energy , is displayed by the components of the intensity of temperature fluctuation.

Figure 4.8 shows the comparison of our results for the intensity of temperature fluctuation ($\sqrt{\overline{T'^2}}/T_s$) with the

experimental measurements of Nicholl (1970) for channel flow. In the region very near the wall, where the laminar sublayer still has influence, the experimental values are larger than ours. But inside the logarithmic region both theory and experiment are much closer and acceptable, considering the different heating conditions. Nicholl's results were obtained with θ_{MAX}=80 ^{o}C and under the influence of buoyancy, while our results are obtained for a θ_{MAX}=30 ^{o}C and no buoyancy effects are considered.

Another interesting parameter in convective heat flows is the relation between the eddy diffusivities of heat and momentum. The eddy diffusivity for momentum (ν_T) is defined by

$$-\overline{u_x u_y} = \frac{\mu_T}{\rho}\frac{\partial}{\partial y}U_x = \nu_T \frac{\partial}{\partial y}U_x \quad . \tag{4.66}$$

The counterpart for heat, the eddy diffusivity for heat (γ_T) is defined by

$$-\rho c_p \overline{u_y T'} = k_T \frac{\partial T}{\partial y} \tag{4.67}$$

or, what is equivalent,

$$-\overline{u_y T'} = \frac{k_T}{\rho c_p}\frac{\partial T}{\partial y} = \gamma_T \frac{\partial T}{\partial y} \quad . \tag{4.68}$$

Thus the diffusivity ratio (γ_T/ν_T) is

$$\frac{\gamma_T}{\nu_T} = \frac{\overline{u_y T'}}{\overline{u_x u_y}} \cdot \frac{\frac{\partial}{\partial y}U_x}{\frac{\partial}{\partial y}T} \quad . \tag{4.69}$$

The inverse of the diffusivity ratio is commonly called turbulent Prandtl number (Pr_t).

In most work on heat transfer it is assumed that $\gamma_T/\nu_T=1$, even though experimental investigation has shown that this assumption is not true. The diffusivity ratio depends on the type of flow, Reynolds number and geometry of the channel. Townsend (1976) states that the diffusivity ratio can vary between 1.0 for large strains and 2.5 for small strains. In figure 4.9 we show our predicted diffusivity ratio for an annulus with small radius ratio. The ratio γ_T/ν_T is calculated using (4.69) with the distributions for shear stress, convective heat flux, temperature gradient and velocity gradient obtained from the five-equation model. As we can see in figure 4.9 , the diffusivity ratio varies from 1.5 near the inner wall to 2.1 in the region of maximum velocity, corroborating the experimental results.

Finally, the heat transfer coefficients, in terms of Nusselt numbers, are compared in figures 4.10 to 4.12 . Nusselt numbers with respect to the heated (or cooled) inner side of an annulus are shown in figure 4.10 . Our predictions with the five-equation model for the case of constant wall temperature are compared with the experimental results of Quarmby and Anand (1970). The theoretical and experimental results are in fairly good agreement. As can be observed, the Nusselt number increases slightly with decreasing radius ratio. Figure 4.11 shows results for a different cooling arrangement. Here the external wall is cooled with constant temperature and the internal wall is insulated. Our predictions for the external Nusselt number (Nu_o) as a function of Reynolds number and radius ratio are shown in figure 4.11 . Our results are again

compared with the corresponding data of Quarmby and Anand(1970) which were obtained experimentally under similar conditions. Again, theory and experiment agree quite well. It is worth noting that in this configuration the external Nusselt number is nearly independent of the radius ratio.

In order to establish the influence of the type of cooling on the wall, we considered a case in which the wall temperature changes step by step (this configuration is equivalent to the case when wall heat flux is constant). We study an annular flow with two different radius ratios, $R^*=0.2$ and $R^*=0.5$. The internal wall temperature is increased linearly from the entrance of the channel to the exit of the channel. The difference of wall temperature from entrance to exit is taken to be 30 ^{o}C. Results for internal Nusselt number as a function of the Reynolds number and radius ratio are plotted in figure 4.12 . Our predictions are compared with the experimental measurements of Kays and Leung (1963) and with the experimental correlation based on the experiments of Quarmby (1967) which is

$$\log Nu = - K_1 + 0.706 \log(Re) \qquad (4.70)$$

where,

$$\log K_1 = 0.1658 - 0.1056 \log(R_o/R_i) \; . \qquad (4.71)$$

As can be seen in figure 4.12, the agreement between our predictions and the experiments is quite good. Comparing the results of figure 4.12 with those of figure 4.10, we see that for the same radius ratio and same Reynolds number, the Nusselt number is slightly higher when the wall heat flux is

constant (fig.4.12) than when the wall temperature is constant (fig. 4.10), which corroborates the experimentally observed result.

4.4.2 Turbulent pipe flow.

The second flow studied is the turbulent pipe flow. Both smooth and rough geometries are considered. The fluid is air and the wall temperature is assumed constant. The maximum difference of temperature between fluid and wall is 30 ^{o}C. Our predictions with the five-equation model are presented in figures 4.13 to 4.17 .

Temperature profiles (θ/ϑ_{MAX}) in a smooth pipe are shown in figure 4.13 . Our predictions are compared with the experimental results of Seban and Shimazaki (1951) which were also obtained for a pipe flow with constant wall temperature. Our results are also compared with the theoretical results obtained by using Martinelli's analogy, as described by Knudsen and Katz (1958). As can be seen in figure 4.13, the results from the Martinelli's analogy are higher than the experimental results in the logarithmic region. The agreement between our predictions and the experimental data is better although our results are slightly larger in the log region. In figure 4.14, velocity and temperature in the non-dimensional forms (u^+ and θ^+) are compared with experimental correlations. Velocity profile is compared with the law of the wall for smooth surfaces, represented by

$$u^+ = B_s + B \ln(y^+) \quad . \tag{4.72}$$

Spalding (1961b) and Kestin and Richardson (1963) surveyed the experimental relations proposed for the law of the wall in smooth surfaces. From the results they included in their review, we take as representative values $B_s=5.5$ and $B=2.5$. The comparison between predicted u^+ and correlation (4.72) shows a fairly good agreement. The temperature profile is compared with (4.65), which was proposed by Leslie (1977), and with (4.64), which was proposed by Spalding (1964). Our results, as shown in figure 4.14, lie between these two sets of results, which indicates the validity of our theoretical model.

Friction factors and Stanton numbers are compared in figure 4.15 . Our calculated friction factors agree quite well with the results from Blasius' formula (3.36). For Stanton numbers, several relations both empirical and semi-empirical have been proposed. All these relations are based on some kind of analogy between heat and momentum. Leslie and Hassid (1973) working with exact equations rather than approximations, and using an improved velocity profile ($u^+=f(y^+)$), developed a relationship applicable to moderate Prandtl numbers. For smooth pipes, they recommend the relation:

$$\frac{1}{St} = \frac{2}{f} + \sqrt{\frac{2}{f}}\, G(Pr) + P + \sqrt{\frac{f}{2}}\, Q \quad , \tag{4.73}$$

where, $P=18.2$ and $Q=15.5$ for pipe flow and $G(Pr)$ is the function introduced in (4.52), $G(Pr)=-2.87$ for $Pr=0.7$. The Stanton numbers given by our model and by (4.73) are compared in figure 4.15 . The results given by the two methods can be

seen to be in good agreement.

Analogies between heat and momentum transfer made by previous workers have been quite successful in predicting heat transfer from smooth surfaces. But they have not been so successful when applied to the much more complex problem of turbulent heat transfer in rough pipes. In order to test the capability of the five-equation model to solve a flow with rough walls, we considered the case of pipe flow with sand-roughening. The roughness ratio (D/e) is taken equal to 200 and the Reynolds number ~~is~~ equal to 1.0×10^5. The results of the calculated velocity and temperature profiles are shown in figure 4.16 . The velocity distribution is compared with the law of the wall (3.15), with $B_r = 8.48$. As we can see, very good agreement is obtained. The temperature profile (θ^+) given by the model is compared with that given by the temperature law of the wall expression, which is

$$\theta^+ = B_{rT}(e^+, Pr) + B \ln\left(\frac{R_o - r}{e}\right) . \qquad (4.74)$$

The calculated values shown in figure 4.16 are obtained using for the boundary condition (4.54) in the five-equation model the following value of $B_{rT}(e^+, Pr)$

$$B_{rT}(e^+, Pr) = 4.70(e^+)^{0.2} Pr^{0.44} . \qquad (4.75)$$

The reason why we choose (4.75) instead of the experimental relation given by (4.55) will be made clear shortly. The comparison of predicted temperature profile obtained with the five equation model and results from (4.74), is shown in figure 4.16 . As can be seen our predictions agree quite well

with results from (4.74) using (4.75). For clarity, the θ^+ profile of (4.74) using (4.55) is not shown in figure 4.16, but this combination gives results no higher than 6% of our predictions.

Stanton numbers for rough pipes with sand roughness are shown in figure 4.17 . Continuing the work of Leslie and Hassid (1973) for smooth pipes, Leslie (1977) proposed the following, theoretically derived, relation for Stanton numbers in rough surfaces:

$$\frac{1}{St_R} = \frac{2}{f_R} + \sqrt{\frac{2}{f_R}}\left[B_{rT}(e^+,Pr) - B_r(e^+)\right] + P + \sqrt{\frac{f_R}{2}}\,Q \,, \quad (4.76)$$

where, the index R is used to indicate the rough condition. All parameters appearing in (4.76) were already described. Based on their experimental data, Dipprey and Sabersky (1963) proposed the relation

$$\frac{1}{St_R} = \frac{2}{f_R} + \sqrt{\frac{2}{f_R}}\left[B_{rT}(e^+,Pr) - B_r(e^+)\right] \,, \quad (4.77)$$

where, $B_{rT}(e^+,Pr)$ is given by (4.55). The Dipprey and Sabersky results are plotted in figure 4.17 . We solve the five-equation model using the Dipprey and Sabersky relation (4.55) as the boundary condition for the rough wall and the results obtained are also shown in figure 4.17 . As can be seen, our predictions are lower than the experimental results; the same discrepancy is observed when Leslie's expression (4.76) is used with (4.55). Therefore, using a trial technique we vary the constants in (4.55), and use this new relation as the boundary condition in our numerical calculations. The iteration is continued until our theoretical values coincide with the experimental data. The

best fit is obtained with expression (4.75). As shown in figure 4.17, in this case, the agreement is very good; using (4.75) in Leslie's relation (4.76), a good agreement is also obtained.

Since the value of $B_{rT}(e^+,Pr)$ given by (4.75), introduced as boundary condition in our five-equation model, gives the best agreement with experiment for Stanton numbers, we assume that this value also predicts more accurate temperature profile (which is the profile shown in figure 4.16). Therefore, we propose that the temperature law of the wall is better represented by (4.74) when the $B_{rT}(e^+,Pr)$ value given by (4.75) is used.

4.4.3 Flat-plate boundary layer.

The experimental results and the predictions of the five-equation model for a smooth flat-plate boundary layer are compared here. An undisturbed velocity (U_∞) equal to 40 m/s is used in all our calculations. The maximum difference of temperature between fluid and wall (θ_{MAX}) is 30 °C. Results from the five-equation model are shown in figures 4.18 to 4.24.

Velocity and temperature profiles are plotted in figure 4.18 . The velocity distribution is compared with the experimental results of Klebanoff (1955) and a good agreement is displayed. The temperature profile, as expected, is slightly lower than the velocity profile, however the shape is similar.

The non-dimensional velocity and temperature profiles are shown in figure 4.20 . The predicted u^+ profile is compared with the experimental relationships proposed by Nikuradse (1950) and Schultz-Grunow (1941). Our results agree well with the Schultz-Grunow expression and are slightly lower than the Nikuradse values. The temperature profile θ^+ is again compared with the expression (4.64), proposed by Spalding (1964) as the best representation of the thermal law of the wall. As can be seen, the predicted values are quite close to those of Spalding's expression.

The shear stress and the convective heat flux profiles are plotted in figure 4.19, while the turbulence energy and the intensity of temperature fluctuation are shown in figure 4.21 . Predictions for exclusively momentum correlations are compared with the experiments of Klebanoff (1950) and the agreement is good for nearly all the flow area. Slight departure of the predicted results from the experimental ones occurs when the free boundary region is approached. But this departure is acceptable considering that near a free boundary the flow is characterised by extreme instability and even the experimental results show an unusual degree of uncertainty in this region. Our calculated values of the convective heat flux and intensity of temperature show a similarity to the shear stress and turbulence energy, respectively.

Figure 4.22 displays the variation of shear stress/turbulence energy ratio ($\overline{u_x u_y}/E_o$). A characteristic of

turbulent flows is the approximate constancy of shear stress/ turbulence energy ratio for nearly all the area across the flow. In figure 4.22 this expected constancy is displayed by the calculated values and a good agreement with the experimental data of Klebanoff (1950) is obtained. Theoretical and experimental values for the ratio shear stress/turbulence energy in the constant region are approximately 0.28 .

One would expect a similar characteristic between the various heat transfer correlations. Thus, the convective heat flux/(turbulence energy x intensity of temperature fluctuation) ratio is also plotted in figure 4.22 . The constancy of the ratio is verified, although the heat correlations ratio is greater than the momentum correlations ratio. Townsend (1976) stated that the heat correlations ratio should be around 0.36 . Launder (1976) summarized the experimental results of this correlation and we make use of his data to produce table 4.2 . In his original summary, Launder listed the ratio $(\overline{u_y T'})^2 / (\overline{u_y^2})(\overline{T'^2})$. The transformed ratio $(\overline{u_y T'}) / (E_o)^{\frac{1}{2}} (\frac{1}{2}\overline{T'^2})^{\frac{1}{2}}$ listed in table 4.2 is obtained assuming $\overline{u_y^2} = 0.5E_o$. Although there is too large a variation among the measurements to make definite conclusions, analysing table 4.2, it seems that a value between 0.40 and 0.50 is the most likely. From our results in figure 4.22 we obtain a value of 0.45 in the constant ratio region and we note that this lies inside the range of experimental data.

Figures 4.23 and 4.24 show, respectively, the turbulence energy balance and the intensity of temperature

Table 4.2 Scalar flux correlation ratio in shear flows in local equilibrium (after Launder (1976)).

Author	$\frac{\overline{u_y T'}}{\sqrt{E_o}.\sqrt{\frac{1}{2}\overline{T'^2}}}$	Geometry
Webster (1964)	0.39-0.55	Homogeneous shear flow
Bremhorst & Bullock(1973)	0.45	Pipe flow
Bourke & Pulling (1970)	0.45	Pipe flow
Lawn & White (1972)	0.40	Pipe flow
Ibragimov et al. (1968)	0.77	Pipe flow
Arya & Plate (1969)	0.33	Smooth flat plate
Johnson (1959)	0.45	Smooth flat plate
Pimenta et al. (1975)	0.55-0.63	Rough flat plate

fluctuation balance. For the turbulence energy as shown in figure 4.23, the dissipation, production, diffusion and advection are in close agreement to the corresponding terms measured by Klebanoff (1950). The distribution of each term contained in the intensity of temperature fluctuation is shown in figure 4.24 . As can be seen, each term has a similar behaviour to the correspondent term in the turbulence energy equation. As expected, the production and dissipation terms are nearly equal at every point across the flow.

4.4.4 Plane mixing layer.

The mixing layer between two streams, initially having uniform velocities $U_{1\infty}$ and $U_{2\infty}$, is called the turbulent plane mixing layer. Cases with and without stagnant surroundings (one of the layers has zero velocity) are considered. Here we show results for two cases, one with zero velocity ratio ($U_{2\infty}=0$) and the other with velocity ratio $\frac{U_{2\infty}}{U_{1\infty}}=0.5$ In both cases, the maximum difference of temperature between the two layers is set to 30 ^{o}C. The fluid considered is air with Prandtl number equal to 0.7 .

The velocity profile obtained by means of the five-equation model is shown in figure 4.25 . The velocity profile for the case of zero velocity ratio is compared with the experimental results of Wygnanski and Fiedler (1970) and with the analytical results obtained by Tollmien (1945). As can be seen, both theories and experiment are in good agreement. It is interesting to note that for the case of a plane mixing layer with a velocity ratio 0.5 , the same velocity distribution is obtained, provided the ratio $(\frac{U(y)-U_{2\infty}}{U_{MAX}-U_{2\infty}})$ is used, instead of $\frac{U(y)}{U_{MAX}}$. The temperature profile obtained with the five-equation model, in terms of $\frac{\theta}{\theta_{MAX}}$, is also plotted in figure 4.25 . The differences of temperature denoted by θ and θ_{MAX} are calculated using, respectively, (4.62) and (4.63), T_{si} being, for this type of flow, the undisturbed temperature at the internal boundary. The temperature ratio is compared with the analytical solution proposed by Tollmien (1945), as we can see, our model gives predictions that are much more realistic than the simple linear

profile proposed by Tollmien.

An important parameter commonly measured in free turbulent flows is the rate of spreading. The rate of spreading for momentum and for heat is defined, respectively, by $\frac{d\, l_u}{dx}$ and $\frac{d\, l_T}{dx}$. Where, l_u and l_T are characteristic lengths across the flow, both parameters depend mainly on the type of flow. For the plane mixing layer we define l_u (or l_T) as the distance across the flow between the points where $\frac{U}{U_{MAX}}$ (or $\frac{\theta}{\theta_{MAX}}$) is equal to 0.1 and 0.9 . In table 4.3 we show a comparison between the measured spreading parameters and those predicted by our model. As can be seen, our predictions for the two types of plane mixing layer are well inside the variation of the experimental data.

The shear stress and convective heat flux profiles are shown in figure 4.26 . Turbulence energy and intensity of temperature fluctuation distributions are plotted in figure 4.27. Both momentum correlations - shear stress and turbulence energy- agree well with the Wygnanski and Fiedler (1970), and Bradshaw et al. (1964) experimental results. Again, a small departure is noticeable in the predicted results when the free boundary is approached. It is impossible to say conclusively that the discrepancy in this region is due to a weakness of the model because is commonly accepted it is difficult to make reliable experiments in this region, therefore, it is reasonable to assume that the experimental results contain a large error. The heat correlations, also plotted in figures 4.26 and 4.27, display a similarity to the momentum relations both in form and location

Table 4.3 Predicted and measured rates of spread in plane mixing layers and plane jets.

Kind of flow	Predicted rates of spread	Experimental data	Data sources
(A) Plane mixing layer 1) Velocity ratio = 0	$\frac{d\,l_u}{dx} = 0.145$	0.130;0.150; 0.160;0.200	Various workers cited by Gibson and Launder(1976)
	$\frac{d\,l_T}{dx} = 0.146$	0.165	
2) Velocity ratio = 0.5	$\frac{d\,l_u}{dx} = 0.050$	0.046	Watt(1967) data cited by Gibson and Launder(1976)
	$\frac{d\,l_T}{dx} = 0.057$	0.051	
(B) Plane jets	$\frac{d\,l_u}{dx} = 0.110$	0.088;0.096; 0.120;0.096	Data cited by Jenkins and Goldschmidt (1973)
	$\frac{d\,l_T}{dx} = 0.144$	0.123;0.137; 0.141;0.170	

of maximum values.

The shear stress/turbulence energy ratio and convective heat flux/(turbulence energy x intensity of temperature fluctuation) ratio are shown in figure 4.28 . The predicted momentum correlation, in agreement with the experimental measurements of Wygnanski and Fiedler (1970), exhibits a constant value for nearly the entire section across the flow. The predicted ratio of 0.28 is quite near the experimental value of 0.26 . The heat correlation also shows the same kind of constancy, with a predicted ratio of 0.46 . This value is nearly the same as predicted for flat-plate boundary layers, which shows that the flux correlations are not affected by the presence of a wall. Of the experimental data summarized in table 4.2, only Webster's (1964) data relates to free shear flow. Our value of 0.46 lies roughly at the mid-point of the Webster data.

For a plane mixing layer, our predicted diffusivity ratio (γ_T/ν_T) defined by (4.69), is plotted in figure 4.29 . As can be seen, a variation from 2.2 in the region of maximum production to 1.5 towards the edges is predicted by our model. Launder's (1976) survey reveals a wide variation in the experimental results and it is not possible to make a concrete conclusion about the best experimental estimate for the diffusivity ratio. But a variation between 2.0 at the region of maximum production to 1.5 at the edge of the boundary agrees with most of the experimental data, and confirms the reliability of the model in the particular context of plane mixing layers.

4.4.5 Plane jet in stagnant surrounding.

A two-dimensional turbulent plane jet results when a jet flows freely through a rectangular orifice into a surrounding fluid of uniform velocity. This type of jet flow occurs when the velocity on the centre-line of the jet is much greater than that of the surrounding flow. Here we consider the case of stagnant surroundings, i.e., the case when the undisturbed velocity of the ambient fluid is zero. We apply the five-equation model to the plane jet, and our predicted results for both thermal and dynamic quantities are summarized in figures 4.30 to 4.33 .

The distributions for velocity ($\frac{U}{U_{MAX}}$) and temperature ($\frac{\theta}{\theta_{MAX}}$) are shown in figure 4.30 . The temperature differences θ and θ_{MAX} are calculated using (4.62) and (4.63), where, T_{si} is the undisturbed temperature of the surrounding flow. $y_{0.5}$ is the value of the cross-stream coordinate, measured from the centre of the jet, where the velocity is half the maximum jet velocity. The velocity profile is compared with the experimental results of Bradbury (1965), while, the temperature distribution is compared with the Jenkins and Goldschmidt (1973) experimental data. As can be seen in figure 4.30, the predictions for both temperature and velocity agree well with the experimental results.

The rates of spreading for momentum and heat, $\frac{d\, l_u}{dx}$ and $\frac{d\, l_T}{dx}$, respectively, are defined in a similar way to that for plane mixing layers. Here we define l_u (or l_T) as the

distance between the centre of the jet and the point where $\frac{U}{U_{MAX}}$ (or $\frac{\theta}{\theta_{MAX}}$) is equal to 0.5 . Our predictions are shown in table 4.3, and our results are well inside the range of variation of the experimental data.

The turbulence energy and intensity of temperature fluctuation profiles are shown in figure 4.31 . The turbulence energy distribution is in close agreement with Bradbury's (1965) experimental results, and the intensity of temperature profile shows a similarity to the turbulence energy profile. The flux correlations shear stress/turbulence energy ratio and convective heat flux/(turbulence energy x intensity of temperature) are plotted in figure 4.32 . The constant value of 0.30 given by the theory for the momentum correlation is very close to the value of 0.32 implied by the experimental data of Bradbury (1965). The constant value of the heat flux correlation over a region is also verified for jet flows. In the constant region, our results give a flux correlation ratio of 0.46 which agrees with most of the experimental ratios summarized in table 4.2 .

Finally, our predictions for the diffusivity ratio are shown in figure 4.33 . Launder (1976) pointed out that the variation of the diffusivity ratio in plane jets should be similar to that in plane mixing layers. If this is true, than one would expect the experimental values of $\frac{\gamma_T}{\nu_T}$ to vary from about 2.0 (in the region of maximum production) to about 1.5 (at the edge). A study of figure 4.33 shows that our results

vary steadily from 2.3 at the centre of the jet to 1.5 at the edge. This tends to confirm our theory and Launder's hypothesis.

CHAPTER - 5

5. Conclusions and recommendations for future developments.

5.1 Conclusions.

The following conclusions regarding two-dimensional incompressible turbulent flows can be drawn from the work presented in this thesis.

(1) An appraisal, both quantitative and qualitative, of some isothermal models of turbulence, already existing in the literature, shows that a three-equation model is the most suitable for predicting turbulent boundary layers, based on such criteria as range of flows, accuracy and computing-time economy.

(2) A study of the influence of varying the constants in a three-equation model, applied to annular flow, discloses an almost negligible (less than 2%) influence on velocity and shear stress distributions even when some constants are varied by as much as 50% . Only the turbulence energy distribution shows any sensitivity to the variation and then only to the variation of the constant C_{sl} (see (2.14)).

(3) The optimum three-equation model is applied to specific problems such as:

(a) prediction of the point of maximum velocity in a smooth annulus, varying the radius ratio,

(b) prediction of the characteristic laws of similarity in a turbulent rough pipe flow, and,

(c) prediction of friction factors in turbulent annular flow with symmetric and asymmetric wall conditions.

A comparison of the predictions of the model with the experimental data for the flows considered confirms the validity of the theoretical model chosen.

(4) A complementary model of convective heat transfer, capable of predicting two-dimensional, incompressible turbulent thermal boundary layers is developed. Numerical solutions of the thermal model, simultaneously with the three-equation model, are performed for annular, pipe, flat-plate, mixing layer and plane jet flows. In general, a good agreement for temperature distributions (θ and θ^+), between the predictions of the theoretical model and experimental results, is achieved.

(5) Predicted profiles for heat transfer correlations, such as convective heat flux and intensity of temperature fluctuation show a strong similarity to the correspondent distributions for momentum - shear stress and turbulence energy. Our predictions of

characteristic flow parameters, such as diffusivity ratio, spreading ratio and convective heat flux/ intensity of temperature ratio, are also in good agreement with the experimental data.

(6) Predicted Nusselt numbers, in concentric annuli heated (or cooled) on one side while the other side is insulated, match well the experimental data. We find the radius ratio effect on the Nusselt number is smaller when the outer wall is heated (or cooled) than when the inner wall is heated (or cooled). Constant wall temperature boundary conditions give slightly lower Nusselt numbers than in the case of a linear rise in wall temperature (which is equivalent to uniform heat flux).

(7) In rough pipe turbulent flow, the relation

$$B_{rT}(e^+, Pr) = 4.70(e^+)^{0.2}Pr^{0.44} \qquad (4.75)$$

gives a better representation to the temperature law of the wall than the relation (4.55) proposed by Dipprey and Sabersky (1963). The relation (4.75) also gives Stanton numbers which are in better agreement with the experimental data.

5.2 Future developments.

To the present time, for most of the real fluid flows, no measurements of fluctuating heat flux quantities such as $\overline{u_i T'}$ and $\overline{T'^2}$ have been reported in the literature. This, undoubtedly, is due to the technical difficulties presented by such measurements, but is also possibly due to the lack of incentive to produce experimental results, since there have been no theoretical results for comparison. Now that some theoretical models of turbulent heat flux are beginning to appear, a great shortage of thermal measurements is apparent. Therefore, parallel to theoretical investigations, the experimental field must now be extensively researched. Thus, we hope that the development and improvement of measurement techniques, either by the well established wire anemometer technique or by the new laser Doppler anemometer technique, will overcome the technical difficulties and enable investigators to produce more basic and comprehensive experimental results relating to thermal turbulence.

The first recommendation for the extension of the model is to include buoyancy effects. Such effects can be represented in the Navier-Stokes equation by the inclusion of external forces due to gravitational effects. Thus, each equation of the model which is derived from the Navier-Stokes equation would then include these terms. Consequently, the shear stress and turbulence energy equations would then have the extra production term $-\frac{g_i}{\bar{T}}\overline{u_i T'}$, where, g_i is the gravitational acceleration in the direction x_i. Also, the

convective heat flux equation would have the additional term $-\frac{g_i}{\bar{T}}\cdot\overline{\frac{1}{2}T'^2}$. There is an influence of the gravitational field in the dissipation equation too, but due to its smallness, as a first approximation it could be neglected. Special attention must be given to the approximation of the pressure-strain terms (in shear stress and convective heat flux equations) because, now, the Poisson equation for the pressure fluctuating term is affected by terms like $\frac{g_i}{\bar{T}}\cdot\frac{\partial T'}{\partial x_i}$. After the inclusion of these additional terms it would then be possible to apply the five-equation model to flows such as the atmospheric stratified shear flow.

Because flows characterized by low Reynolds number are important in engineering applications, it is desirable to extend our model in order to include flows of this nature. Unlike the high Reynolds number flows, the low Reynolds number flows are affected by the viscous sub-layer, where the molecular properties affect the process of production, diffusion and, mainly, dissipation of turbulence. Tentative solutions using simple models such as the mixing length or the eddy viscosity have resulted in unsatisfactory predictions. Some published work suggest that models based on transport equations have a better likelihood of success. Thus, a model for low Reynolds number flows, based on our model, can be developed provided that: (1) molecular diffusion terms are included, (2) further terms are added to allow for the fact the dissipation process near the wall are not isotropic. It should be noted that some molecular terms (viscosity and thermal conductivity) are already included in our model, but there are others neglected

whose inclusion should now be considered. Also, a study and verification of the value of the constants should be made, it being possible that they depend upon the Reynolds number.

The present model was entirely developed for incompressible flows (constant properties). To comply with this condition, our model can only be applied when the difference of temperature between boundary and undisturbed flow is relatively small. Many real flows have differences of temperature not so small, thus, it should be of value to include compressibility effects in our model in order to extend the model to predict such flows. A simple method is to incorporate the best possible functional relationships for the variation of density, viscosity and thermal conductivity with pressure and temperature. Naturally, a careful study of the validity of some of the approximations must be made. Such a model could then be applied to flows with greater temperature differences, for example, it could be used for the design of gas-cooled reactor fuel elements in order to predict temperature distributions, as well as velocity, turbulence energy, convective heat flux profiles and many other important correlations.

The study of two-dimensional flows was our main objective, but some three-dimensional flows have similar characteristics and it is possible to extend our model to apply to these flows. Such three-dimensional flows as the round jet, the flow over an aerofoil, flow in a non-circular channel come into this category. These flows are characterized by the fact that there is a predominant direction of flow, and also the

gradients in two of the directions (say, x and z) are small compared with the gradient normal to the surface. Consequently, the ordinary boundary layer approximations apply and the upstream conditions alone determine the conditions downstream. In these flows all Reynolds stresses are important, thus, one of the first considerations would be to develop an individual equation for each normal stress $\overline{u_x^2}$, $\overline{u_y^2}$ and $\overline{u_z^2}$ instead of using the turbulence energy equation. Equations for the lateral shear stress $\overline{u_x u_z}$ and lateral convective heat flux $\overline{u_z T'}$ would be approximated, in addition to the already developed equations for $\overline{u_x u_y}$ and $\overline{u_y T'}$. Due to the parabolic character of the equations, the same numerical method (marching procedure) could be employed. In most of these flows there is a variation of pressure in the direction normal to the flow, thus, an allowance for the pressure variation in the cross-stream plane should be included in the numerical calculations.

REFERENCES

BATCHELOR, G.K. and TOWNSEND, A.A. (1948): "Decay of isotropic turbulence in the initial period", Proc. of Royal Society (London), A.193 , p.539 .

BETTERMANN, D. (1966): "Contribution à l'étude de la convection forcée turbulente ~~au~~ le long de plaques rugueuses", Int. Journ. of Heat and Mass Transfer, vol. 9 , pp.153-164 .

BRADBURY, L.J.S. (1965): "The structure of a self-preserving turbulent plane jet", Journ. of Fluid Mech., vol.23 part 1, pp.31-64 .

BRADSHAW, P. (1976) (ed.): "Turbulence", Topics in Applied Physics, vol.12, Springer-Verlag, Berlin.

BRADSHAW, P. ; FERRISS, D.H. and ATWELL, N.P. (1967): "Calculation of boundary layer developments using the turbulent energy equation", Journ. of Fluid Mech., vol.28 , pp.593-616 .

BRADSHAW, P. ; FERRISS, D.H. and JOHNSON, R.F. (1964): "Turbulence in the noise-producing region of a circular jet", Journ. of Fluid Mech., vol.19, part 4, pp.591-624 .

BRIGHTON, J.A. and JONES, J.B. (1964): "Experimental studies through annular sections", Journ. of Basic Engin., Trans. ASME, vol.86, pp.835-844 .

CHAMPAGNE, F.H. ; HARRIS, V.G. and CORRSIN, S. (1970): "Experiments on nearly homogeneous turbulent shear flow", Journ. of Fluid Mech., vol.41, part 1, pp.81-139 .

CHOU, P.Y. (1945): "On velocity correlations and the solution of the equations of turbulent fluctuation", Quart. Appl. Math., vol.3 , pp.38-54 .

COLBURN, A.P. (1933): "A method of correlating forced convection heat transfer data and comparison with fluid friction", Trans. AIChE, vol.29, pp.174-210 .

DALY, B.J. and HARLOW, F.H. (1970): "Transport equations of turbulence", Physics of Fluids, vol.13, pp.2634-2649.

DAVIDOV, B.I. (1961): "On the statistical dynamics of an incompressible fluid", Dokl. AN SSSR, vol.136, p.47.

DEISSLER, R.G. (1955): "Analysis of turbulent heat transfer, mass transfer and friction in smooth tubes at high Prandtl and Schmidt numbers", N.A.C.A. Report No.1210 .

DIPPREY, D.F. and SABERSKY, R.H. (1963): "Heat and momentum transfer in smooth and rough tubes at various Prandtl numbers", Int. Journ. of Heat and Mass Transfer, vol.6 , pp.329-353 .

DONALDSON, C.P. ; SULLIVAN, R.D. and ROSENBAUM, H. (1972): "A theoretical study of the generation of atmospheric turbulence", AIAA Journal, vol.10, p.162.

EDWARDS, F.J. and SHERIFF, N. (1961): "The heat transfer and friction characteristics for forced convection of air flow over a particular type of rough surface", Int. Develop. in Heat Transfer, ASME, vol.2 , pp.415-425 .

FERNHOLZ, H.H. (1976): "External flows", Topics in Applied Physics, Turbulence, Bradshaw (ed.), vol.12 , pp. 45-107 .

GARDNER, G.C. and KESTIN, J. (1963): "Calculation of the Spalding function over a range of Prandtl numbers", Int. Journ. of Heat and Mass Transfer, vol.6, pp.289-299 .

GIBSON, C.H. and SCHWARTZ, W.H. (1963): "The universal equilibrium spectra of turbulent velocity and scalar fields", Journ. of Fluid Mech., vol.16 , pp.365-384 .

GIBSON, M.M. and LAUNDER, B.E. (1976): "On the calculations of horizontal, turbulent, free shear flows under gravitational influence", Trans. of ASME, Journ. of Heat Transfer, pp.81-87 .

GLUSHKO, G.S. (1965): "Turbulent boundary layer on a flat plate in an incompressible fluid", NASA TT F-10080 , translation from Izvestiya Akademii Nauk SSSR, Seriya Mekhanika No.4 , pp.13-23 .

GOWEN, R.A. and SMITH, J.W. (1967): "The effect of Prandtl number on transport profiles for heat transfer in turbulent pipe flow", Chem. Eng. Sci., vol.22 , pp.1701-1711 .

HALL, W.B. (1962): "Heat transfer in channels having rough and smooth surfaces", Journ. of Mech. Eng. Sci., vol.4 , No.3 , pp.287-291 .

HANJALIC, K. (1970): "An experimental and theoretical investigation on the asymmetric, quasi-parallel flow of turbulent incompressible fluids", Ph.D. Thesis, London University.

HANJALIC, K. and LAUNDER, B.E. (1972-a): "Fully developed asymmetric flow in a plane channel", Journ. of Fluid Mech., vol.51 , part 2 , pp.301-335 .

HANJALIC, K. and LAUNDER, B.E. (1972-b): "A Reynolds stress model of turbulence and its applications to thin shear flows", Journ. of Fluid Mech., vol.52 , part 4 pp.609-638 .

HINZE, J.O. (1959): "Turbulence", McGraw-Hill, New York .

JENKINS, P.E. and GOLDSCHMIDT, V.W. (1973): "Mean temperature and velocity in a plane turbulent jet", Journ. of Fluids Eng., Trans. ASME, pp.581-584 .

JONES, W.P. and LAUNDER, B.E. (1972): "The prediction of laminarization with a 2-equation model of turbulence" Int. Journ. of Heat and Mass Transfer, vol.15 , pp.301-314 .

JONES, W.P. and LAUNDER, B.E. (1973): "Calculation of low Reynolds numbers phenomena with a two-equation model of turbulence", Int. Journ. of Heat and Mass Transfer, vol.16 , pp.1119-1130 .

JOHNK, R.E. and HANRATTY, T.J. (1962): "Temperature profiles for turbulent flow of air in a pipe", Chem. Eng. Sci., vol.17 , pp.867-879 .

JOHNSTON, J.P. (1976): "Internal flows", Topics in Applied Physics, Turbulence, Bradshaw (ed.), vol.12, pp.109-169 .

JONSSON, V.K. and SPARROW, E.M. (1966): "Experiments on turbulent flow phenomena in eccentric annular ducts", Journ. of Fluid Mech., vol.25, part 1, pp.65-86 .

KAYS, W.M. and LEUNG, E.Y. (1963): "Heat transfer in annular passages - hydrodynamically developed turbulent flows with arbitrary prescribed heat flux", Int. Journ. of Heat and Mass Transfer, vol.6, pp.537-557.

KESTIN, J. and PERSEN, L.N. (1962): "Application of Schmidt's method to the calculation of Spalding's function and of the skin-friction coefficient in turbulent flow", Int. Journ. of Heat and Mass Transfer, vol.5, pp.143-152 .

KESTIN, J. and RICHARDSON, P.D. (1963): "Heat transfer across turbulent incompressible boundary layers", Int. Journ. of Heat and Mass Transfer, vol.6, pp.147-189.

KLEBANOFF, P.S. (1955): "Characteristics of turbulence in a boundary layer with zero pressure gradient", N.A.C.A. Report No. 1247 .

KLINE, S.J.;MORKOVIN, M.V.;SOVRAN, G. and COCKRELL, D.J.(1969) (ed.) : Proc. of AFOSR/IFP Conference on Computation of Turbulent Boundary Layers 1968, vol. I, Stanford University.

KNUDSEN, J.G. and KATZ, D.L. (1958): "Fluid dynamics and heat transfer", McGraw-Hill, New-York.

KOLAR, V. (1965): "Heat transfer in turbulent flow of fluids through smooth and rough tubes", Int. Journ. of Heat and Mass Transfer, vol.8 , pp.639-653 .

KOLOVANDIN, B.A. and VATUTIN, I.A. (1969): "On the statistical theory of non-uniform turbulence", Int. Seminar on Heat and Mass Transfer, Herceg Novi, Yugoslavia.

LAUNDER, B.E. (1975): "On the effects of gravitational field on the turbulent transport of heat and momentum", Journ. of Fluid Mech., vol.67, part 3, pp.569-581 .

LAUNDER, B.E. (1976): "Heat and mass transport", Topics in Applied Physics, Turbulence, Bradshaw (ed.), vol.12, pp.231-287 .

LAUNDER, B.E. ; REECE, G.J. and RODI, W. (1975): "Progress in the development of a Reynolds stress turbulence closure", Journ. of Fluid Mech., vol.68, part 3 , pp.537-566 .

LAUNDER, B.E. and SPALDING, D.B. (1972): "Mathematical models of turbulence", Academic Press, London .

LAWN, C.J. (1969): "Turbulent heat transfer at low Reynolds numbers", Trans. ASME, vol.91, serie C, number 4 .

LAWN, C.J. (1970): "Application of the turbulence energy equation to fully developed flow in simple ducts", CEGB Report, RD/B/R1575, parts I to IV, Berkeley Nuclear Laboratory.

LAWN, C.J. and HAMLIN, M.J. (1968): "Velocity measurements in an internally roughened pipe", CEGB Report, RD/B/N1156, Berkeley Nuclear Laboratory.

LEE, C.J. (1972): "Investigation of flow parameters for a series of concentric rough pin and smooth channel assemblies", CEGB Report, RD/B/N2404, Berkeley Nuclear Laboratory.

LEE, Y. and BARROW, H. (1964): Institute of Mechanical Engineers - Thermodynamics and Fluid Mechanics Symposium, paper 12 .

LESLIE, D.C. (1973): "Developments in the theory of turbulence" Clarendon Press, London.

LESLIE, D.C. (1975): "Turbulence models", Nuclear Engineering Department, TU 8/75, Queen Mary College.

LESLIE, D.C. (1976): "Thermal analysis of Hinkley B AGR", lecture notes for Part III students, QMC-ET-6022, Queen Mary College, Nuclear Eng. Dep. .

LESLIE, D.C. (1977): "Lecture notes on heat transfer in a pipe flow", Nuclear Engineering Department, Queen Mary College.

LESLIE, D.C. and HASSID, (1973): "Improvements to the von Karman analogy for heat transfer at moderate Prandtl numbers", QMC-EP-6001, Nuclear Eng. Dep., Queen Mary College.

LUMLEY, J.L. (1970): "Stochastic tools in turbulence", Academic Press, New York.

LUMLEY, J.L. (1972): "A model of computation of stratified turbulent flows", International Symposium on Stratified Flows, Novosibirsk.

LYON, R.N. (1951): "Liquid metal heat transfer coefficients", Chemical Eng. Progress, vol.47, p.75 .

MARTINELLI, R.C. (1947): Trans. ASME, vol.69, pp.947-959 .

MONIN, A.S. and YAGLOM, A.M. (1975): "Statistical fluid mechanics", MIT Press, vol.2, Cambridge, Mass..

NATHAN, D.I. and PIRIE, M.A.M. (1970): "On the interpretation of heat transfer and pressure drop tests on roughened rods in smooth circular channels", CEGB Report, RD/B/N1370, Berkeley Nuclear Laboratories.

NEE, V.W. and KOVASZNAY, L.S.G. (1969): "The calculation of the incompressible turbulent boundary layers by a single theory", Proc. of 1968 AFOSR/IFP Conference on Computation of Turbulent Boundary Layers, vol.I, pp.300-319 , Stanford University.

NG, K.H. and SPALDING, D.B. (1976): "Predictions of two-dimensional boundary layers on smooth walls with a two-equation model of turbulence", Int. Journ. of Heat and Mass Transfer, vol.19 , pp.1161-1172 .

NICHOLL, C.I.H. (1970): "Some dynamical effects of heat on a turbulent boundary layer", Journ. of Fluid Mech., vol.40 , part 2 , pp.361-384 .

NIKURADSE, J. (1950): "Laws for flow in rough pipes", NACA Report TM 1292 .

ORSZAG, S.A. (1973): "The statistical theory of turbulence", Cambridge University Press, London.

OWEN, P.R. and THOMSON, W.R. (1963): "Heat transfer across rough surfaces", Journ. of Fluid Mech., vol.15, part 3, pp.321-334 .

PATANKAR, S.V. and SPALDING, D.B. (1970): "Heat and mass transfer in boundary layers", Intertex Books, London.

PRANDTL, L. (1910): Z. Phys., vol.11, pp.1072-1078 .

PRANDTL, L. (1925): "Bericht uber untersuchungen zur ausgebildeten turbulenz", ZAMM, vol.5, p.136 (also NACA TM 1231, 1949).

QUARMBY, A. (1967): "Some measurements of turbulent heat transfer in the thermal entrance region of concentric annuli", Int. Journ. of Heat and Mass Transfer, vol.10 , pp.267-276 .

QUARMBY, A. and ANAND, R.K. (1970): "Turbulent heat transfer in concentric annuli with constant wall temperatures" Trans. of ASME, vol.92, serie C, number 1, pp.33-43.

RANNIE, W.D. (1956): "Heat transfer in turbulent shear flow", Journ. of Aeron. Sci., vol.23, number 5, pp.485-489.

REYNOLDS, A.J. (1974): "Turbulent flows in engineering", John Wiley and Sons, London.

REYNOLDS, O. (1883): Phil. Trans. Royal Society (London), series A, vol.174 , p.935 .

REYNOLDS, O. (1901): "Scientific papers of Osborne Reynolds", vol.II, Cambridge University Press.

REYNOLDS, W.C. and CEBECI, T. (1976): "Calculation of turbulent flows", Topics in Applied Physics, Turbulence, Bradshaw (ed.), vol.12, pp. 193-229 .

ROTTA, J. (1962): "Turbulent boundary layers in incompressible flow", Progress in Aeron. Sciences, MacMillan, vol.2, pp.1-221 .

SCHLICHTING, H. (1968): "Boundary layer theory", McGraw-Hill, New York.

SCHULTZ-GRUNOW, F. (1941): NACA TM Report No.986 .

SEBAN, R.A. and SHIMAZAKI, T.T. (1951): "Proceedings of the general discussion on heat transfer", Institution of Mechanical Engineers, p.122 , London.

SMITH, A.G. and SHAH, V.L. (1962): "The calculation of wall and fluid temperatures for the incompressible turbulent boundary layer, with arbitrary distribution of wall heat flux", Int. Journ. of Heat and Mass Transfer, vol.5, pp.1179-1189 .

SPALDING, D.B. (1961-a): "Heat transfer to a turbulent stream from a surface with step-wise discontinuity in wall temperature", Int. Develop. in Heat Transfer, Proc. of Conf. organized by ASME, Colorado, part II, pp.439-446 .

SPALDING, D.B. (1961-b): "A single formula for the law of the wall", Journ. of Applied Mech., Trans. ASME, vol.28, serie E, number 3, pp.455-458 .

SPALDING, D.B. (1964): "Contribution to the theory of heat transfer across turbulent boundary layer", Int. Journ. of Heat and Mass Transfer, vol.7, pp.743-761 .

SPARROW, E.M. and HALLMAN, T.M. (1958): "Turbulent heat transfer in the thermal entrance region of a pipe with uniform heat flux", Applied Sci. Resch., A7, pp.37-52.

TAYLOR, G.I. (1935): "Statistical theory of turbulence", Proc. Royal Society (London), series A, vol.151, parts I-IV, p.421 .

TENNEKES, H. and LUMLEY, J.L. (1973): "A first course in turbulence", MIT Press, London.

TOLLMIEN, W. (1945): "Berechnung turbulenter ausbreitungsvorgange", NACA TM Report No.1085 .

TOWNSEND, A.A. (1958): "Turbulent flow in a stably stratified atmosphere", Journ. of Fluid Mech., vol.3, pp.361-372.

TOWNSEND, A.A. (1976): "The structure of turbulent shear flow", Cambridge University Press, London.

WATSON, M.A.P. (1970): "The performance of a square rib type of heat transfer surface", CEGB Report, RD/B/N 1738, Berkeley Nuclear Laboratories.

WEBB, R.L. ; ECKERT, E.R.G. and GOLDSTEIN, R.J. (1971): "Heat transfer and friction in tubes with repeated-rib roughness", Int. Journ. of Heat and Mass Transfer, vol.14, pp.601-617 .

WEBSTER, C.A.G. (1964): "An experimental study of turbulence in a density stratified shear flow", Journ. of Fluid Mech., vol.19, pp.221-245 .

WILKIE, D. (1966): "Calculation of heat transfer and flow resistance of rough and smooth surfaces contained in a single passage", Proc. of 3rd Int. Heat Transfer Conf. (Chicago), AIChE, vol.I, paper 2, pp.20-31 .

WYGNANSKI, I. and FIEDLER, H.E. (1970): "The two-dimensional mixing region", Journ. of Fluid Mech., vol.41. part 2, pp.327-361 .

ZEMAN, O. and LUMLEY, J.L. (1976): "Modeling buoyancy driven mixed layers", Journ. of the Atmospheric Sciences, vol.33 , pp.1974-1988 .

APPENDIX - 1

A brief description of the numerical method of Patankar and Spalding.

Patankar and Spalding (1970) developed a general method of calculating boundary layer flows, by solving numerically the partial differential equations by a finite-differences procedure. A brief description of the method is given in this appendix.

Each one of the models of turbulence presented in this thesis has two or more partial differential equations to be solved. An inspection of these equations, which are summarized in section 4.1.4, shows that they have a similar mathematical structure, therefore, it is possible to develop a general form of solution, as follows. It is common in turbulent boundary layers to use the stream function ψ as the cross-stream variable in place of y. The x-ψ system is known as the von Mises coordinate system. The stream function ψ is defined by

$$\frac{\partial \psi}{\partial y} = \rho U_x r \quad ; \quad \frac{\partial \psi}{\partial x} = -\rho U_y r \ . \qquad (A.1)$$

In practice, it is more convenient to use a dimensionless stream function w as the cross-stream variable. The function w (called grid function) is defined by

$$w = \frac{\psi - \psi_I}{\psi_E - \psi_I} \quad ; \quad \frac{\partial \psi_I}{\partial x} = -r_I \dot{m}''_I \quad ; \quad \frac{\partial \psi_E}{\partial x} = -r_E \dot{m}''_E \qquad (A.2)$$

where, $\dot{m}''_I$ and $\dot{m}''_E$ are the mass flows entering the internal and external boundaries, respectively. Then, using (A.1) and (A.2), the set of turbulence equations of section 4.1.4 is transformed from the system x-y to the system x-w. Any of the seven transport equations is then reduced to the general form

$$\frac{\partial \Phi}{\partial x} + (a + b w) \frac{\partial \Phi}{\partial w} = \frac{\partial}{\partial w}\left(c \frac{\partial \Phi}{\partial w}\right) + d \qquad (A.3)$$

where,

Φ is the general dependent variable (see table A.1)

$$a = r_I \dot{m}''_I / (\psi_E - \psi_I) \qquad (A.4)$$

$$b = (r_E \dot{m}''_E - r_I \dot{m}''_I)/(\psi_E - \psi_I) \qquad (A.5)$$

c and d are relations between dependent variables. The exact expressions for c and d are in table A.1 .

Table A.1 : Terms c and d for set of equations.

Φ	c	d
U_x	$\frac{r^2 \rho U_x \mu}{(\psi_E - \psi_I)^2}$	$-\frac{\partial}{\partial w}\left(\frac{r\rho\overline{u_x u_y}}{\psi_E - \psi_I}\right) - \frac{1}{\rho U_x}\frac{dp}{dx}$
$\overline{u_x u_y}$	$\frac{r^2 \rho U_x}{(\psi_E - \psi_I)^2}\left(\mu + \rho C_s \frac{E_o^2}{\varepsilon}\right)$	$-\frac{C_{s2}}{U_x}\left(C_{s1} E_o \frac{\partial U_x}{\partial y} + \frac{\varepsilon \overline{u_x u_y}}{E_o}\right)$
E_o	$\frac{r^2 \rho U_x}{(\psi_E - \psi_I)^2}\left(\mu + \rho C_e \frac{E_o^2}{\varepsilon}\right)$	$-\frac{1}{U_x}\left(\overline{u_x u_y}\frac{\partial U_x}{\partial y} + \varepsilon\right)$
ε	$\frac{r^2 \rho U_x}{(\psi_E - \psi_I)^2}\left(\mu + \rho C_\varepsilon \frac{E_o^2}{\varepsilon}\right)$	$-\frac{1}{U_x}\left(C_{\varepsilon 1}\frac{\varepsilon \overline{u_x u_y}}{E_o}\frac{\partial U_x}{\partial y} + C_{\varepsilon 2}\frac{\varepsilon^2}{E_o}\right)$
T	$\frac{r^2 \rho U_x}{(\psi_E - \psi_I)^2}\left(\frac{k}{c_p}\right)$	$-\frac{1}{U_x}\left(\frac{\partial}{\partial y}(\overline{u_y T'})\right)$
$\overline{u_y T'}$	$\frac{r^2 \rho U_x}{(\psi_E - \psi_I)^2}\left(C_{UT2}\frac{E_o^2}{\varepsilon}\right)$	$-\frac{1}{U_x}\left(C_{UT1}\frac{\varepsilon}{E_o}\overline{u_y T'} + C_U E_o \frac{\partial T}{\partial y}\right)$
$\overline{\frac{1}{2}T'^2}$	$\frac{r^2 \rho U_x}{(\psi_E - \psi_I)^2}\left(\frac{k}{c_p} + C_{TT2}\frac{E_o^2}{\varepsilon}\right)$	$-\frac{1}{U_x}\left(\overline{u_y T'}\frac{\partial T}{\partial y} + C_{TT1}\frac{\varepsilon}{E_o}\left(\overline{\frac{1}{2}T'^2}\right)\right)$

The general equation (A.3) is solved by a micro-integral evaluation. The cross-flow is divided into N strips (N is therefore, the number of grid points), each strip corresponds to one value of w, which varies from 0 to 1 (w_I=0 at inner boundary and w_e=1 at outer boundary). A control volume is defined between 3 consecutive grid points as shown in figure A.1 .

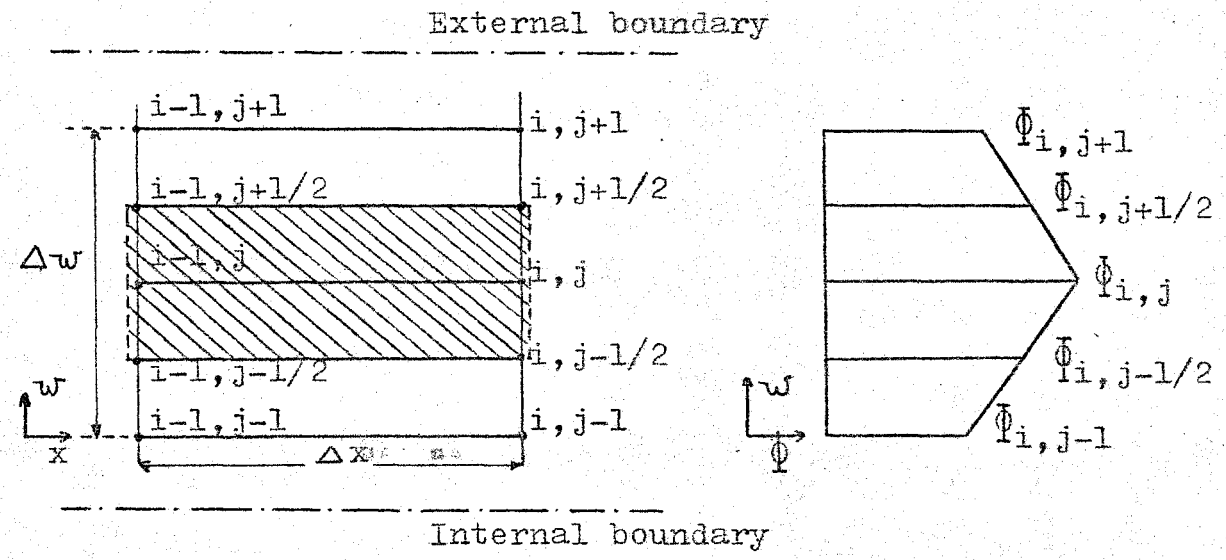

Figure A.1: A typical control volume (shaded) for which micro-integrals are formulated.

Applying (A.3) to the control volume of figure A.1 we have the following micro-integral equation:

$$\int_{i-1}^{i}\int_{j-1/2}^{j+1/2}\left[\frac{\partial \Phi}{\partial x}+(a+bw)\frac{\partial \Phi}{\partial w}\right]dw\,dx=\int_{i-1}^{i}\int_{j-1/2}^{j+1/2}\left[\frac{\partial}{\partial w}\left(c\frac{\partial \Phi}{\partial w}\right)+d\right]dw\,dx \qquad (A.6)$$

The integral equation (A.6) is solved using the trapezoidal rules and the following assumptions:

(i) w is constant with i, thus, $w_{i-1,j}=w_{i,j}$

(ii) Φ varies linearly between adjacent cross-strips, that is, for $\omega = \omega_{i,j+1/2}$

$$\Phi_{i,j+1/2} = \frac{1}{2}(\Phi_{i,j} + \Phi_{i,j+1}) \quad .$$

(iii) Values of Φ_j between x_{i-1} and x_i are uniform and equal to $\Phi_{i,j}$, i.e.,

$$\text{for} \quad x_{i-1} < x \leqslant x_i \longrightarrow \Phi = \Phi_{i,j} \quad .$$

Thus, after extensive algebra (A.6) becomes:

$$\Phi_{i,j} = A_j \Phi_{i,j+1} + B_j \Phi_{i,j-1} + C_j \quad . \qquad (A.7)$$

Coefficients A_j, B_j and C_j are functions of a, b, c and d, as well as the grid parameters. All three coefficients are calculated for the previous step (say, x_{i-1}) were all parameters are known.

Equation (A.7) can be transformed into the simpler form:

$$\Phi_{i,j} = A^*_j \Phi_{i,j+1} + B^*_j \quad . \qquad (A.8)$$

Where,

$$A^*_j = A_j/(1-B_j A^*_{j-1}) \qquad (A.9)$$

$$B^*_j = (B_j B^*_{j-1} + C_j)/(1-B_j A^*_{j-1}) \qquad (A.10)$$

$$A^*_2 = A_2 \qquad (A.11)$$

$$B^*_2 = B_2 \Phi_1 + C_2 \qquad (A.12)$$

At start of calculations (section x_{i-1}) all parameters and distributions $\Phi_{i-1,j}$ are assigned thus, A^*_j and B^*_j can be calculated for all the grid points (j=1,N+3). Equation (A.8) is then solved by back-substitution from j=N+3 (external boundary whose conditions are imposed or

known, i.e., $\Phi_{i,N+3}$ is fixed) to j=1 (internal boundary) for section x_i. This procedure enables the calculation of the profile of the dependent variable $\Phi_{i,j}$ for the whole section x_i. New values for A_j^* and B_j^* can now be calculated. An increase in x is then given and all the operations are repeated for the next step, and so on, until the end of the channel.

Based on this numerical method we develop a computer program called TTBL (Two-dimensional Turbulent Boundary Layers), capable of solving any one of the models proposed in chapter - 2, as well as the thermal model described in chapter-4. The selection of the model to be solved is made through the index NEQ which stands for the number of equations to be solved. The flow geometry can be a combination of any two of the three boundaries: wall, free and symmetry line. The specification of geometry is made by using indices KIN and KEX , which refer to the internal and external boundaries, respectively. KIN and KEX are attributed the values 1, 2 or 3 depending on whether the boundary is a wall, free or a symmetry line.

Two grid functions (ω) are incorporated; one is the uniform grid, where all the grid points are equally spaced between internal and external boundaries; the other is the logarithmic grid, where the density of grid points is greater as the boundary is approached. Any one of the two grids can be selected at the start of the program via the data. The logarithmic grid is particularly used in flows where there is an asymmetry in the profiles of turbulent quantities; it has the advantage of giving more accurate results, but the disadvantage of being more sensitive to instabilities in the solution of differential equations in comparison to the uniform grid.

The tendency of instabilities of the numerical solution in general can be prevented by selecting a suitable grid distribution with an adequate number of grid points and/or

choosing a smaller forward increment, Δx . There is no exact rule to establish either w or Δx . But from our experience we found that grids with N between 40 and 60 points are suitable; and forward increments Δx of about 4% of the distance between the two boundaries of the fluid flow proved to be sufficient.

Computing time, obviously, depends on the number of equations, number of grid points and size of forward step. Our program was run on a CDC 7600 computer. In a typical case, for N=60 points and a Δx about 4% of cross-stream distance between boundaries, a run of the thermal model (7 differential equations to be solved) took less than 15 seconds. Whereas a run of the three-equation model (4 differential equations to be solved) took less than 10 seconds per case.

APPENDIX - 2

Approximation of pressure-rate term in the convective heat flux equation.

The pressure-rate of strain term appearing in the Reynolds shear stress equation was approximated by Hanjalic and Launder (1972b) and Launder et al. (1975) following proposal by Chou (1945) and Rotta (1962). We will use a similar procedure in order to approximate the pressure-rate term ($\overline{\frac{p'}{\rho}\frac{\partial T'}{\partial x_i}}$) which appears in the convective heat flux equation.

Taking the divergent of the Navier-Stokes equation for turbulent flow and using the continuity equation, we find the transport equation for the pressure fluctuation

$$\frac{1}{\rho}\frac{\partial^2 p'}{\partial x_k^2} = -2\frac{\partial u_m}{\partial x_k}\frac{\partial U_k}{\partial x_m} - \frac{\partial^2}{\partial x_k \partial x_m}(u_m u_k - \overline{u_k u_m}) \quad . \tag{B.1}$$

A formal integration of (B.1) over the volume of the flow gives the fluctuating pressure at a position $\vec{r}_o$:

$$p'(\vec{r}_o) = \frac{\rho}{4\pi}\int_{vol}\left[-2\frac{\partial u_m}{\partial x_k}\frac{\partial U_k}{\partial x_m} - \frac{\partial^2}{\partial x_k \partial x_m}(u_m u_k - \overline{u_k u_m})\right]_{\vec{r}} \cdot \frac{d(vol)}{|\vec{r}_o - \vec{r}|} \quad . \tag{B.2}$$

Multiplying (B.2) by $(\frac{\partial T'}{\partial x_i})_{\vec{r}_o}$ and averaging, we obtain

$$\left[\overline{\frac{p'}{\rho}\frac{\partial T'}{\partial x_i}}\right]_{\vec{r}_o} = \frac{1}{4\pi}\int_{vol}\left[\left(-2\overline{\frac{\partial u_m}{\partial x_k}\frac{\partial U_k}{\partial x_m}}\right)_{\vec{r}}\left(\frac{\partial T'}{\partial x_i}\right)_{\vec{r}_o} - \left(\overline{\frac{\partial^2 u_m u_k}{\partial x_k \partial x_m}}\right)_{\vec{r}}\left(\frac{\partial T'}{\partial x_i}\right)_{\vec{r}_o}\right]\frac{d(vol)}{|\vec{r}_o - \vec{r}|} \tag{B.3}$$

The left hand side of (B.3) is just the pressure-rate term of the convective heat flux equation, whose approximated form we are seeking. By inspection of (B.3) we see that the

pressure strain originates from two processes: (1) effects due to mean velocity over fluctuating components u_m and T', and (2) effects from purely turbulence interactions. From this we can assume that the pressure strain (B.3) is the sum of the two terms,

$$\overline{\frac{p'}{\rho}\frac{\partial T'}{\partial x_i}} = \left(\overline{\frac{p'}{\rho}\frac{\partial T'}{\partial x_i}}\right)_{\substack{\text{mean}\\ \text{flow}}} + \left(\overline{\frac{p'}{\rho}\frac{\partial T'}{\partial x_i}}\right)_{\text{turbulent}} \qquad \text{(B.4)}$$

Turbulent component in (B.4).

A similar term appears when the pressure-strain term for the Reynoldsshear stress equation is approximated, it then has the form

$$\overline{\frac{p'}{\rho}\left(\frac{\partial u_i}{\partial x_j} + \frac{\partial u_j}{\partial x_i}\right)}_{\text{turbulent}} .$$

Rotta (1962) proposed (and thereafter every worker who made closure approximations for the pressure-strain term did the same) the relation,

$$\overline{\frac{p'}{\rho}\left(\frac{\partial u_i}{\partial x_j} + \frac{\partial u_j}{\partial x_i}\right)}_{\text{turbulent}} = -C_{\phi 1}\frac{\varepsilon}{E_o}\left(\overline{u_i u_j} - \frac{2}{3}\delta_{ij}E_o\right)$$

where, $C_{\phi 1}$ is a constant.

By analogy, we will assume that the turbulent component in (B.4) can be approximated by

$$\left(\overline{\frac{p'}{\rho}\frac{\partial T'}{\partial x_i}}\right)_{\text{turbulent}} = -C_{UT1}\frac{\varepsilon}{E_o}\overline{u_i T'} \quad , \qquad \text{(B.5)}$$

where, C_{UT1} is also a constant.

Mean flow component in (B.4).

From (B.3), the mean flow component is

$$\overline{\left(\frac{p'}{\rho}\frac{\partial T'}{\partial x_i}\right)}_{\substack{\text{mean}\\ \text{flow}}} = -\frac{1}{2\pi}\int_{vol}\overline{\left(\frac{\partial u_m}{\partial x_k}\frac{\partial U_k}{\partial x_m}\right)_{\vec{r}}\left(\frac{\partial T'}{\partial x_i}\right)_{\vec{r}_o}}\cdot\frac{d(vol)}{\left|\vec{r}_o-\vec{r}\right|} \quad . \tag{B.6}$$

Assuming a flow with homogeneous turbulence, where the mean properties can be assumed independent of position, (B.6) can be written as

$$\overline{\left(\frac{p'}{\rho}\frac{\partial T'}{\partial x_i}\right)}_{\substack{\text{mean}\\ \text{flow}}} = a_{k\ i}^{m\ T'}\cdot\frac{\partial U_k}{\partial x_m} \tag{B.7}$$

where the tensor $a_{k\ i}^{m\ T'}$ is defined by,

$$a_{k\ i}^{m\ T'} = -\frac{1}{2\pi}\int_{vol}\frac{\partial^2}{\partial x_k \partial x_i}\left(\overline{u_m T'}\right)\cdot\frac{d(vol)}{\left|\vec{r}_o-\vec{r}\right|} \quad . \tag{B.8}$$

Again, following Rotta (1962), the fourth-order tensor $a_{k\ i}^{m\ T'}$ must satisfy the following conditions, in order to satisfy the symmetry requirements and the laws of conservation:

$$a_{k\ i}^{m\ T'} = a_{k\ i}^{T'\ m} = a_{i\ k}^{T'\ m} \tag{B.9}$$

$$a_{i\ i}^{m\ T'} = 2\,\overline{u_m T'} \quad . \tag{B.10}$$

The condition (B.10) suggests a form for the tensor $a_{k\ i}^{m\ T'}$ that is a combination of convective heat flux terms. Therefore with this assumption, the most general form for $a_{k\ i}^{m\ T'}$ should be

$$a_{k\ i}^{m\ T'} = \alpha\delta_{ik}\overline{u_m T'} + \beta\delta_{im}\overline{u_k T'} + \eta\delta_{mk}\overline{u_i T'} \tag{B.11}$$

where, α, β and η are constants and m, k and i are indices which can be any of the coordinates x, y or z. Subscripts m, k and i refer only to velocity components, and terms like $\delta_{jT'}$ are meaningless, thus the only way (B.11) can satisfy all the

symmetry conditions in (B.9) is by making

$$a_{k\,i}^{m\,T'} = \alpha \delta_{ik} \overline{u_m T'} \quad . \tag{B.12}$$

As δ_{ik} is different from zero only when i=k, (B.12) can be written as

$$a_{k\,i}^{m\,T'} = \alpha \overline{u_m T'} \quad . \tag{B.13}$$

If (B.13) must satisfy the law of conservation (B.10), then

$$2\,\overline{u_m T'} = \alpha \overline{u_m T'} \quad \text{and} \quad \alpha = 2.0 \tag{B.14}$$

Thus, relating (B.7) and (B.13) we obtain the mean flow component of the pressure-rate term, namely,

$$\left(\overline{\frac{p'}{\rho}\frac{\partial T'}{\partial x_i}}\right)_{\substack{\text{mean}\\ \text{flow}}} = \alpha \overline{u_m T'} \frac{\partial U_i}{\partial x_m} \quad . \tag{B.15}$$

Finally, substituting (B.15) and (B.5) in (B.4) we derive the total pressure-rate term to be used in the convective heat flux equation:

$$\left(\overline{\frac{p'}{\rho}\frac{\partial T'}{\partial x_i}}\right) = - C_{UT1} \frac{\varepsilon}{E_o} \overline{u_i T'} + \alpha \overline{u_m T'} \frac{\partial U_i}{\partial x_m} \quad . \tag{B.16}$$

APPENDIX - 3

Approximation of the triple-correlation term in the convective heat flux equation.

The analysis of a triple-correlation equation provides a foundation for approximating the triple-correlation term appearing in the convective heat flux equation. The equation for triple-correlation is obtained, after some mathematical manipulation, by multiplying two similar Navier-Stokes equations in 'i' and 'k' coordinates and the temperature equation, for turbulent flows, by $u_k T'$, $u_i T'$ and $u_i u_k$, respectively, then summing the 3 resultant equations and averaging each term. Finally, making use of the mean momentum equations for 'i' and 'k' coordinates as well as the mean temperature equation, we obtain the triple-correlation equation $(\frac{D}{Dt}\overline{u_i u_k T'})$ in its exact form, neglecting only external forces effects. This general form is:

$$\frac{D}{Dt}(\overline{u_i u_k T'}) = -\frac{\partial}{\partial x_m}(\overline{u_i u_k u_m T'}) \qquad \text{(I)}$$

$$+ (\overline{u_k T'}\frac{\partial}{\partial x_m}\overline{u_i u_m} + \overline{u_i T'}\frac{\partial}{\partial x_m}\overline{u_k u_m} + \overline{u_i u_k}\frac{\partial}{\partial x_m}\overline{u_m T'}) \qquad \text{(II)}$$

$$+ \nu(\overline{u_k T'\frac{\partial^2 u_i}{\partial x_m^2}} + \overline{u_i T'\frac{\partial^2 u_k}{\partial x_m^2}}) + \gamma\overline{u_i u_k\frac{\partial^2 T'}{\partial x_m^2}} \qquad \text{(III)}$$

$$- \frac{1}{\rho}(\overline{T' u_k\frac{\partial p'}{\partial x_i}} + \overline{T' u_i\frac{\partial p'}{\partial x_k}}) \qquad \text{(IV)}$$

$$- \Big[U_m(\overline{u_k T'}\frac{\partial}{\partial x_m}U_i + \overline{u_i T'}\frac{\partial}{\partial x_m}U_k + \overline{u_i u_k}\frac{\partial T}{\partial x_m}) + \qquad \text{(V)}$$

$$+ \overline{u_m u_k T'}\frac{\partial}{\partial x_m}U_i + \overline{u_m u_i T'}\frac{\partial}{\partial x_m}U_k + \overline{u_m u_i u_k}\frac{\partial T}{\partial x_m}\Big]. \qquad \text{(C.1)}$$

Following Hanjalic and Launder (1972), the fourth-order correlation term (I) in (C.1) can be approximated in terms of second-order correlations as follows:

$$\overline{u_i u_k u_m T'} = \overline{u_i u_m}.\overline{u_k T'} + \overline{u_i u_k}.\overline{u_m T'} + \overline{u_m u_k}.\overline{u_i T'} \quad . \quad (C.2)$$

Using this approximation for (I) and adding it to term (II) of (C.1) gives

$$(I)+(II) = -\left(\overline{u_i u_m}\frac{\partial}{\partial x_m}\overline{u_k T'} + \overline{u_m T'}\frac{\partial}{\partial x_m}\overline{u_i u_k} + \overline{u_k u_m}\frac{\partial}{\partial x_m}\overline{u_i T'}\right). \quad (C.3)$$

Each of the first two compenents of term (III) has order of magnitude $\left[\nu\frac{u^2\,\theta}{\ell}\right] \equiv \left[\frac{u^3\,\theta}{\ell.Re}\right]$, where, u , θ and ℓ are a velocity-scale, a temperature-scale and a length-scale. Any term of (C.3) has the order of $\left[\frac{u^3\,\theta}{\ell}\right]$, thus, as we only consider flows with high Reynolds numbers, the first two components of (III) are negligible when compared with the terms of (C.3). The same applies to the last component of (III), because we are considering fluids which have ν and α of the same order. Therefore, we can neglect all components of term (III) in (C.1). A comparison of each term of (IV) with the approximation of turbulent terms on pressure-rate (Appendix-2, relation (B.5)), suggests the relationship

$$(IV) = -\frac{1}{\rho}\left(\overline{u_k T'\frac{\partial p'}{\partial x_i}} + \overline{u_i T'\frac{\partial p'}{\partial x_k}}\right) = -C_{sa}\frac{\varepsilon}{E_o}\overline{u_i u_k T'} \quad . \quad (C.4)$$

The last term (V) in (C.1) is itself a sum consisting of products of average mean quantities and fluctuating correlations. Although, when considered theoretically, each term of (V) has the same order of magnitude as each term in (C.3), as a first approximation we are going to neglect all

terms which are products of fluctuating terms and mean flow terms. By this argument, term (V) can be neglected. For the same reason, the convective term in (C.1), $\frac{D}{Dt}(\overline{u_i u_k T'})$, is also negligible. We concede that this approximation is somewhat crude, but triple-correlations are already small in magnitude and the exclusion of one or two terms should not introduce a significant error.

Introducing the approximations discussed above, with relations (C.3) and (C.4) into (C.1) we obtain

$$\overline{u_i u_k T'} = - C_{UT2} \frac{E_o}{\varepsilon}\left(\overline{u_i u_m}\frac{\partial}{\partial x_m}\overline{u_k T'} + \overline{u_m T'}\frac{\partial}{\partial x_m}\overline{u_i u_k} + \overline{u_k u_m}\frac{\partial}{\partial x_m}\overline{u_i T'}\right) \qquad (C.5)$$

where, C_{UT2} is a new constant ($= 1/C_{sa}$).

The triple-correlation term given by expression (C.5) is the approximated form of $\overline{u_i u_k T'}$ which we use to close the turbulent diffusion term in the equation of convective heat flux.

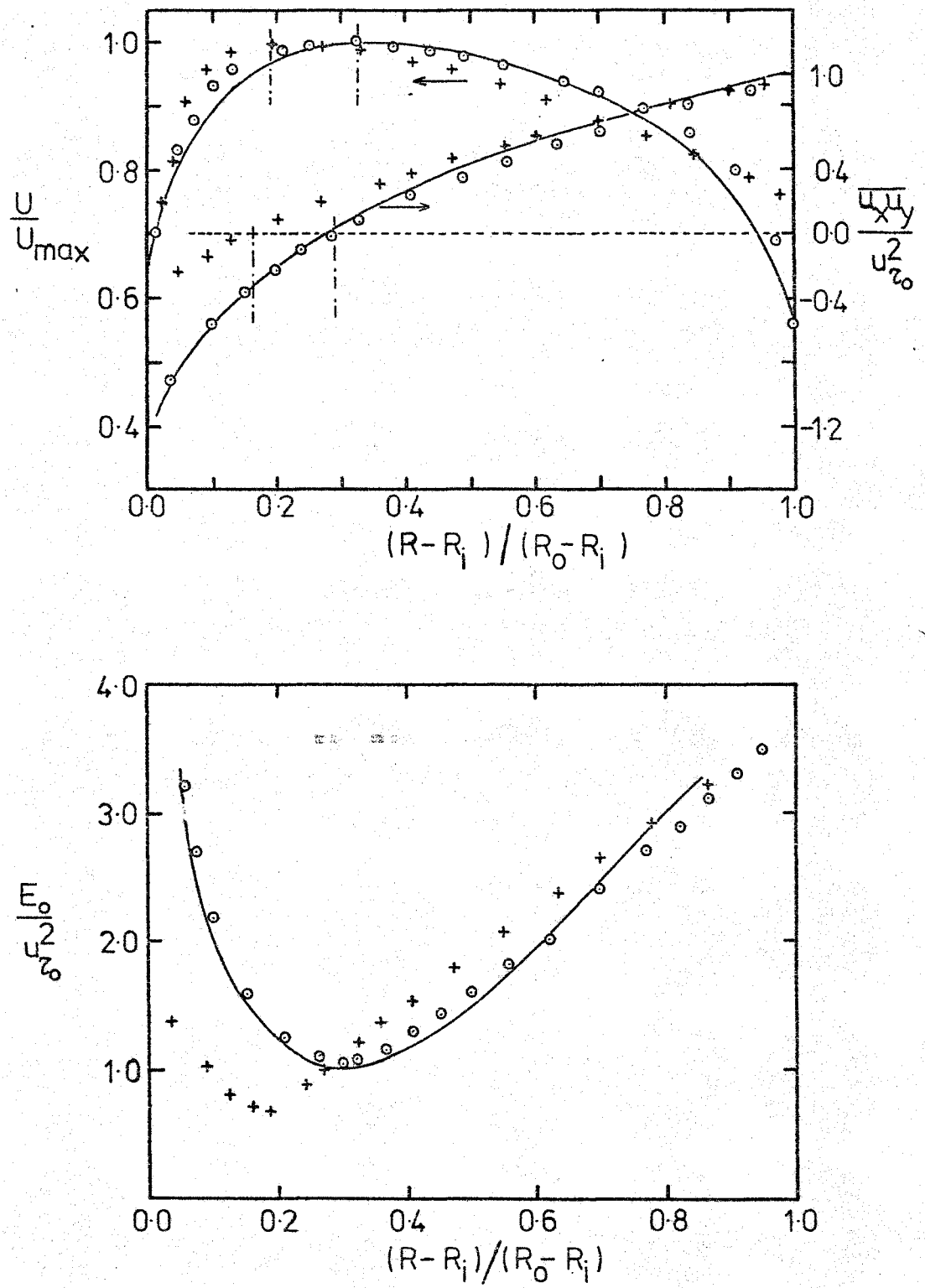

Fig. 2.1 Length scale influence in velocity, shear stress and turbulence energy profiles in a smooth annulus using a two-equation model (E_o, $\overline{u_x u_y}$). R_i/R_o=0.088; Re=2.4x10^5.

Lawn's (1970) experiment: —— . Predictions: ⊙ with (2.10) and (2.11) expressions; + with expression(2.12).

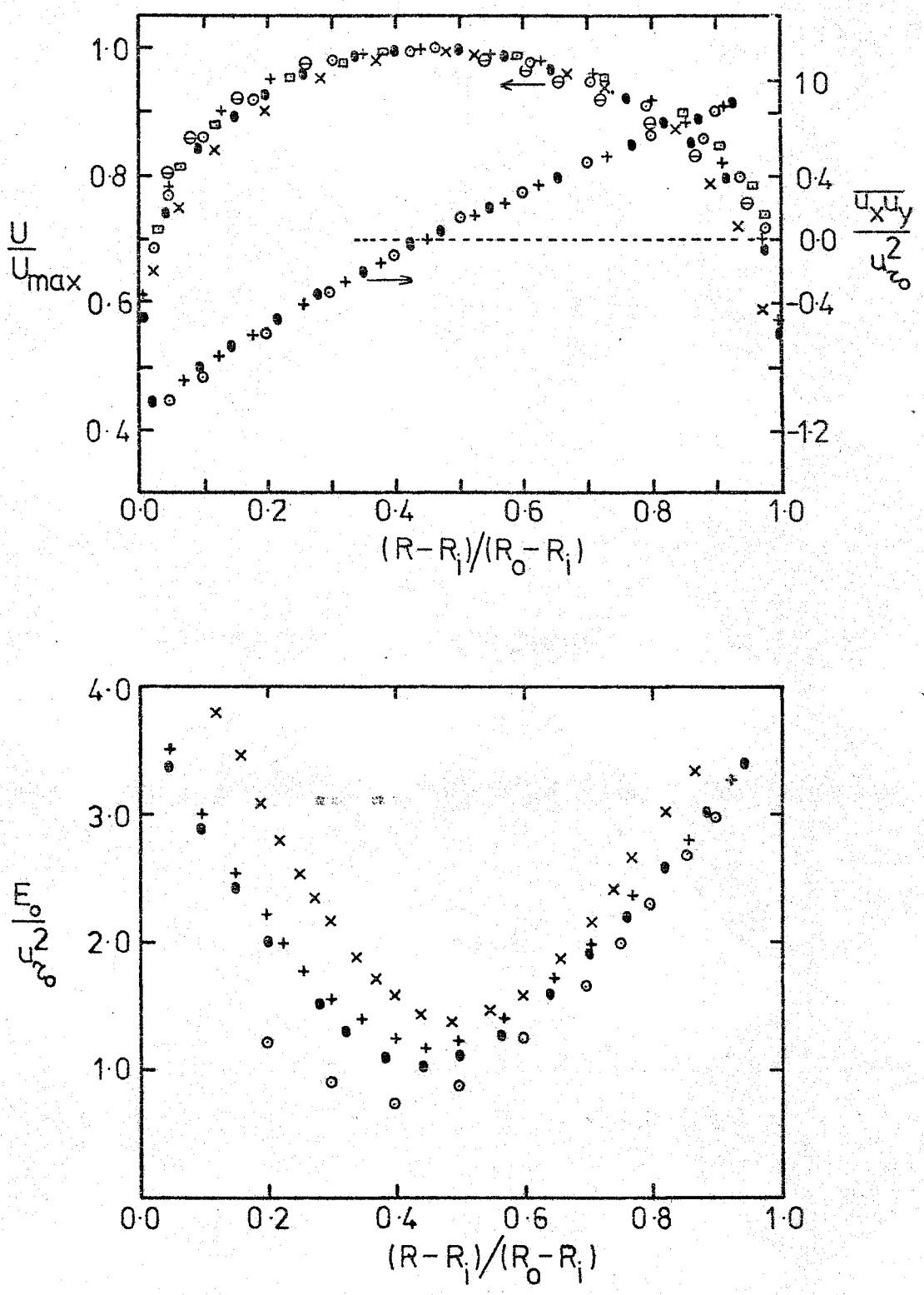

Fig. 2.2 Comparison between models of turbulence: velocity, shear stress and turbulence energy profiles in a smooth annulus. $R_i/R_o=0.562$; $Re=1.46\times10^5$.

- experiment, Brighton and Jones (1964). Predictions:
- 3-eq. model; + 2-eq. model (E_o,$\overline{u_x u_y}$); ⊖ 1-eq.model;
- × 2-eq. model (E_o,ε); ▫ mixing length.

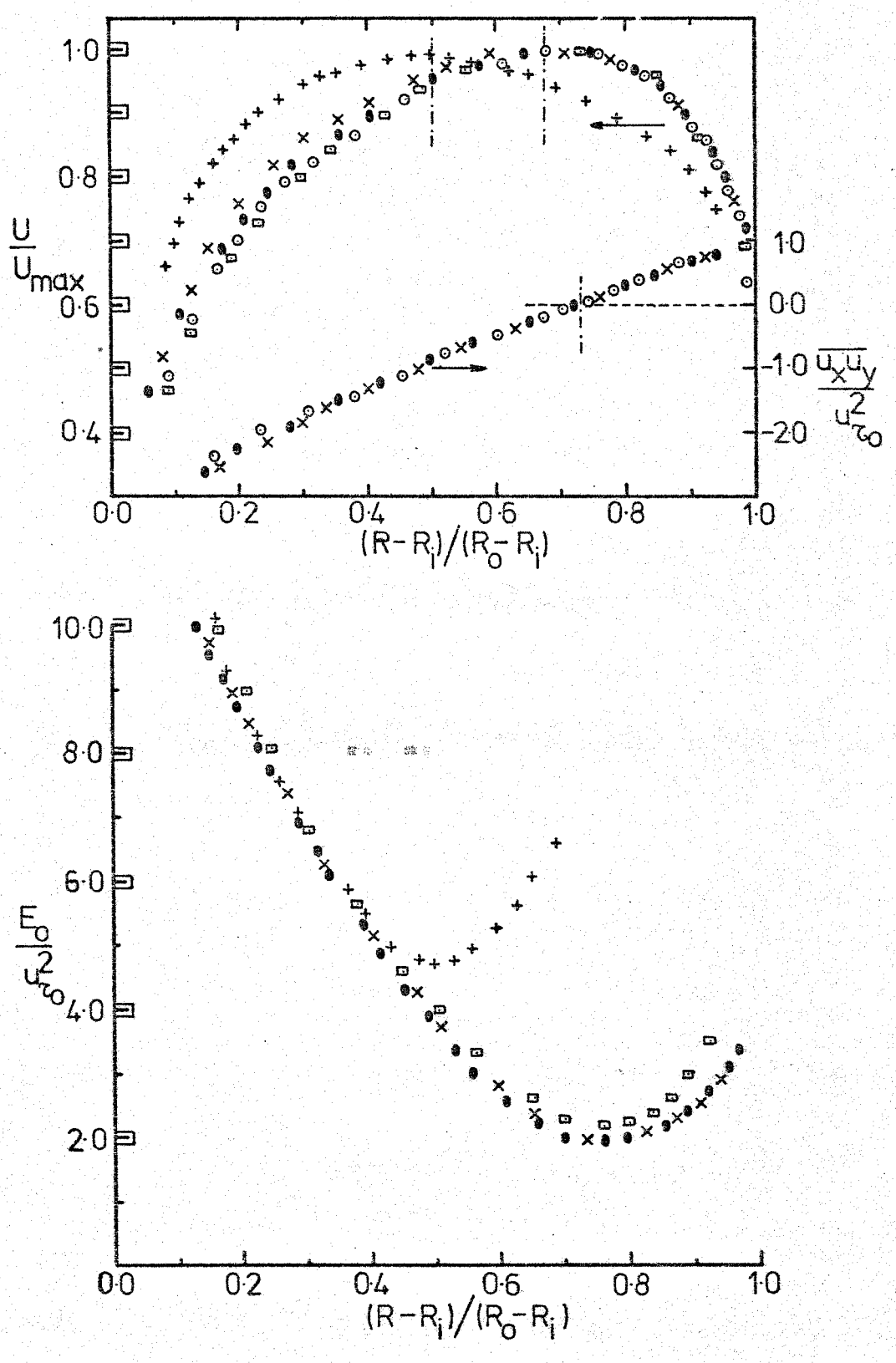

Fig. 2.3 Comparison between models of turbulence: velocity, shear stress and turbulence energy profiles in an annulus internally roughened. R_i/R_o=0.521; Re=7.1x10^4; e/D_e=0.0198.

o experiment, Lawn (1970). Predictions: • 3-eq.model;
× 2-eq. model (E_o, $\overline{u_x u_y}$); 1-eq. model + ;
▫ 2-eq. model (E_o, ε).

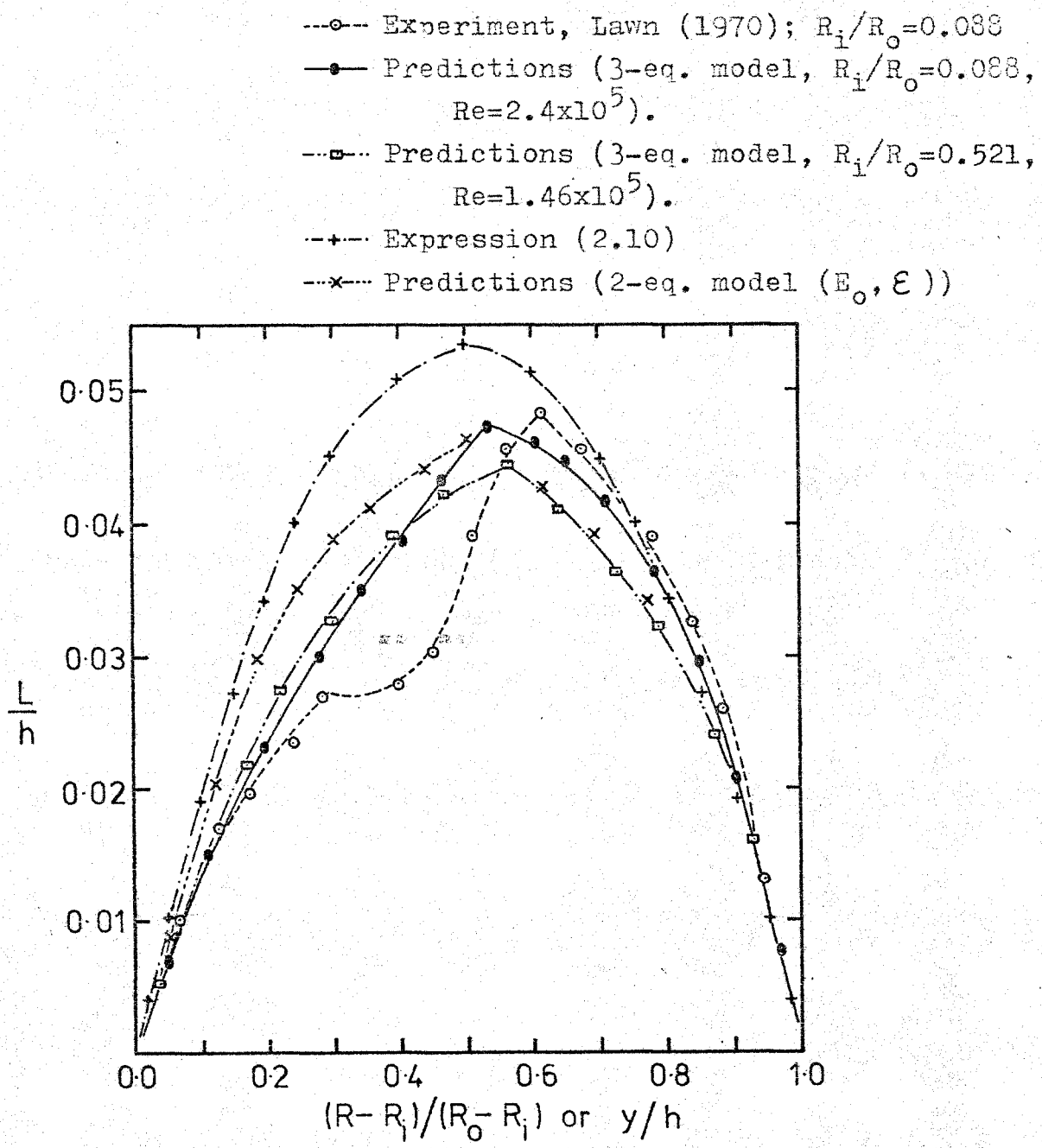

Fig. 2.4 Length scale variation in a smooth annulus.

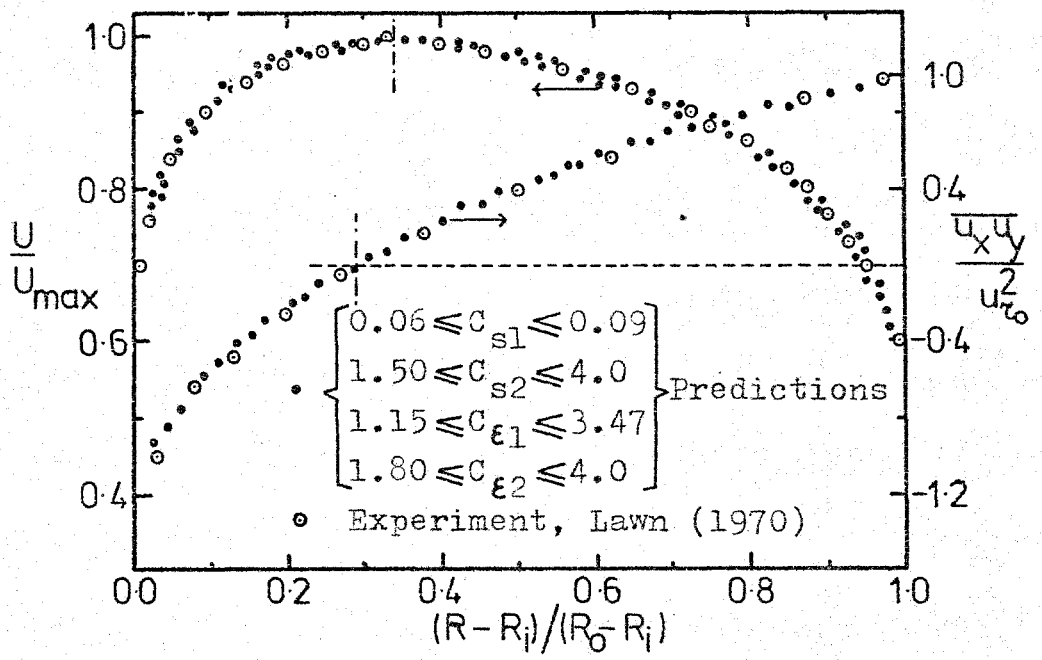

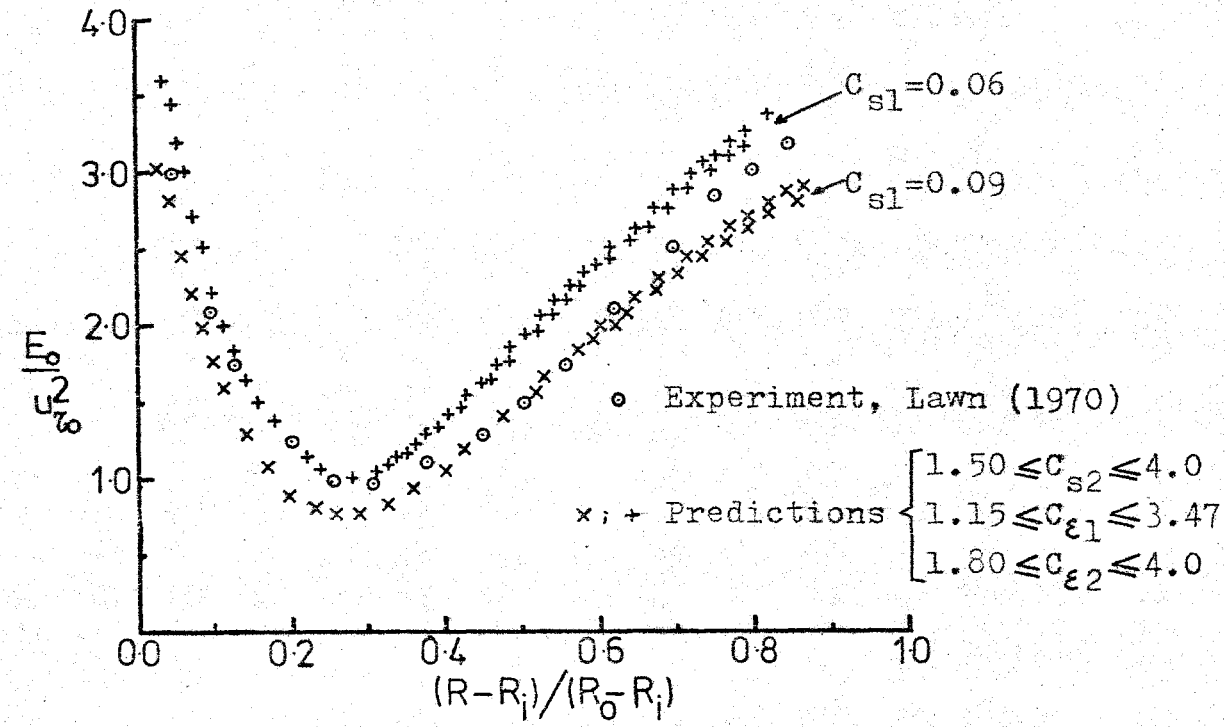

Fig. 3.1 Influence of constants C_{s1}, C_{s2}, $C_{\varepsilon 1}$ and $C_{\varepsilon 2}$ in velocity, shear stress and turbulence energy profiles in a smooth annulus; R_i/R_o=0.088 ; Re=2.4×10^5; Prandtl-Schmidt numbers from 0.5 to 1.1

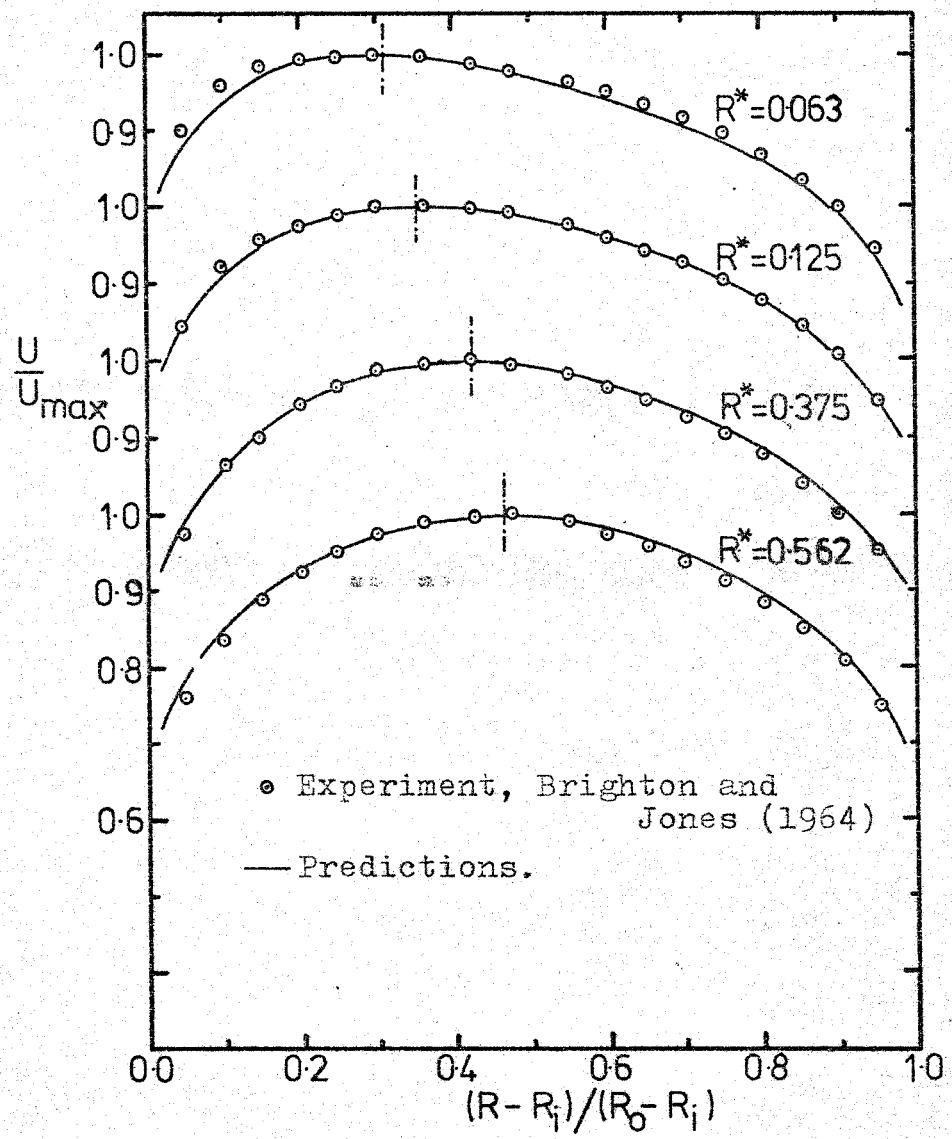

Fig. 3.2 Mean velocity distribution in a smooth annulus, varying radius ratio. $1.46 \times 10^5 \leqslant Re \leqslant 3.27 \times 10^5$.

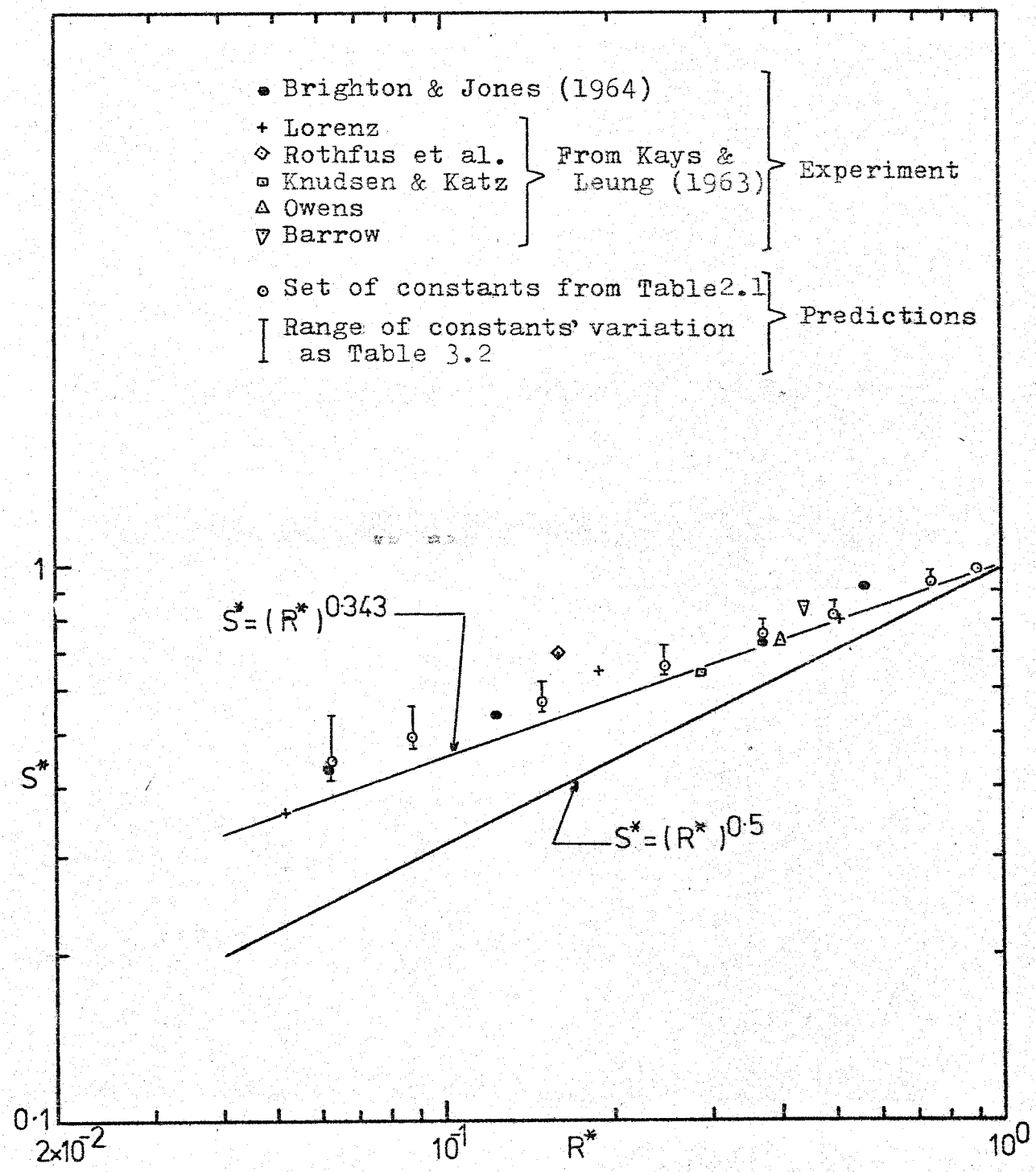

Figure 3.3 : Experimental and predicted data on the point of maximum velocity for turbulent flow in smooth annulus. $1.0 \times 10^4 \leq Re \leq 7.0 \times 10^5$.

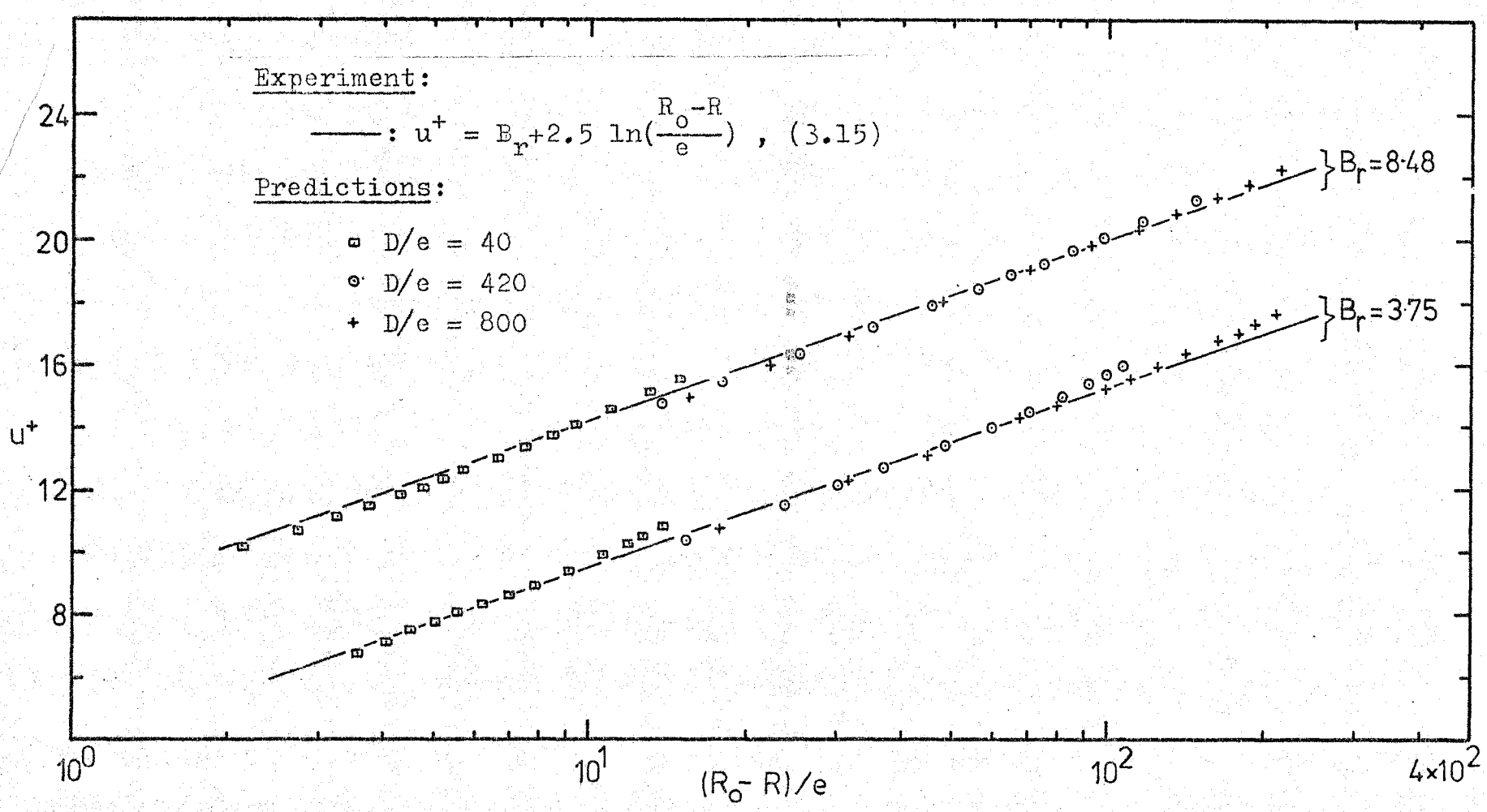

Figure 3.4 Non-dimensional velocity profile in a sand roughened pipe with different degrees of roughness. Re=5.0×10^5 .

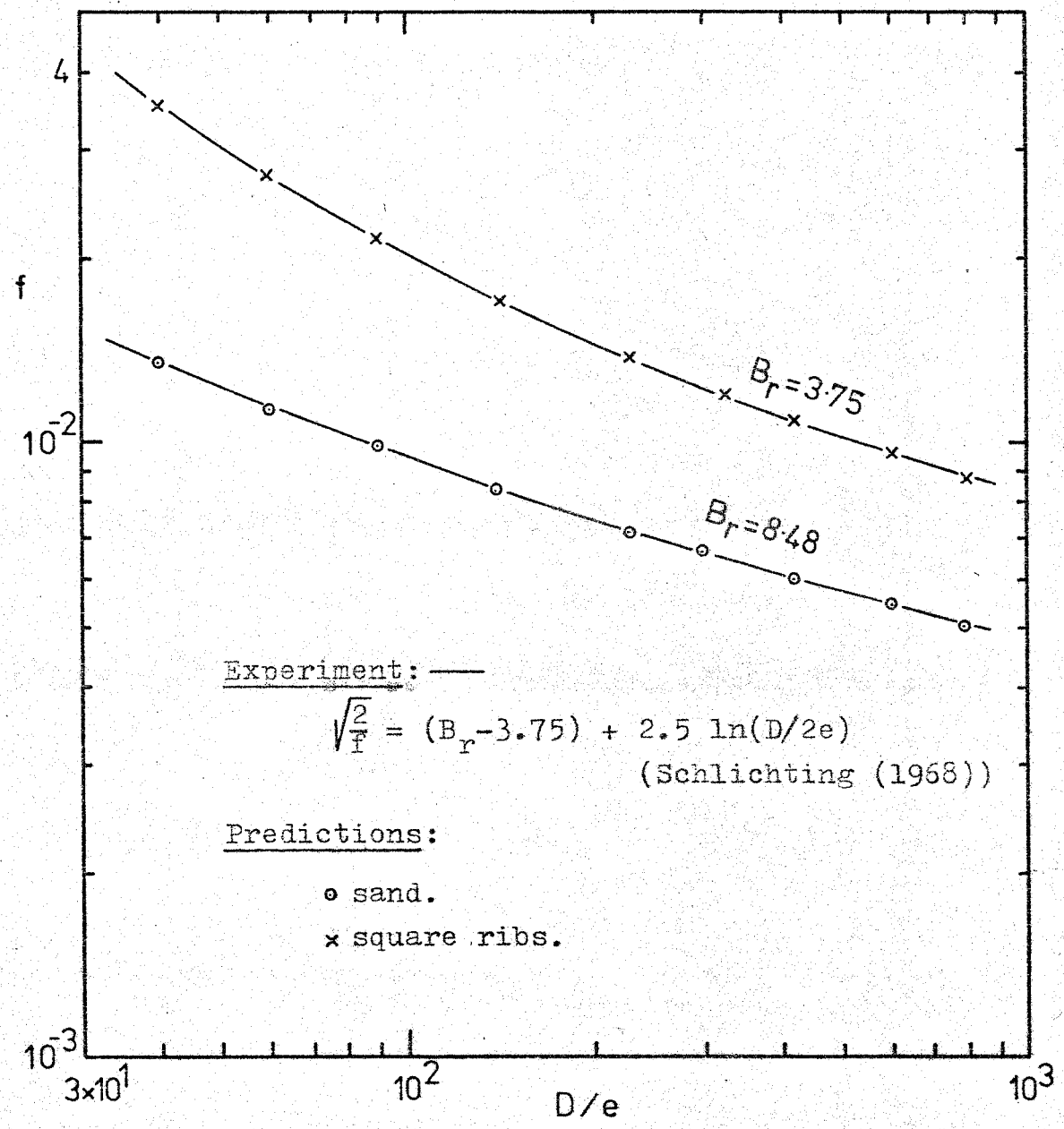

Fig. 3.5 Friction factors in a turbulent pipe flow with sand and square ribs roughness. $Re=5.0\times10^{5}$.

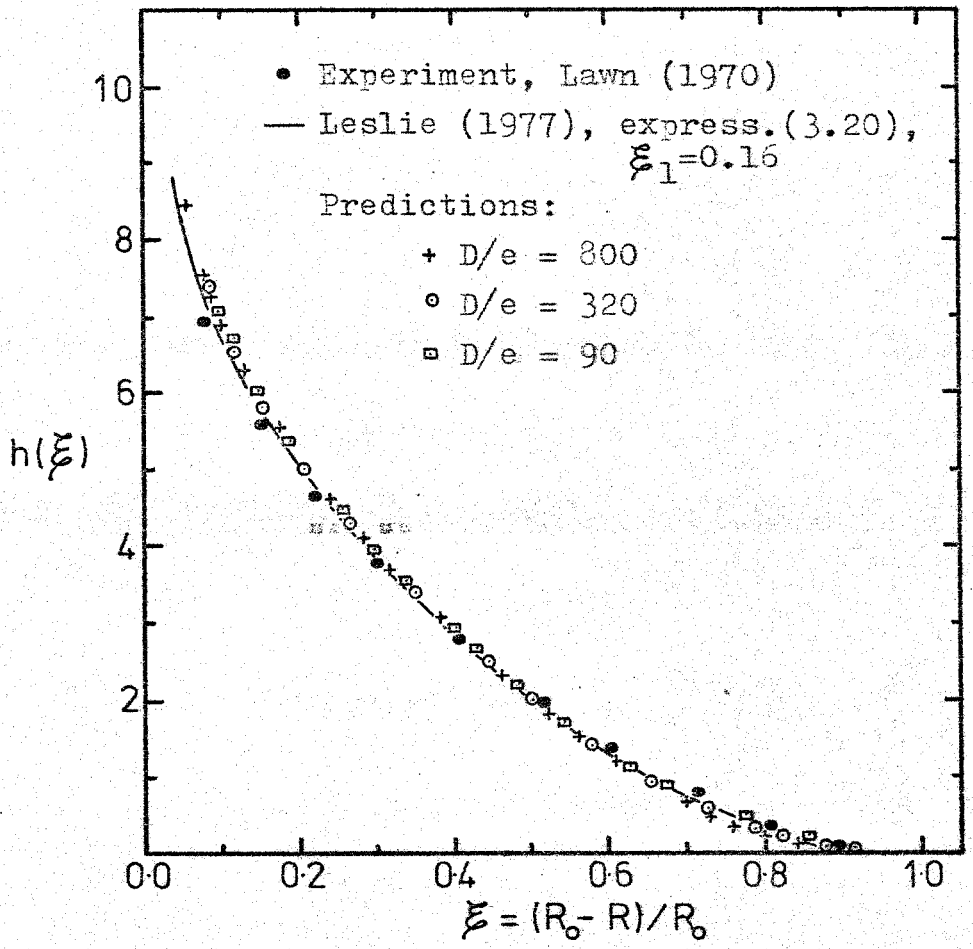

Fig. 3.6 Defect function ($h(\xi)$) in a pipe with sand roughness. $Re=5.0\times10^5$.

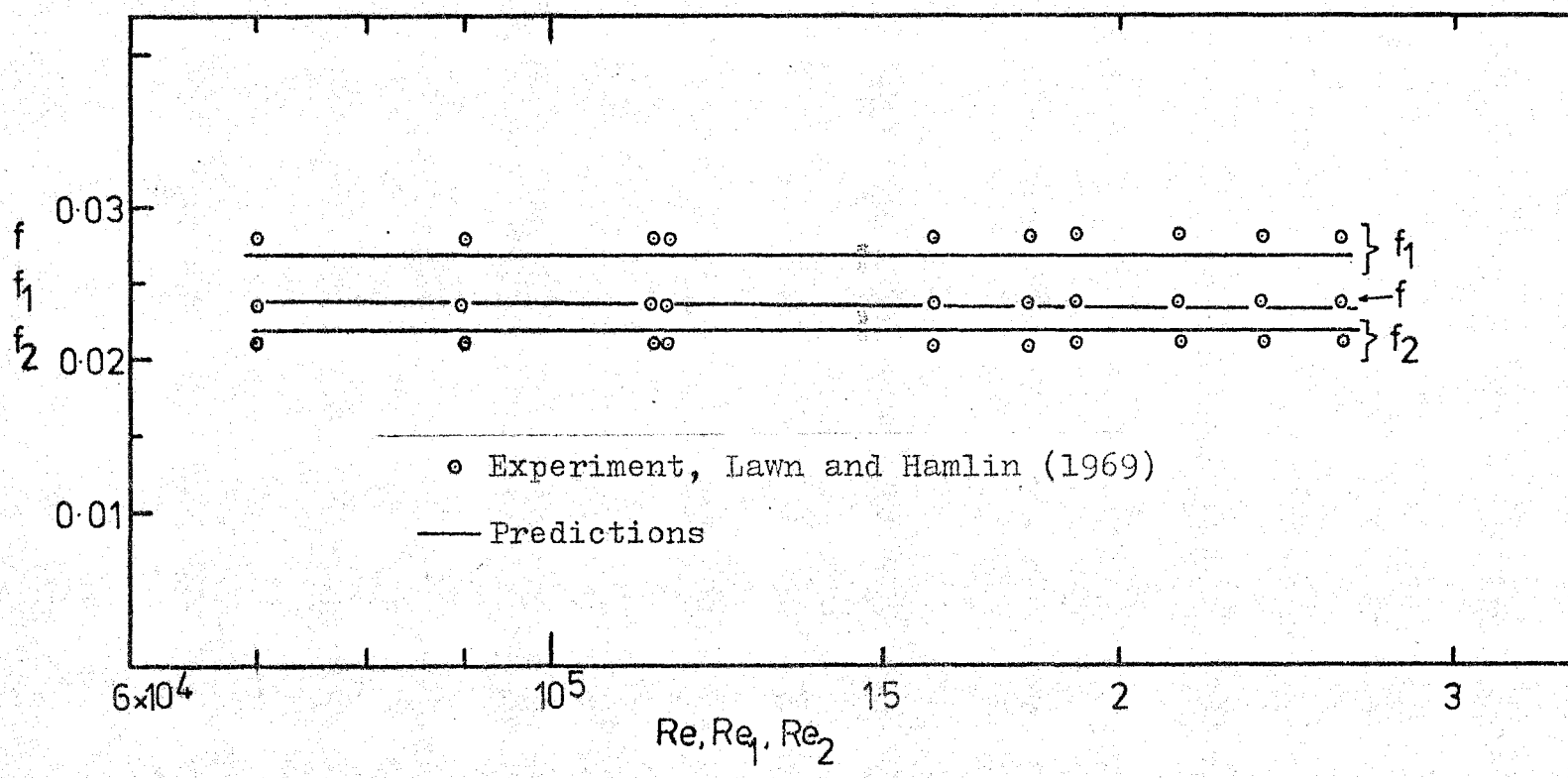

Figure 3.7 Friction factors in an annulus roughened on both sides.
R_i/R_o=0.405 ; De/e=113.64 .

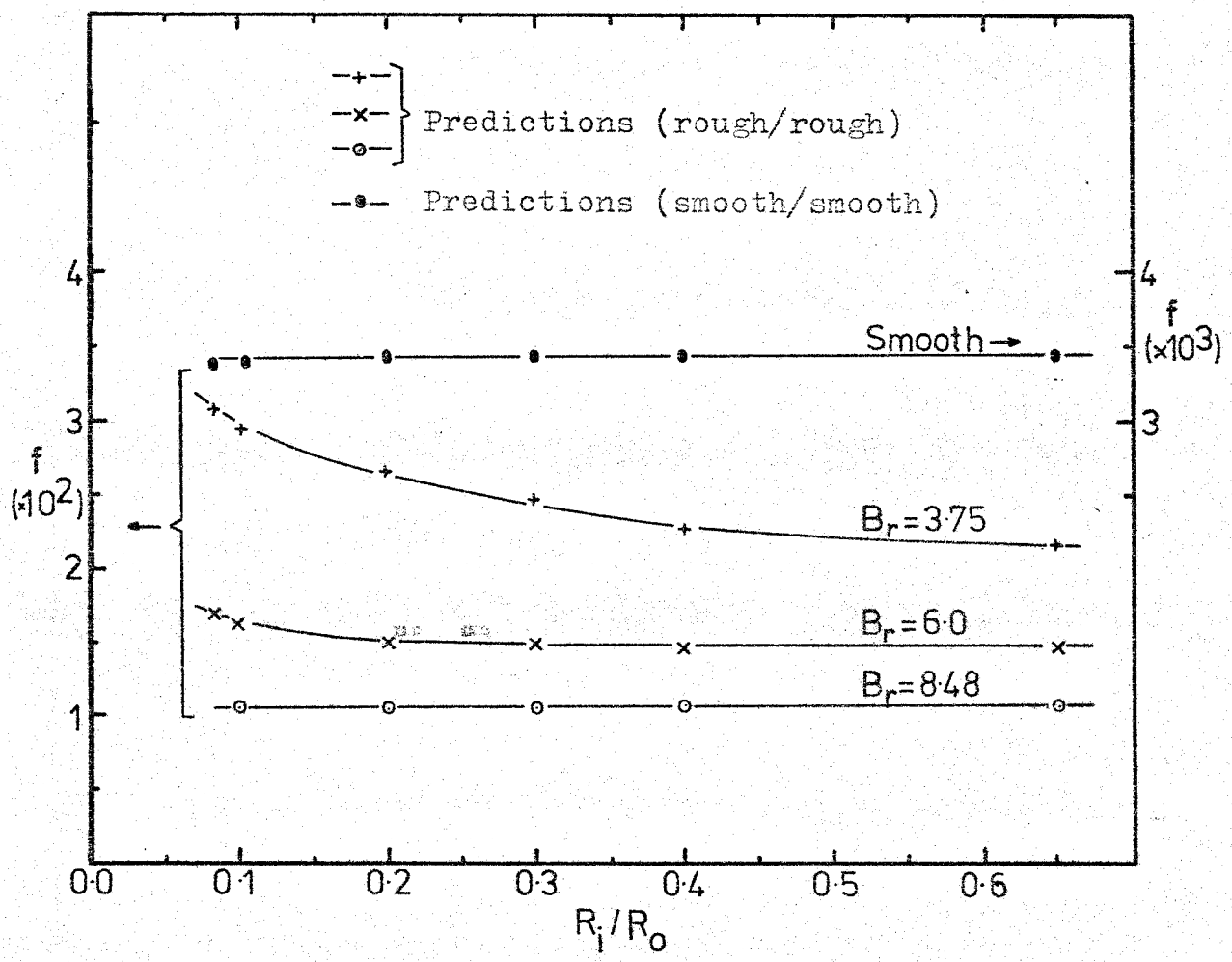

Fig. 3.8 Radius ratio (R_i/R_o) influence on friction factors in rough/rough and smooth/smooth annuli. Re = 5.0×10^5; D_e/e = 100 .

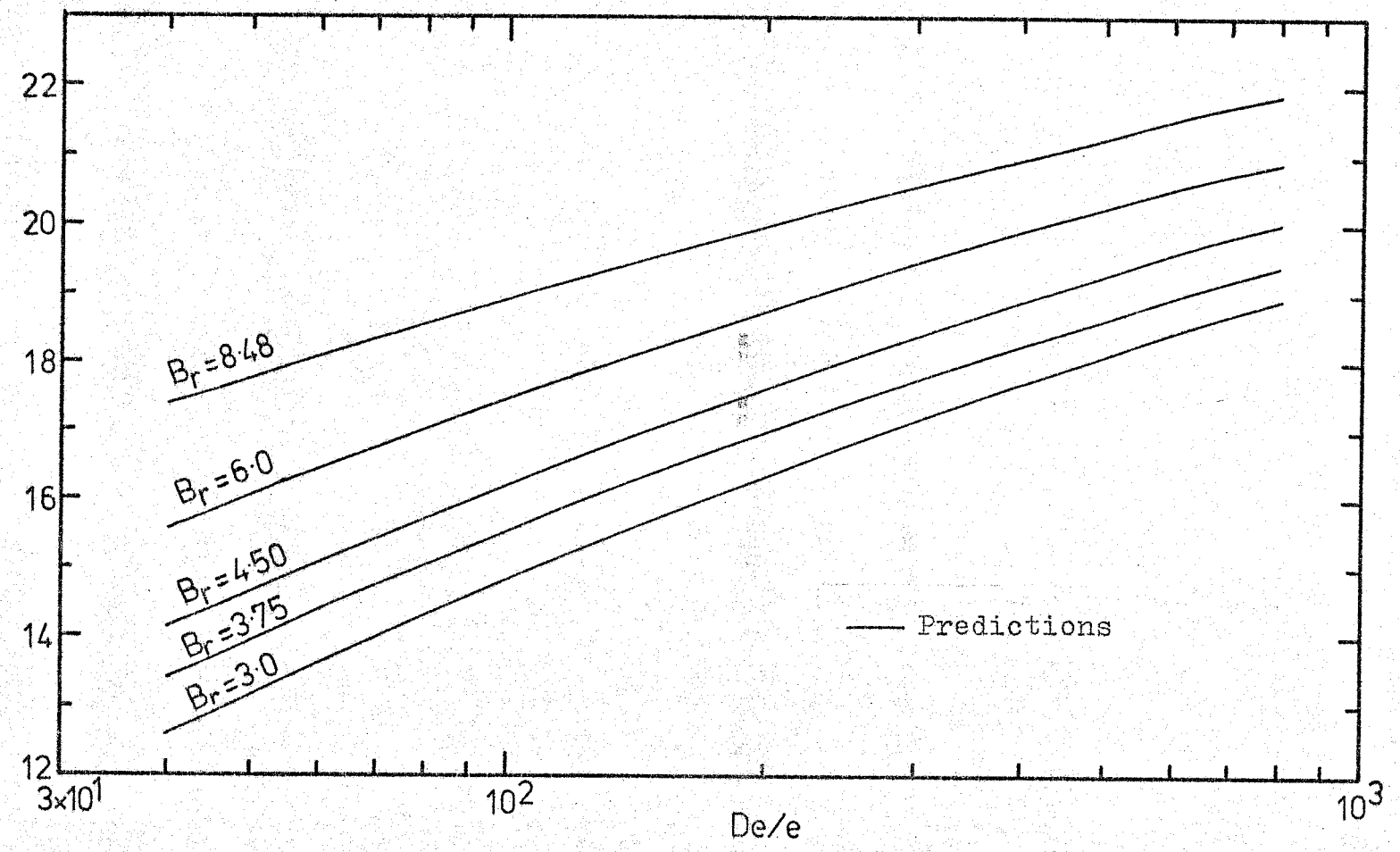

Figure 3.9 Variation of overall friction factor ($\sqrt{2/f}$) with roughness ratio (De/e) in an annulus internally roughened. Re=5.0x10^5; R_i/R_o=0.5 .

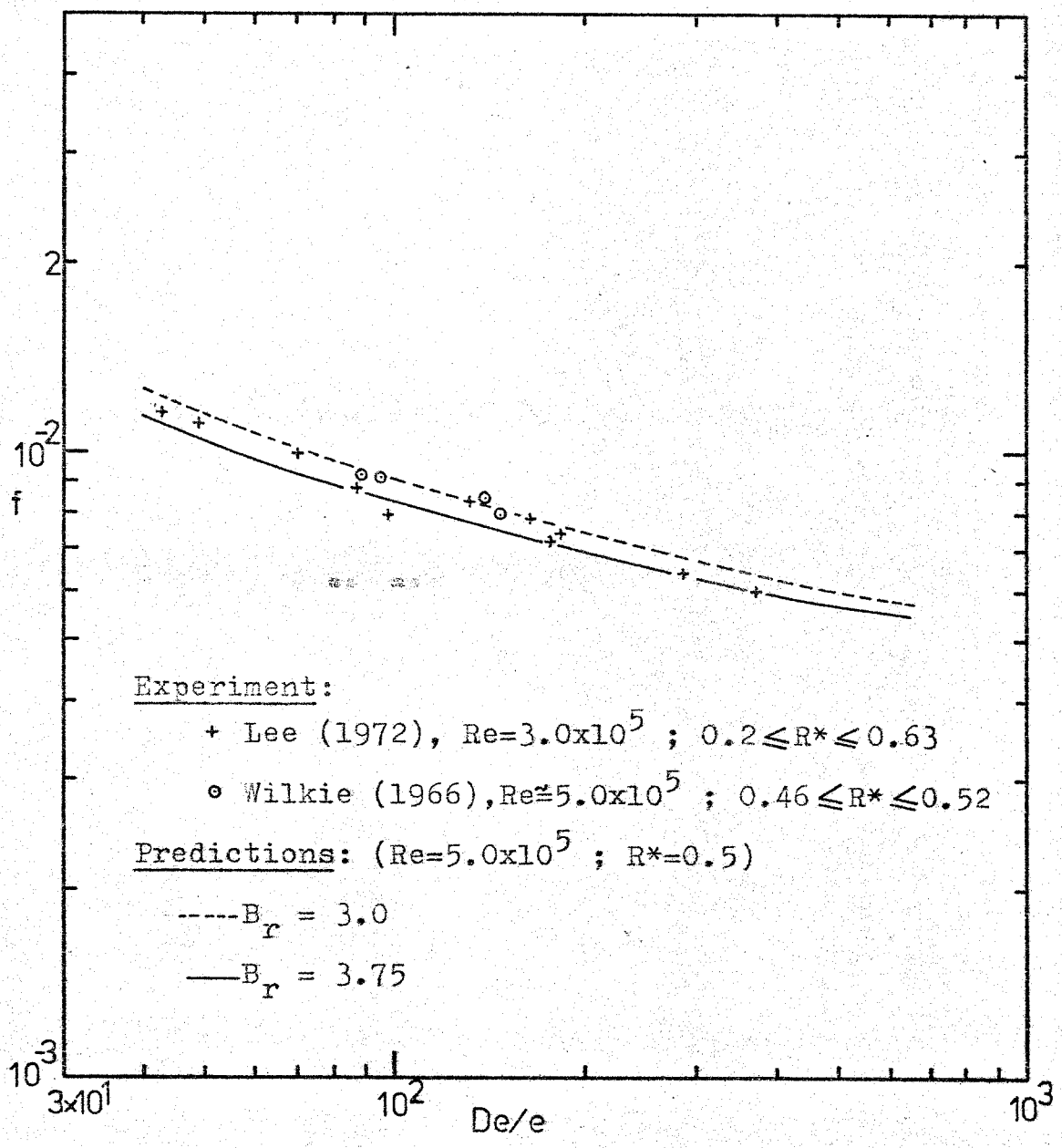

Fig. 3.10 Comparison between experimental and predicted overall friction factors in an annulus internally roughened.

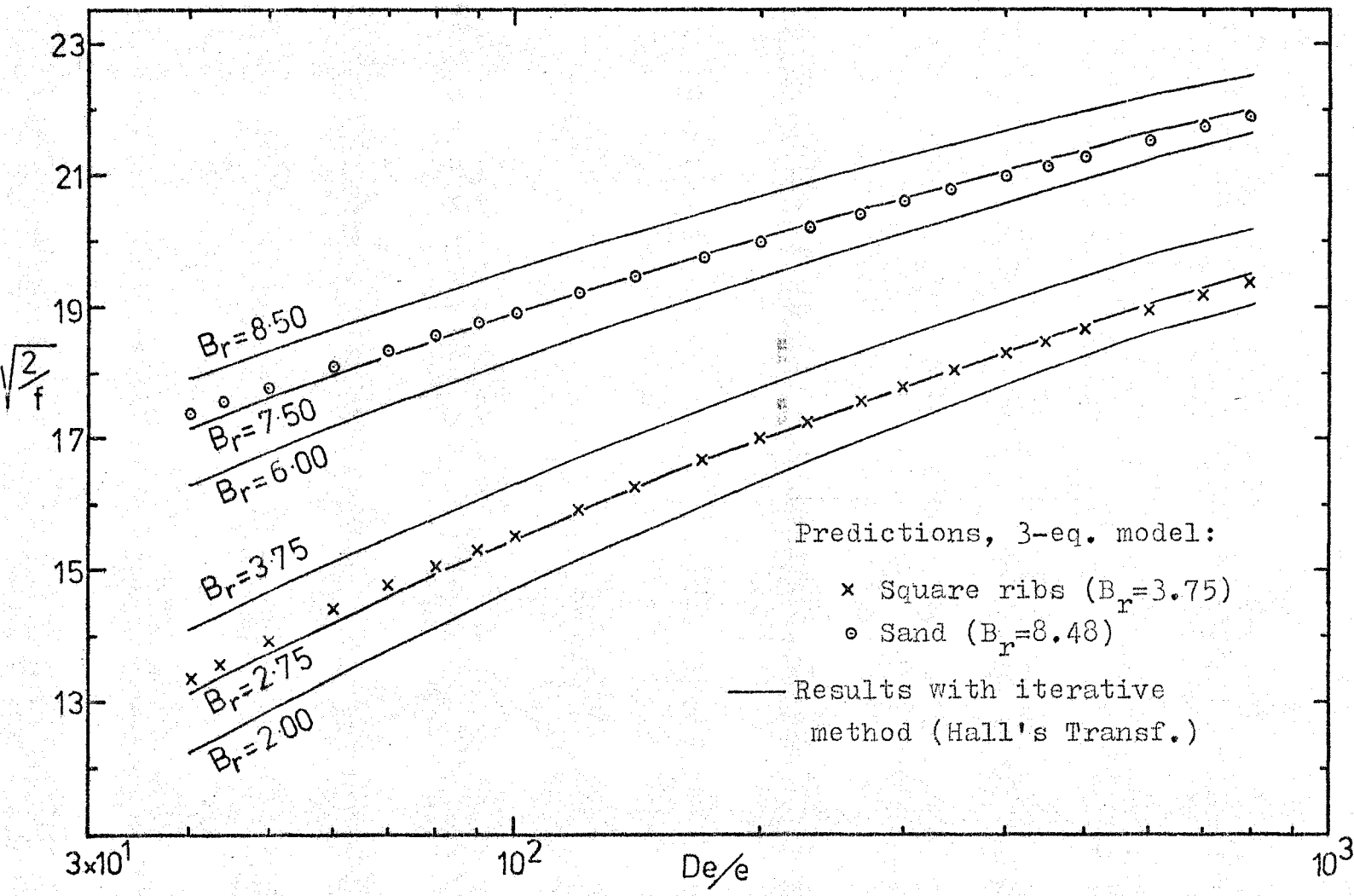

Figure 3.11 Friction factors obtained with the 3-equation model compared with friction factors obtained using iterative method, in an annulus internally roughened. Re=5.0×10^5 ; R*=0.5 .

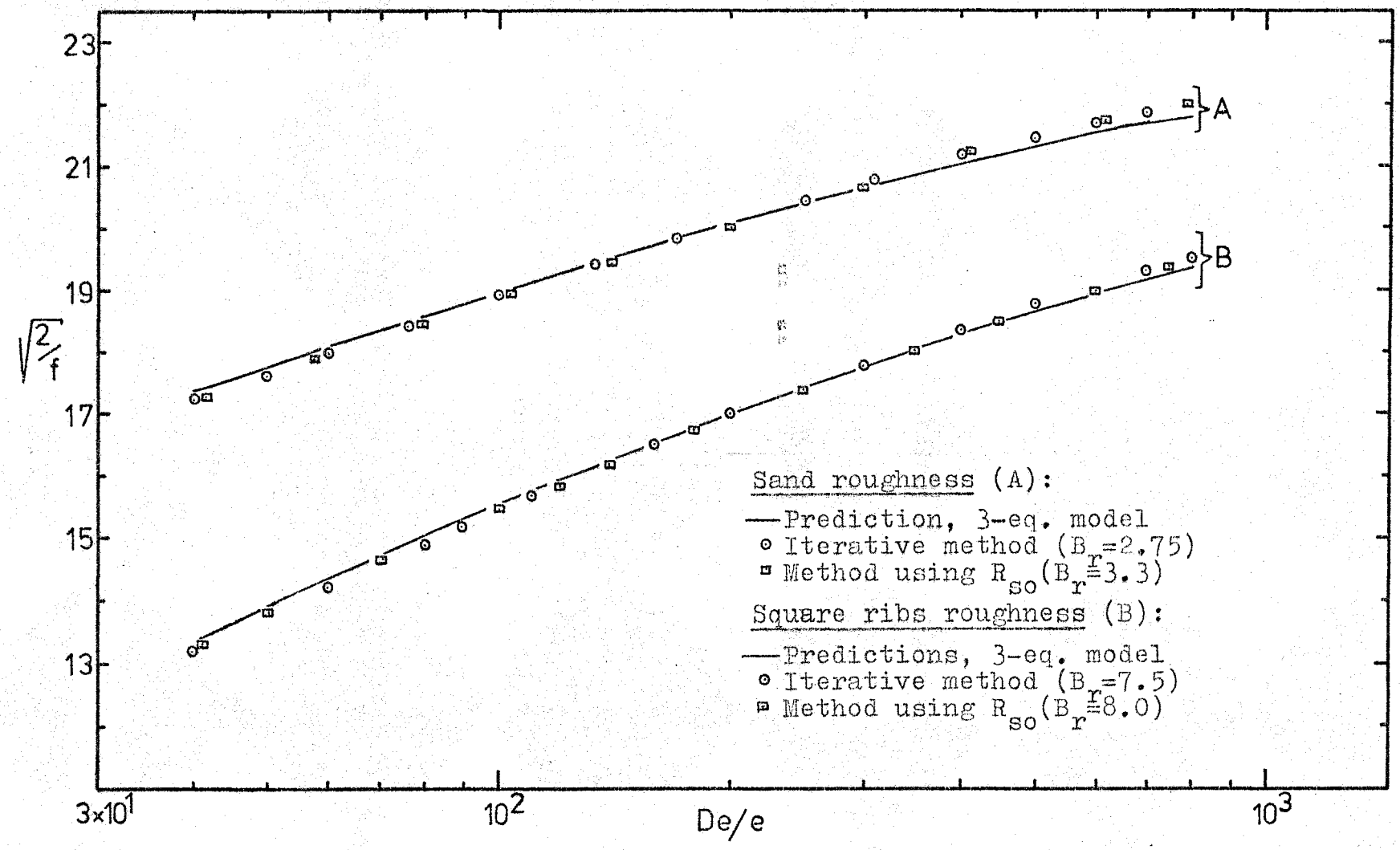

Figure 3.12 Overall friction factors obtained with the 3-equation model compared with friction factors obtained using Hall's transformation in an annulus internally roughened.

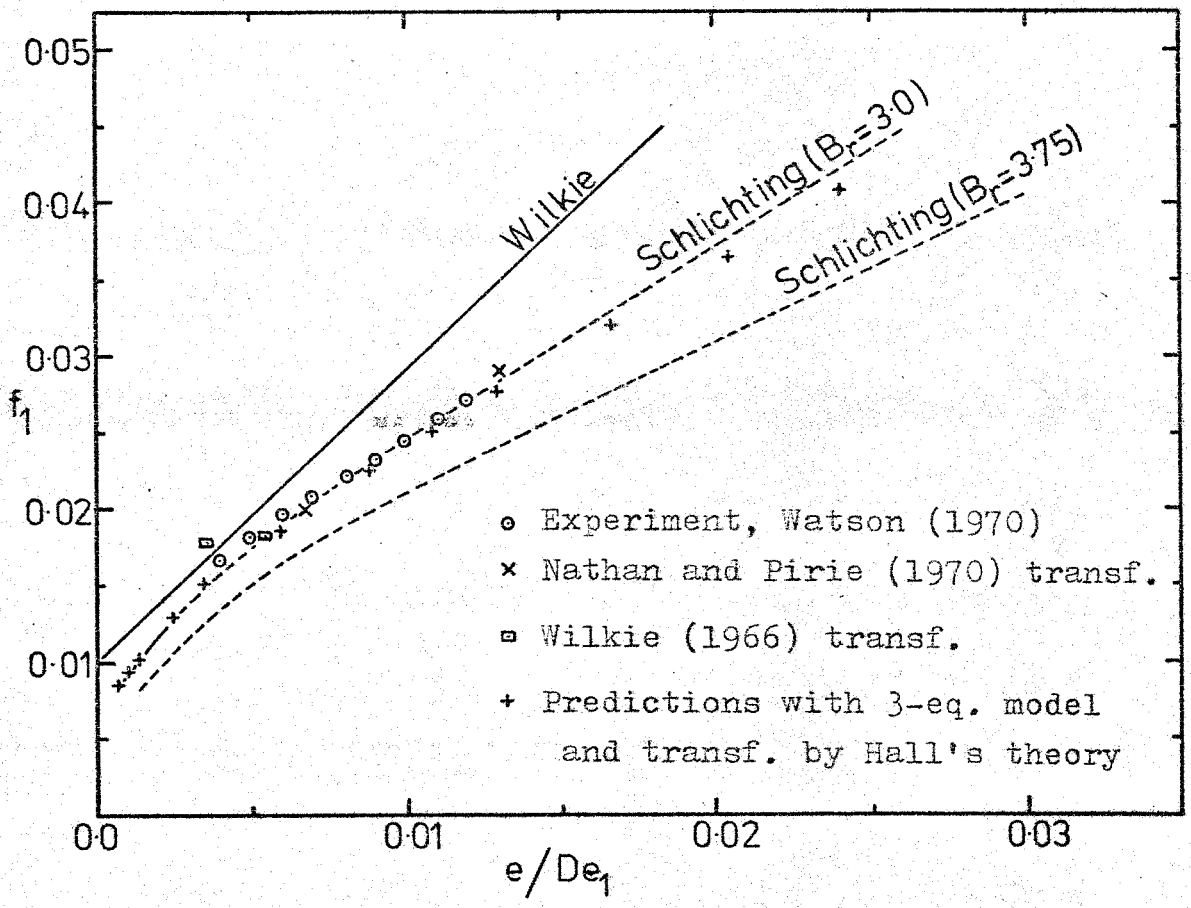

Fig. 3.13 Transformed friction factors in an annulus internally roughened: square ribs. Re = 5.0×10^5; $R^* = 0.5$. ----- Schlichting relation (3.18) —— Wilkie relation (3.39).

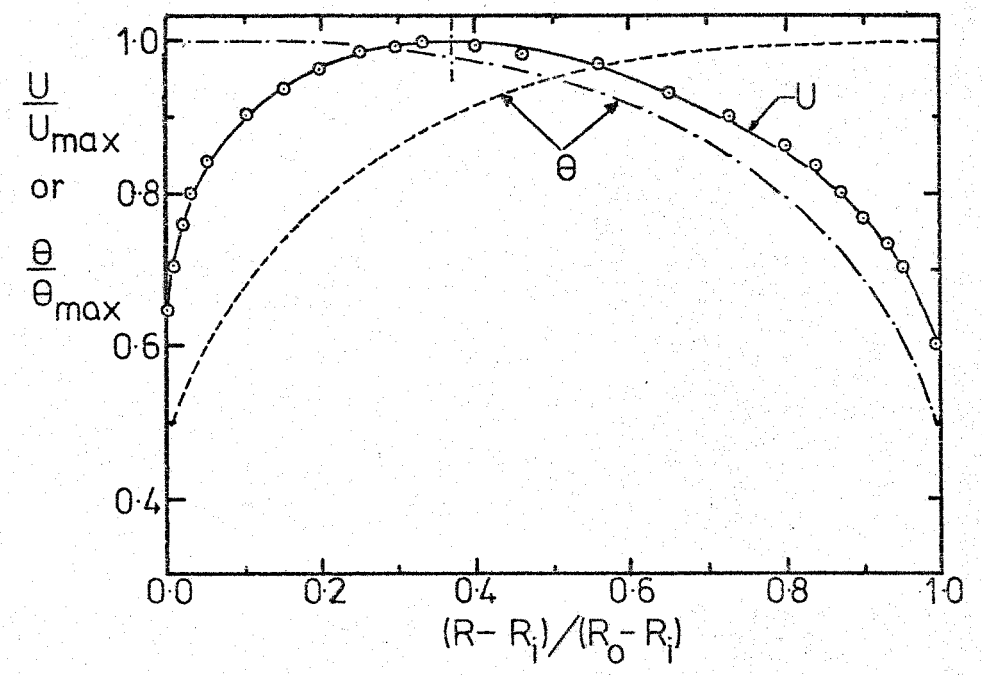

Fig. 4.1 Velocity and temperature profiles in a smooth annulus: inner wall heated (or cooled) and outer wall insulated Pr=0.7 ; Re=1.0x10^5 ; R*=0.18 and θ_{max}=30 °C .
Velocity: ⊙ Experiment, Lawn (1970) ; —— Predictions.
Temperature: ------ Predictions (internal wall cooled)
—·—· Predic. (external wall heated or cool.)

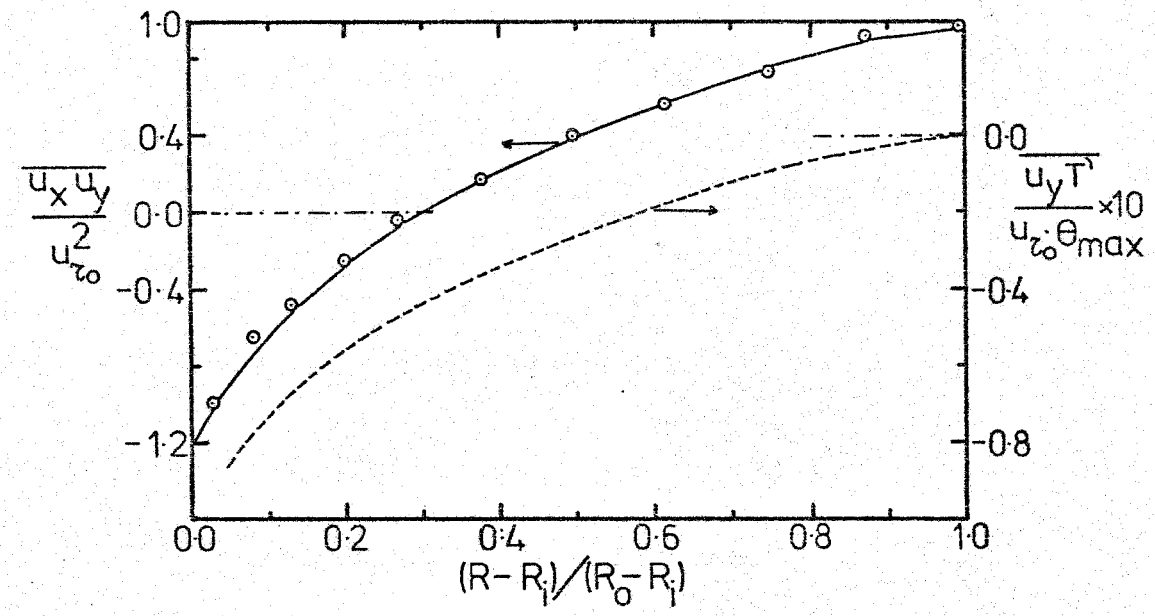

Fig. 4.2 Shear stress and convective heat flux profiles in symmetric smooth annulus with small radius ratio.
Shear stress ($\overline{u_x u_y}$): ⊙ Experiment, Lawn (1970); —— Predictions.
Convective heat flux ($\overline{u_y T'}$):---- Predictions.

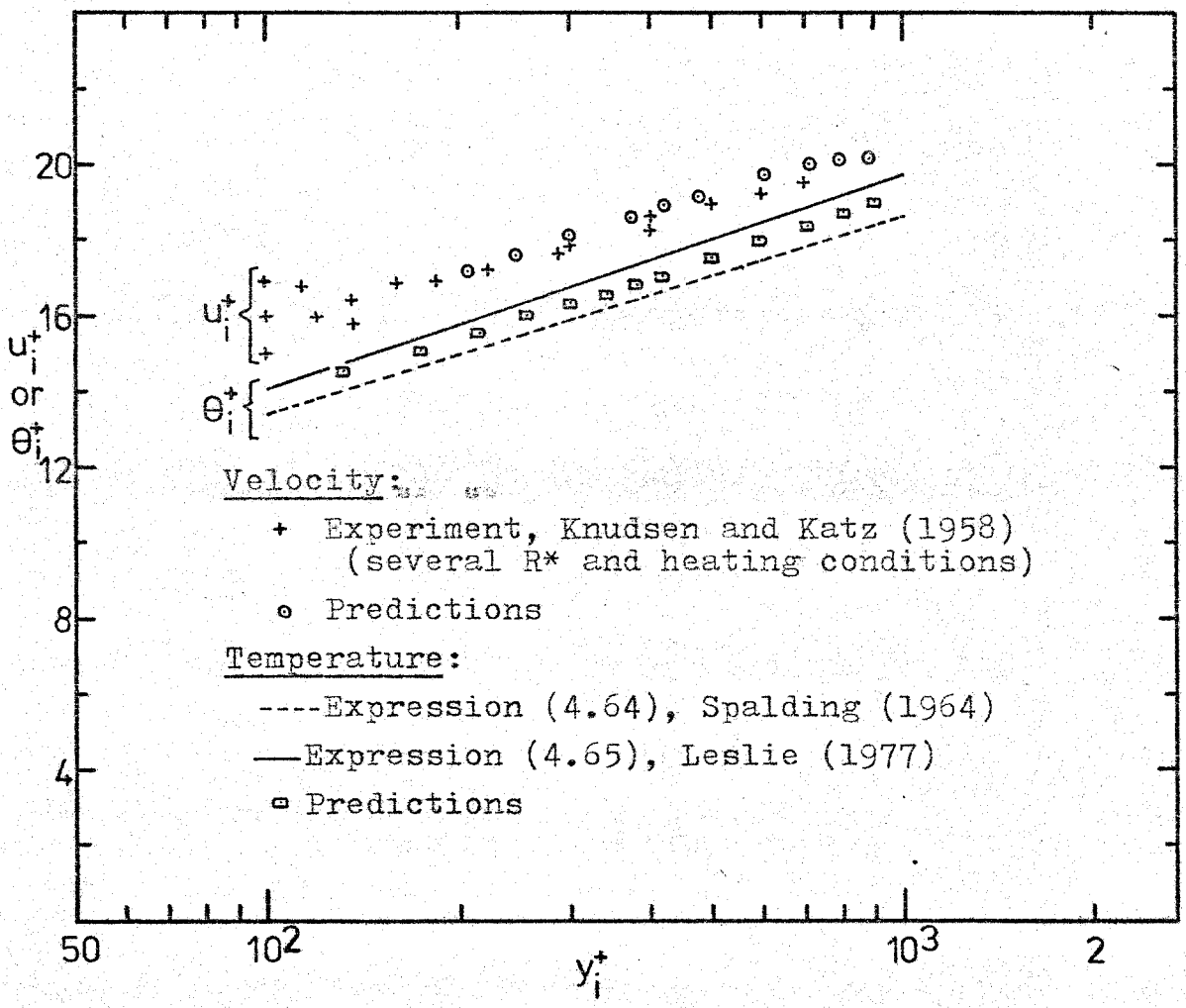

Fig. 4.3 Non-dimensional velocity (u_i^+) and temperature (θ_i^+) profiles for the inner portion of a smooth annulus with small radius ratio. Pr=0.7 ; Re=1.0x10^5 ; R*=0.18 ; θ_{max}=30 ^oC .

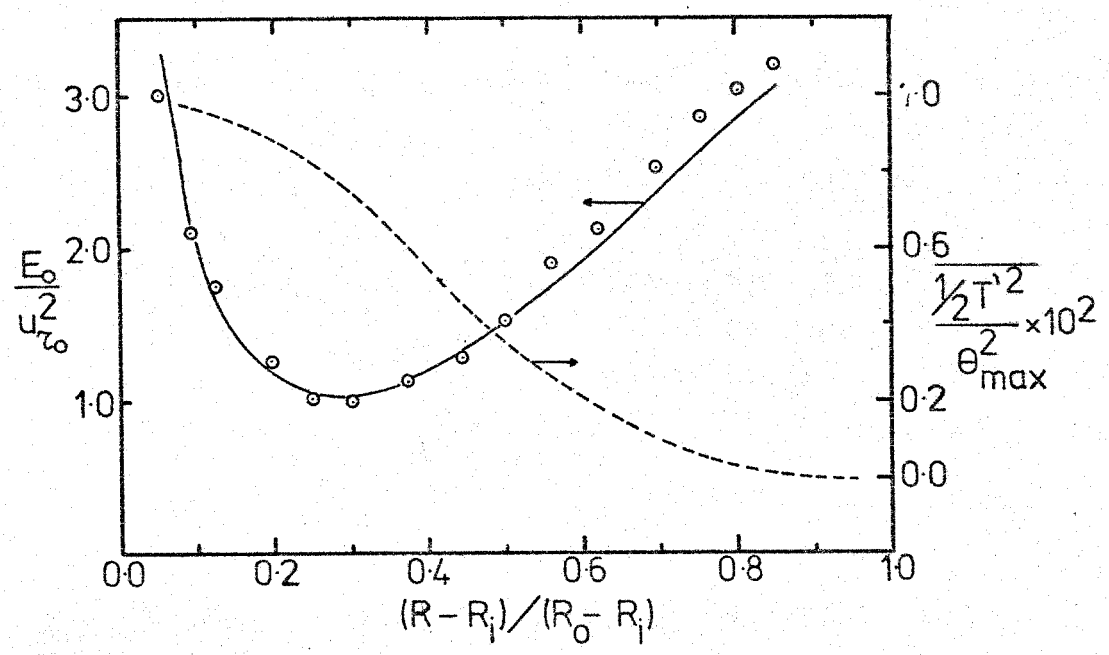

Fig. 4.4 Turbulence energy and intensity of temperature profiles in a symmetric annulus: inner wall heated (or cooled) and outer wall insulated.
Turbulence energy (E_o): ∘ Experiment, Lawn (1970). —— Predictions.
Intensity of temperature ($1/2T'^2$):---- Predictions.

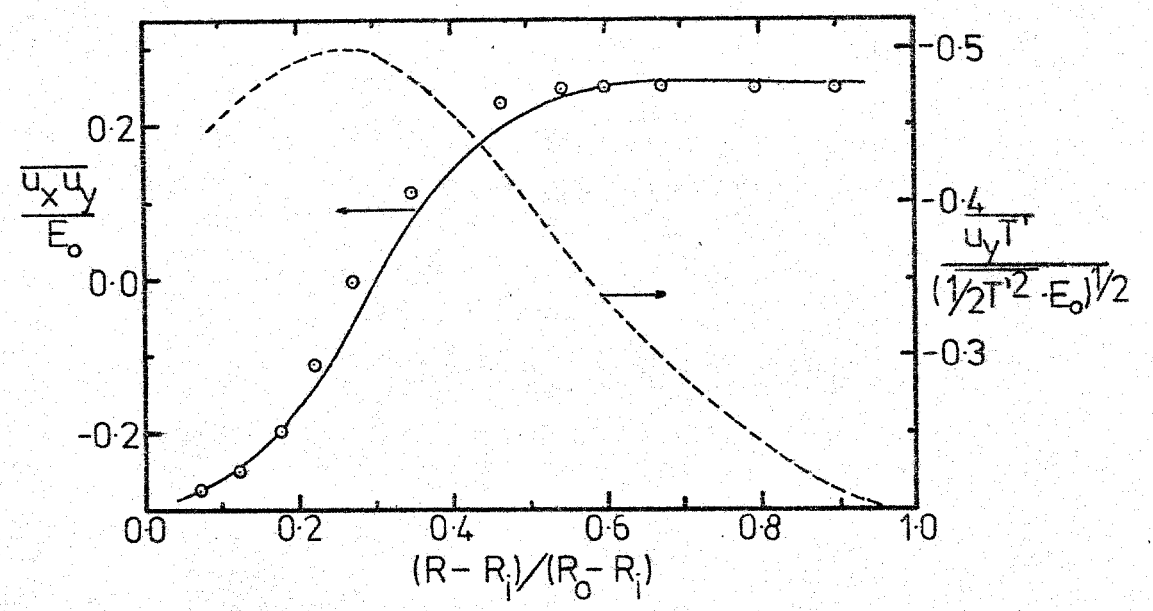

Fig. 4.5 The ratios shear stress/turbulence energy and convective heat/(intensity of temperature x turbulence energy) in a smooth annulus.
Shear stress ($\overline{u_x u_y}/E_o$): ∘ Experiment, Lawn (1970). —— Predictions.
Convective heat:------Predictions.

(1) Production: $(-\overline{u_x u_y}\frac{\partial U}{\partial y})(R_o-R_i)/u_{\tau o}^3$

(2) Dissipation: $(\varepsilon.(R_o-R_i))/u_{\tau o}^3$

(3) Diffusion: $(\frac{\partial}{\partial y}(\nu_{eff})\frac{\partial E_o}{\partial y})(R_o-R_i)/u_{\tau o}^3$

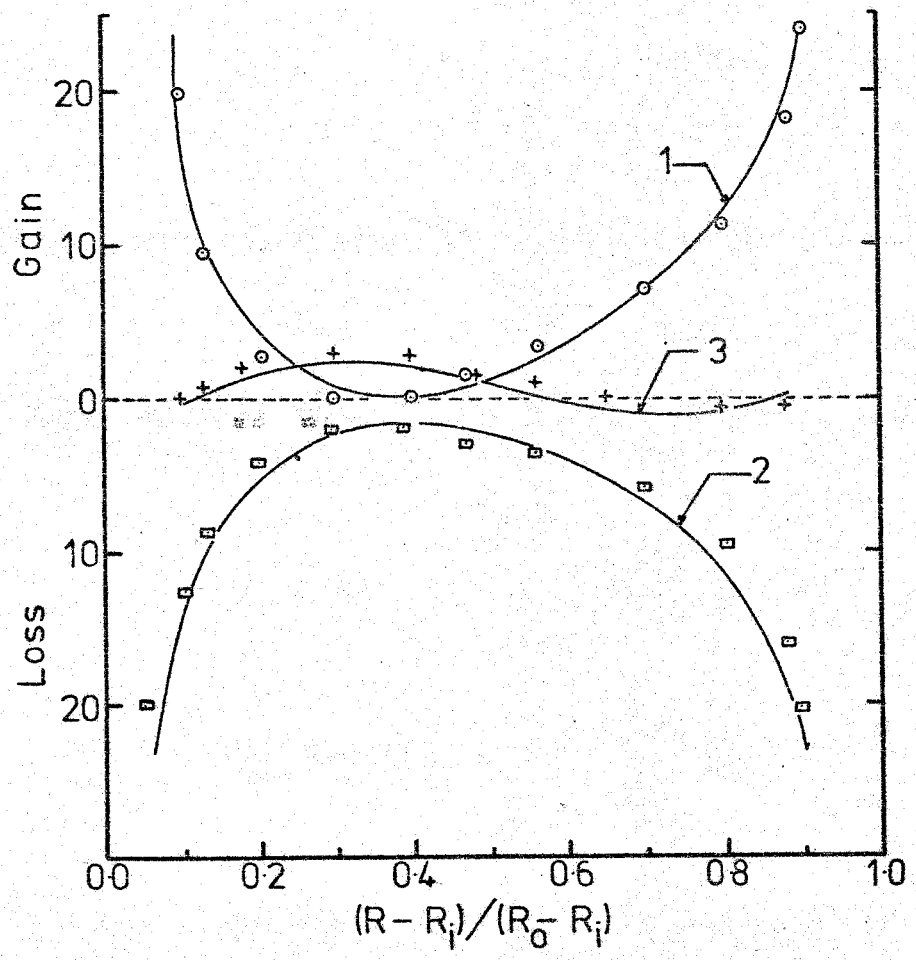

Fig. 4.6 Turbulence energy balance in a symmetric smooth annulus.

⊙ + ▫ Experiment, Lawn (1970).

——— Predictions.

(1) Production: $(-\overline{u_y T'}\frac{\partial T}{\partial y})(R_o-R_i)/u_{\tau o}.\theta^2_{max}$

(2) Dissipation: $(C_{TT1}\ \overline{\frac{1}{2}T'^2}/E_o)(R_o-R_i)/u_{\tau o}.\theta^2_{max}$

(3) Diffusion: $(\frac{\partial}{\partial y}(\gamma_{eff})\frac{\partial}{\partial y}\ \overline{\frac{1}{2}T'^2})(R_o-R_i)/u_{\tau o}.\theta^2_{max}$

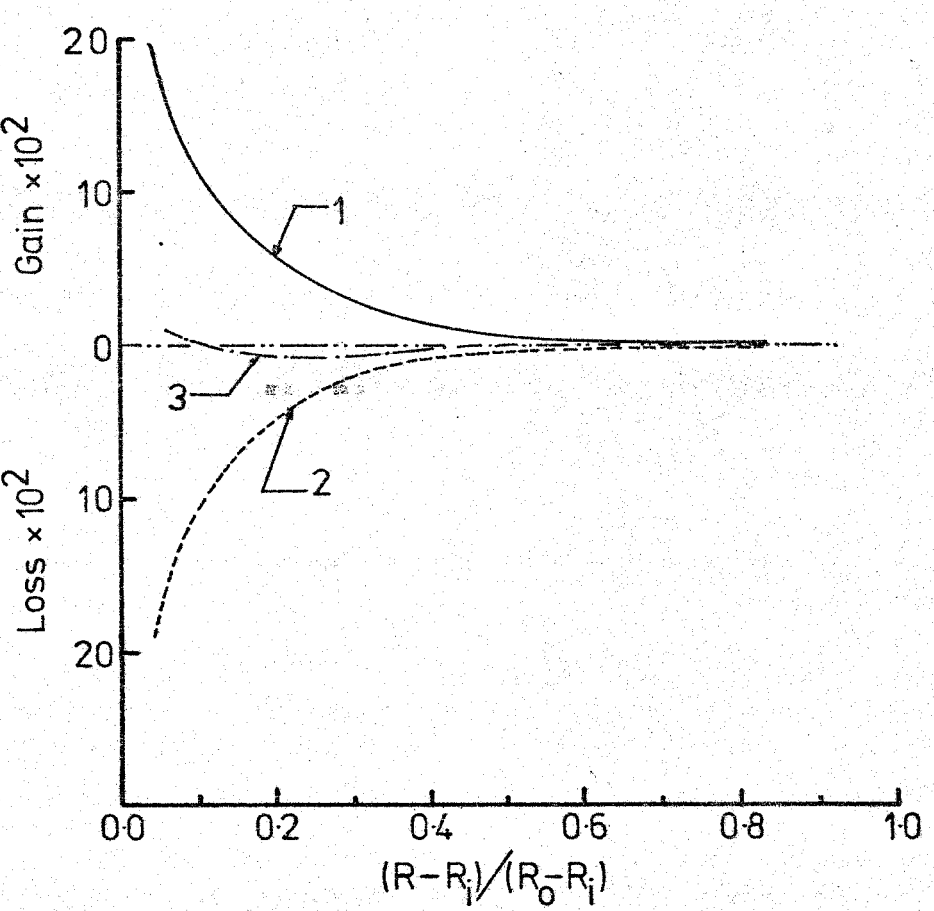

Fig. 4.7 Intensity of temperature fluctuation balance in a symmetric smooth annulus: heated (or cooled) on inner wall and insulated on outer wall.

——; —·—·; ----- Predictions.

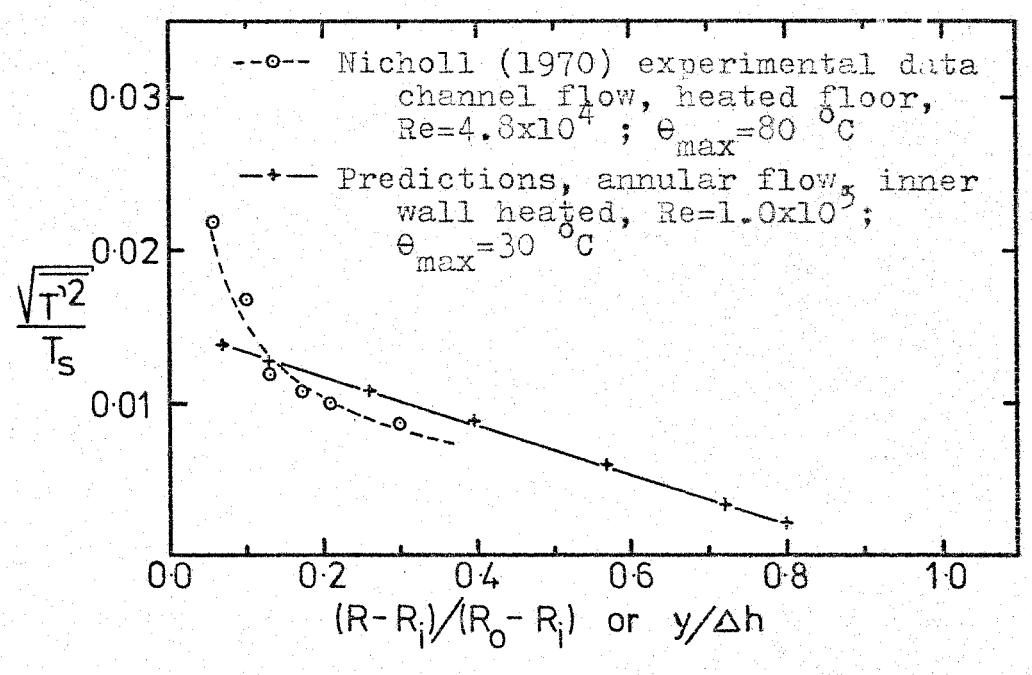

Fig. 4.8 Intensity of temperature fluctuation profiles in smooth annular and channel flows. Pr=0.7 .

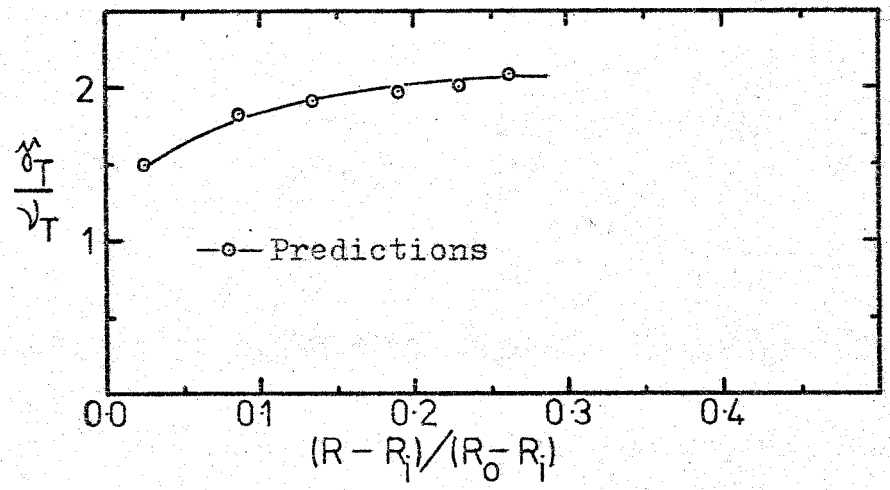

Fig. 4.9 Eddy diffusivity of heat and momentum ratio (γ_T/ν_T) in a symmetric smooth annulus: inner wall heated (or cooled) and outer wall insulated. Pr=0.7 ; Re=1.0x10^5 θ_{max}=30 °C .

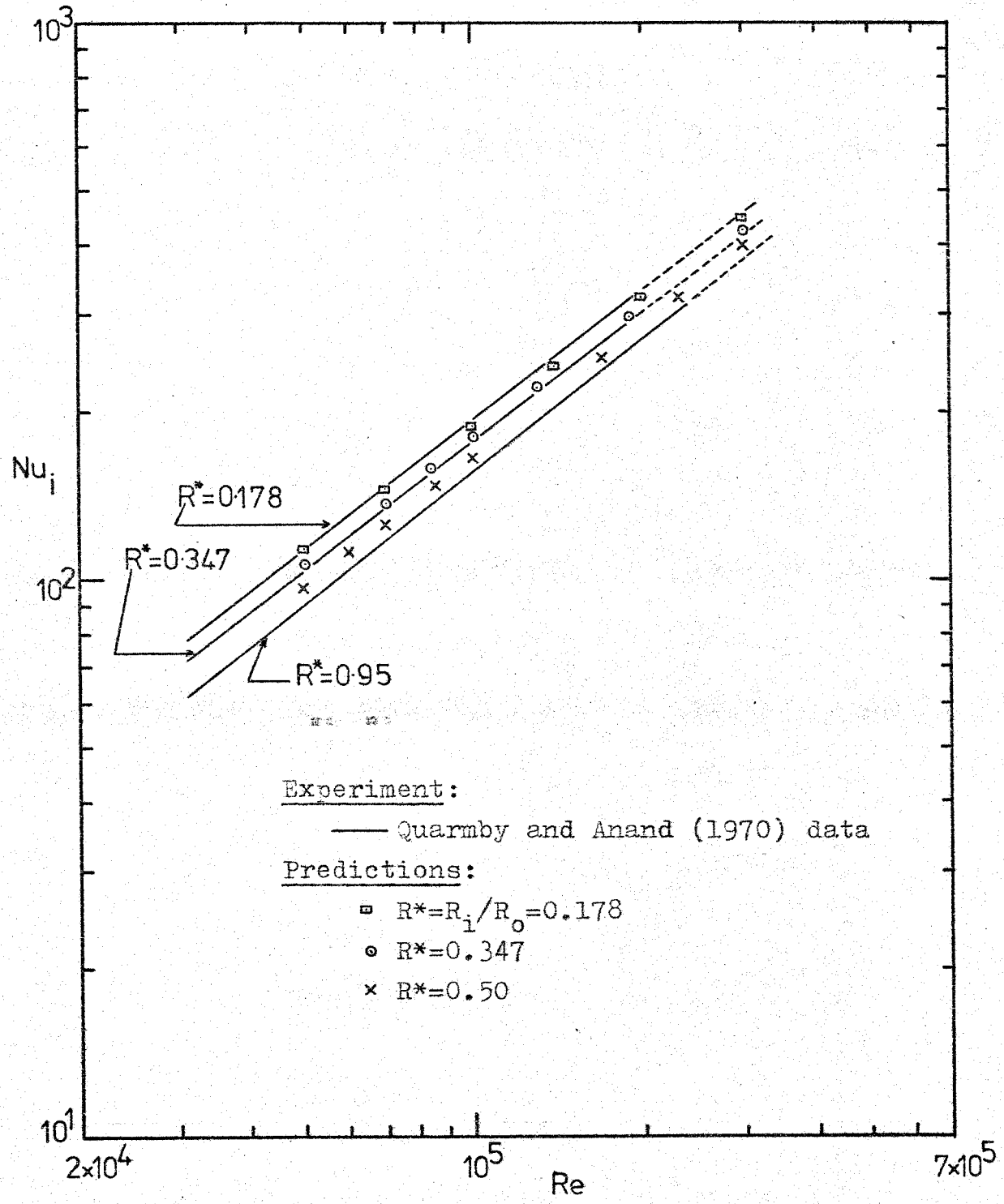

Fig. 4.10 Fully developed Nusselt numbers for the inner wall of a turbulent flow in a smooth annulus: heated (or cooled) on the inner side; constant wall temperature. Pr=0.7 ; θ_{max}=30 °C .

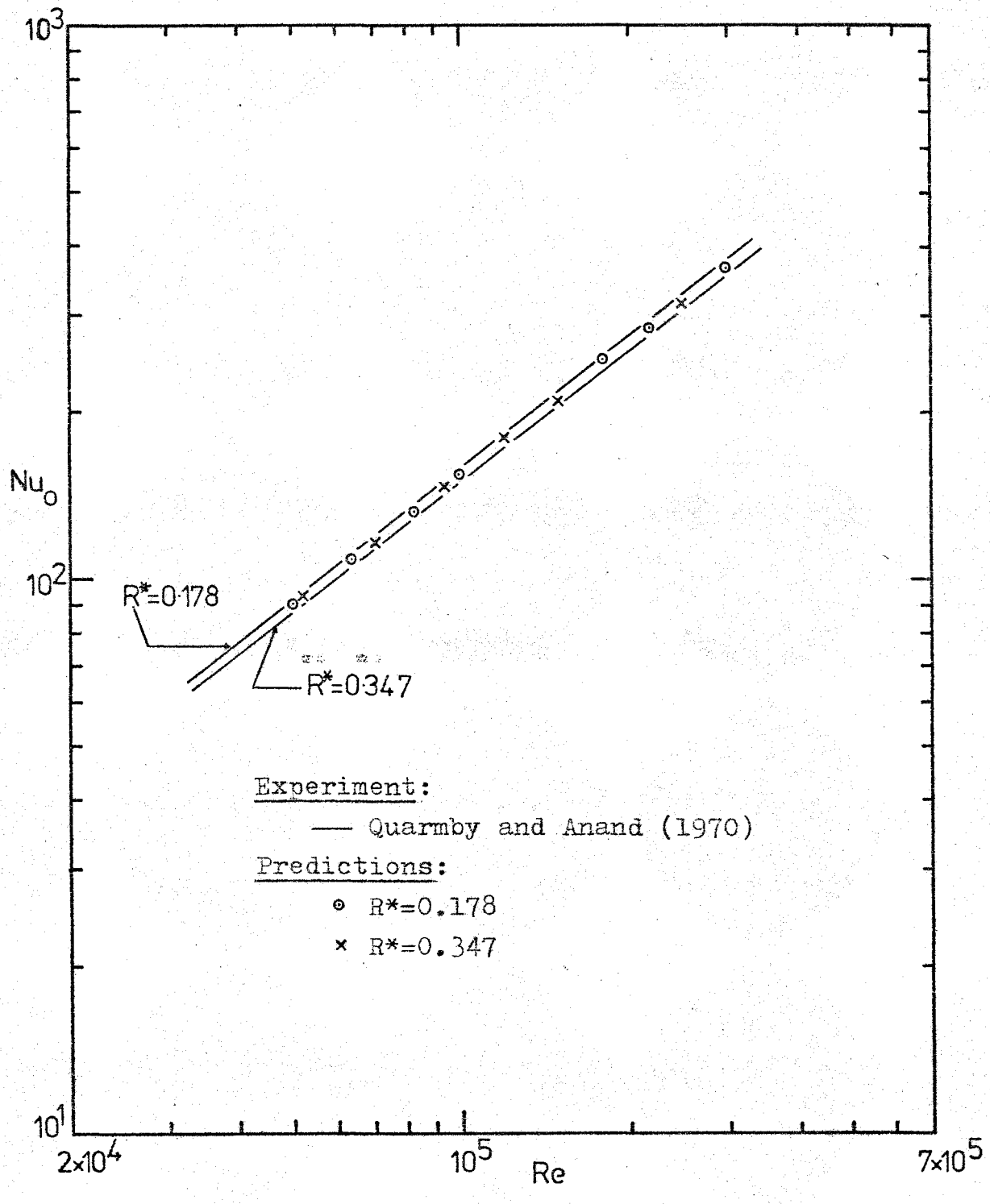

Fig. 4.11 Fully developed Nusselt numbers for the outer wall of a turbulent flow in a smooth annulus: heated (or cooled) on the outer side; constant wall temperature. Pr=0.7 ; θ_{max}=30 °C .

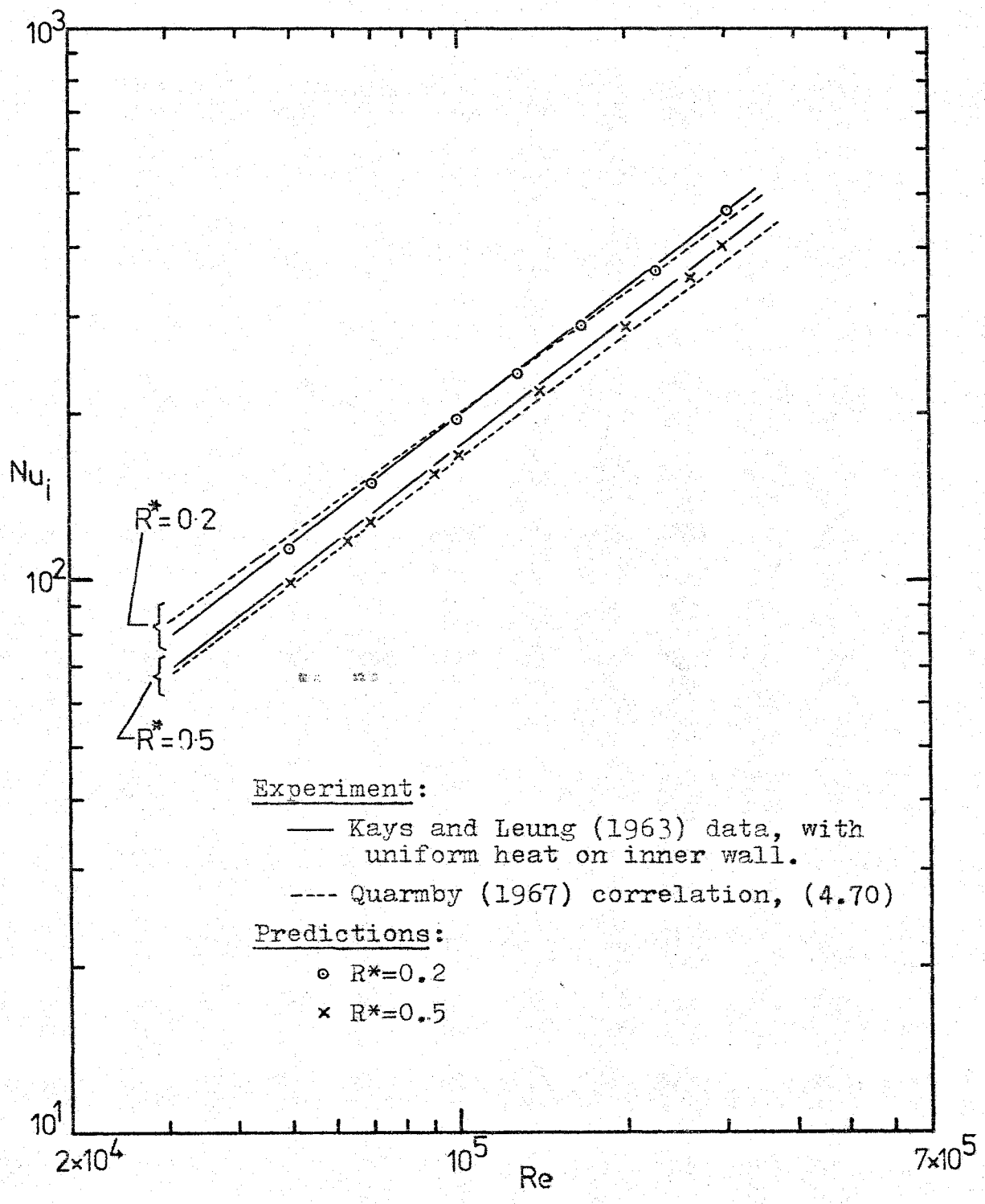

Fig.4.12 Fully developed Nusselt numbers for the inner wall of a turbulent flow in a smooth annulus: heated (or cooled) on the inner side; wall temperature increasing linearly in direction of flow. Pr=0.7 ; $\theta_{max}=30^{o}C$.

Experiment:

▫ Seban and Shimazaki (1951)

\+ Martinelli analogy, from Knudsen and Katz (1958)

Predictions: ——

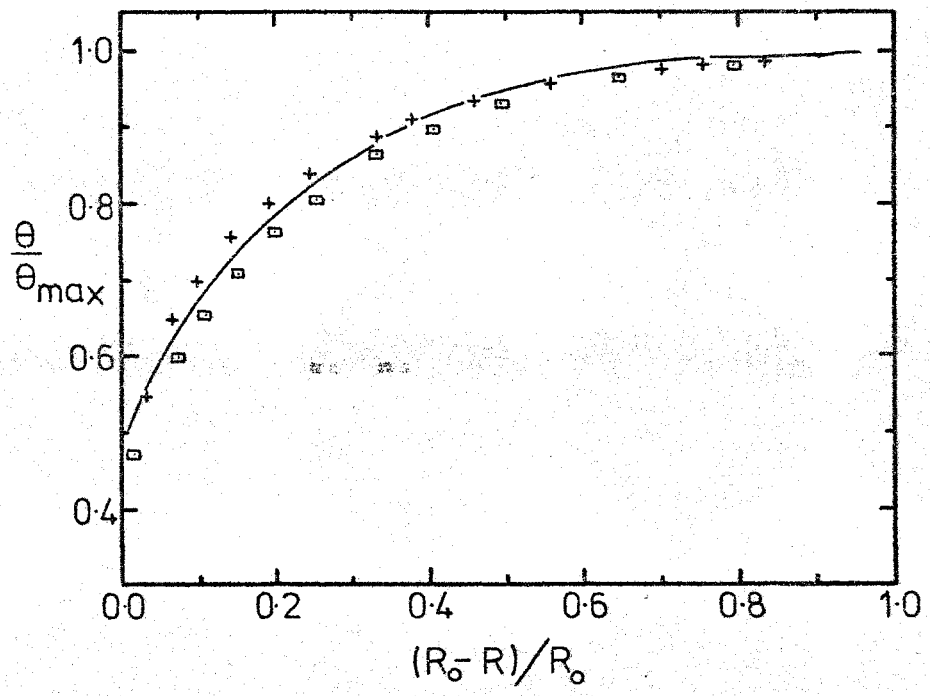

Fig. 4.13 Temperature profiles in a heated (or cooled) smooth pipe. Pr=0.7 ; Re=1.0x10^5 ; θ_{max}=30 ^{o}C .

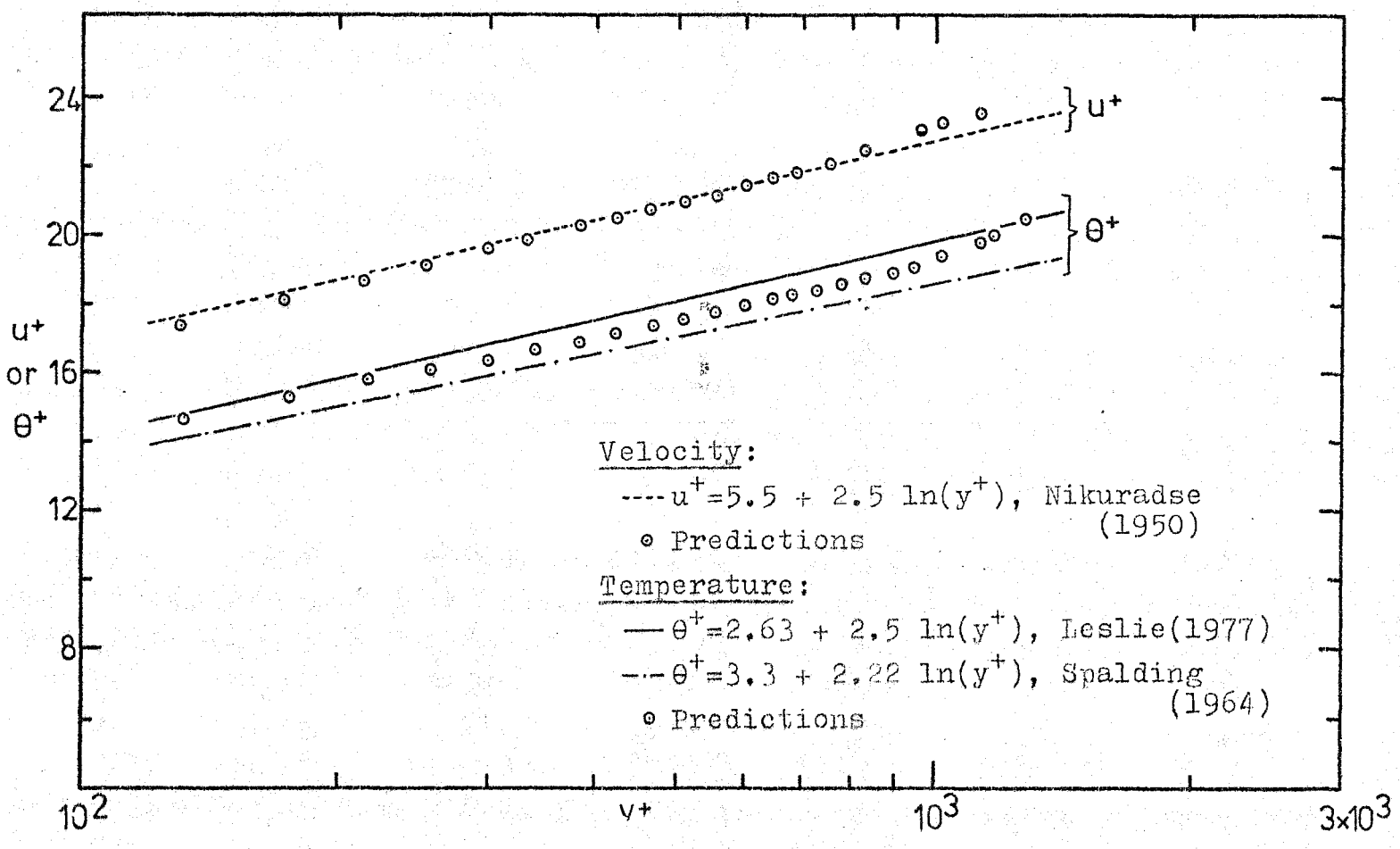

Figure 4.14 Non-dimensional velocity (u^+) and temperature distribution (θ^+) in a smooth pipe flow. Pr=0.7 ; Re=1.0x10^5.

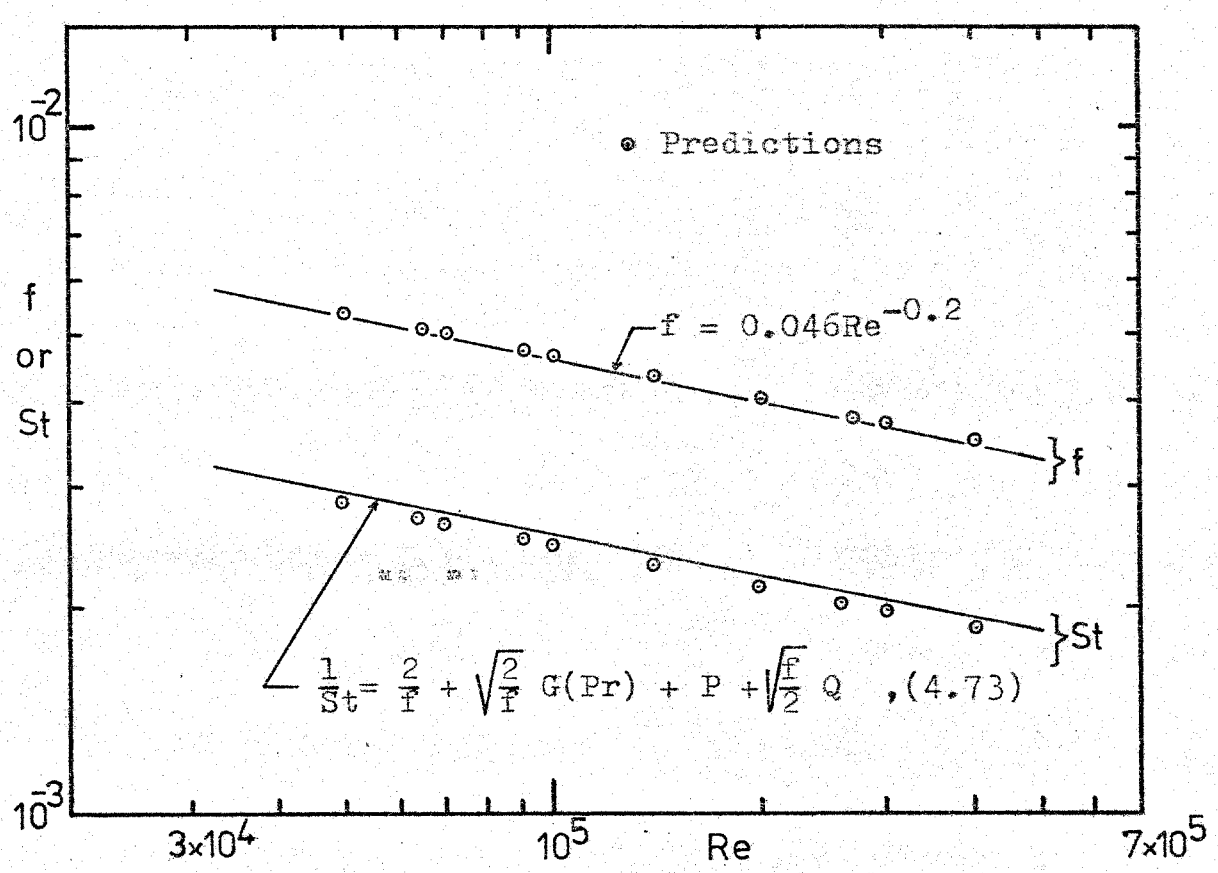

Fig. 4.15 Friction factors and Stanton numbers in a smooth pipe flow. Pr=0.7 .

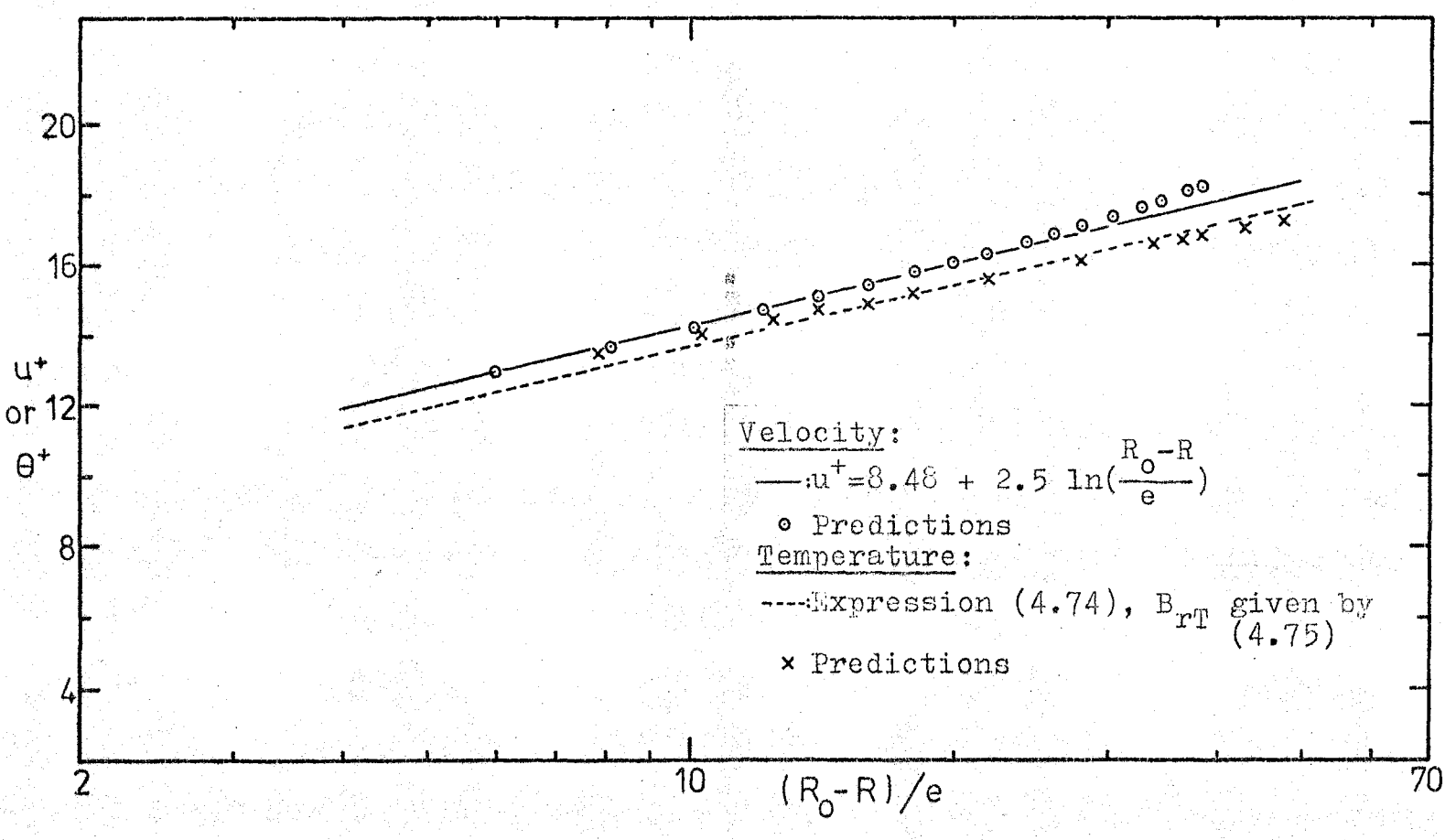

Figure 4.16 Velocity and temperature distributions in a rough (sand) pipe flow. $Re=1.0\times10^5$; $Pr=0.7$; $D/e=200$.

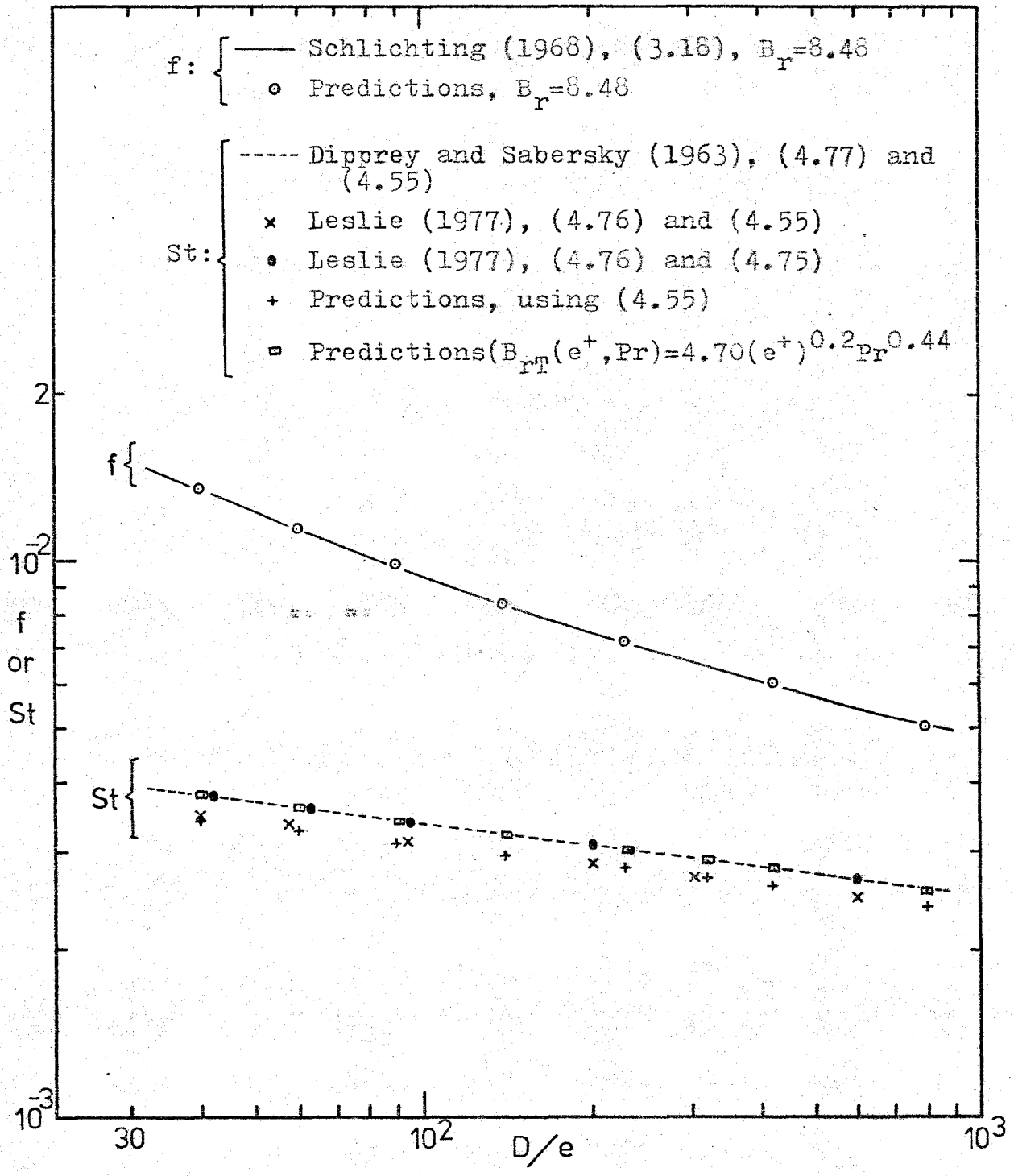

Fig. 4.17 Friction factors and Stanton numbers in a pipe with 'sand' roughness. Re=5.0x10^5 ; Pr=0.7 .

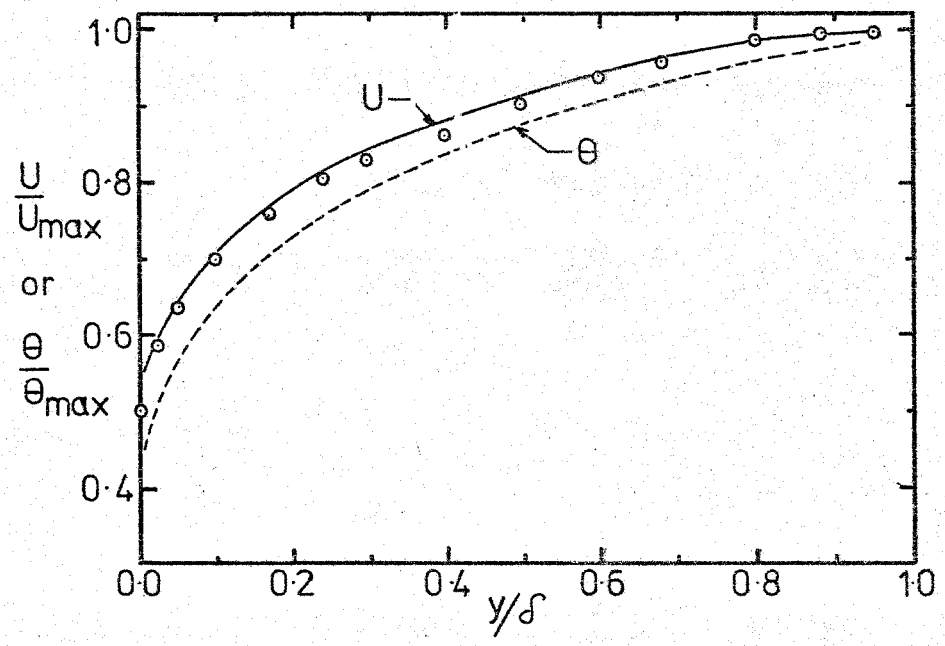

Fig. 4.18 Velocity and temperature profiles in a heated (or cooled) flat-plate boundary layer. Pr=0.7; θ_{max}=30°C.
Velocity (U/U_{max}): ○ Experiment, Klebanoff (1955)
— Predictions
Temperature (θ/θ_{max}): ----- Predictions.

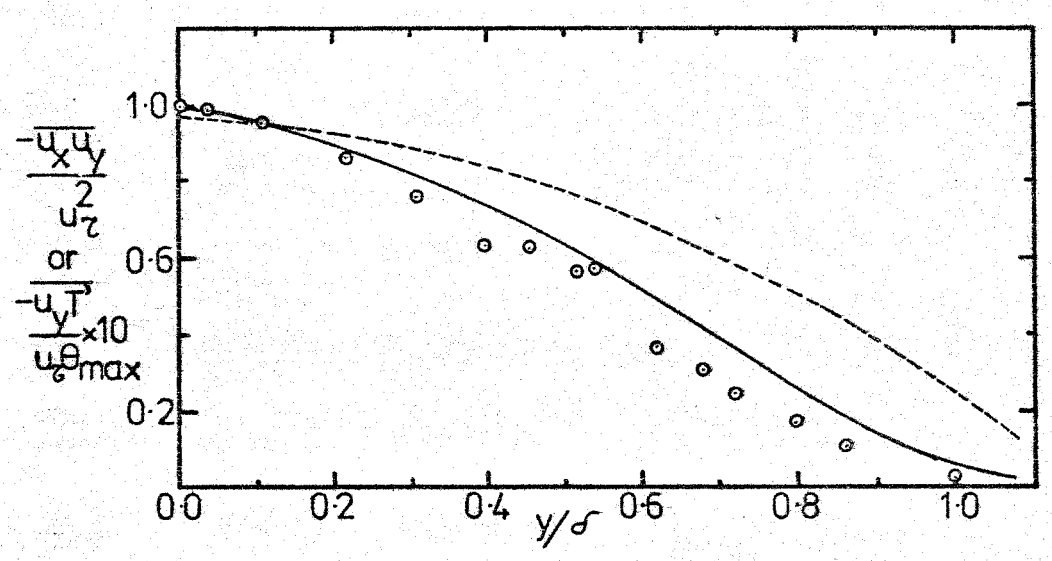

Fig. 4.19 Shear stress and convective heat flux profiles in a heated (or cooled) flat-plate boundary layer.
Shear stress($\overline{u_x u_y}$): ○ Experiment, Klebanoff (1955)
— Predictions
Convective heat flux($\overline{u_y T'}$): ----- Predictions.

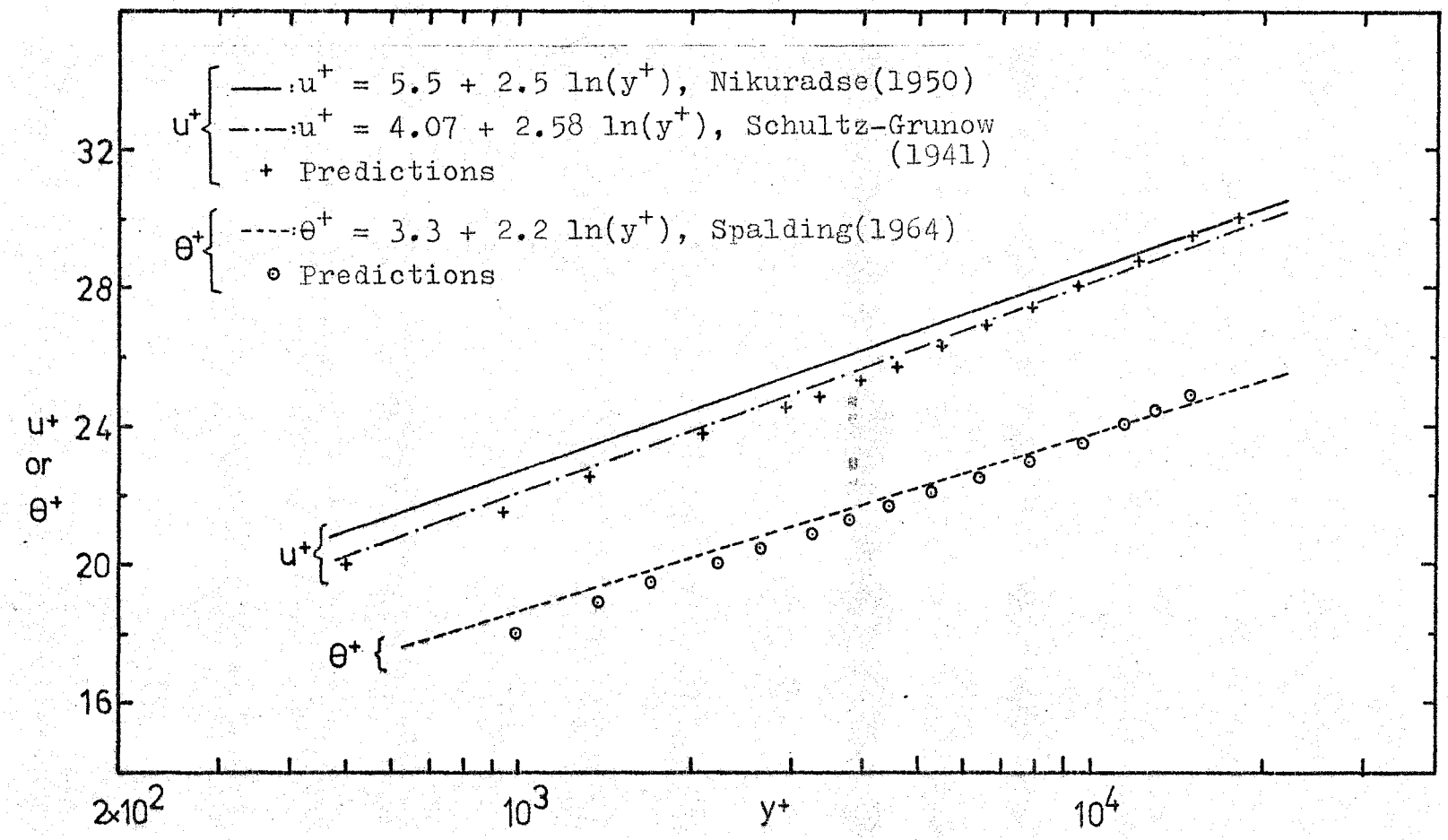

Figure 4.20 Non-dimensional velocity (u^+) and temperature (θ^+) distributions in a smooth flat-plate. Pr=0.7 ; θ_{MAX}=30 ^{o}C.

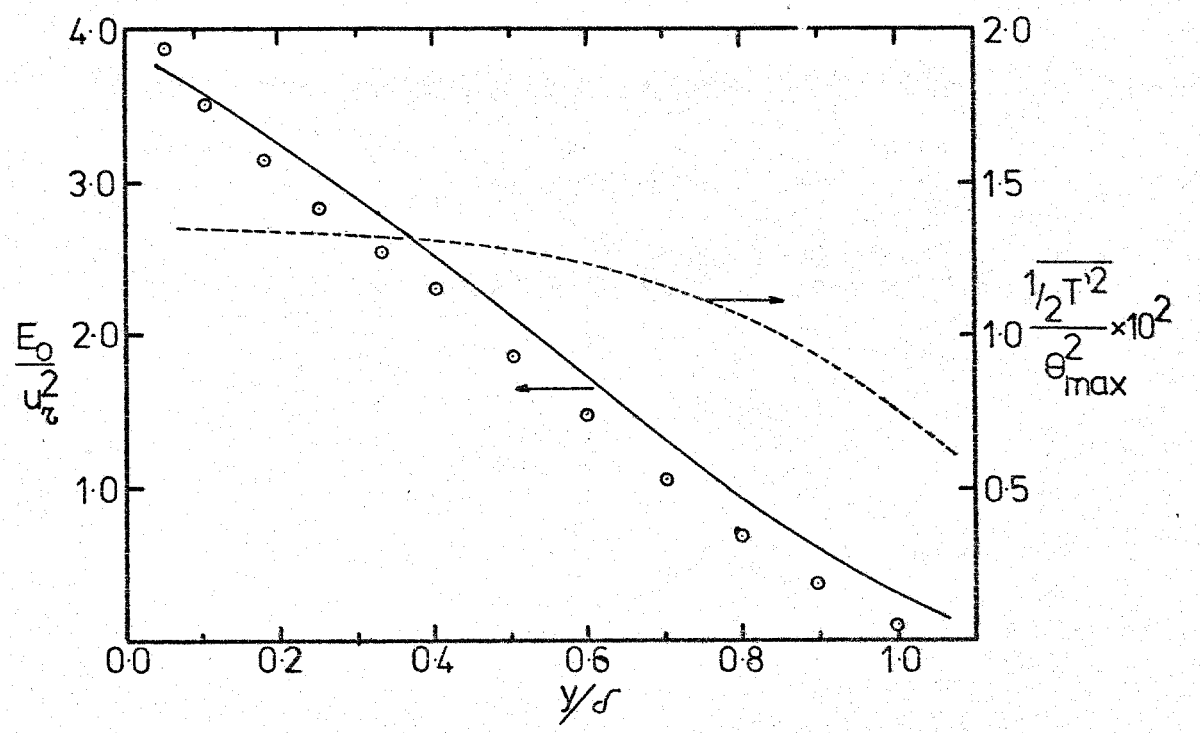

Fig. 4.21 Turbulence energy and intensity of temperature profiles in a flat-plate boundary layer.

Turbulence energy(E_o): ⊙ Experiment, Klebanoff (1955)
—— Predictions

Intensity temperature($1/2\overline{T'^2}$):----- Predictions.

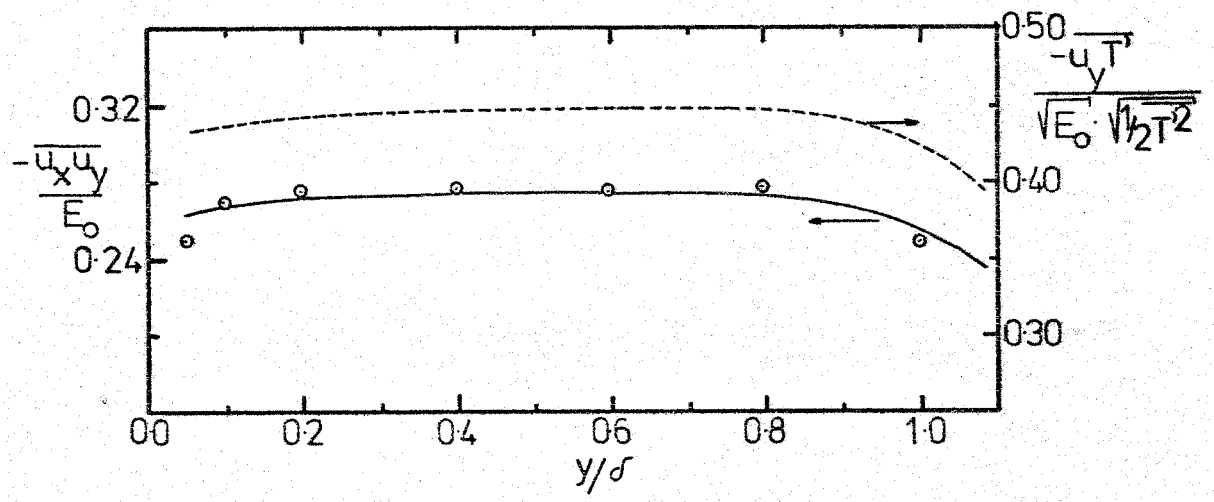

Fig. 4.22 Momentum and heat transfer flux correlations in a flat-plate boundary layer.

Momentum($-\overline{u_x u_y}/E_o$): ⊙ Experiment, Klebanoff (1955)
—— Predictions

Heat flux correlation:---- Predictions.

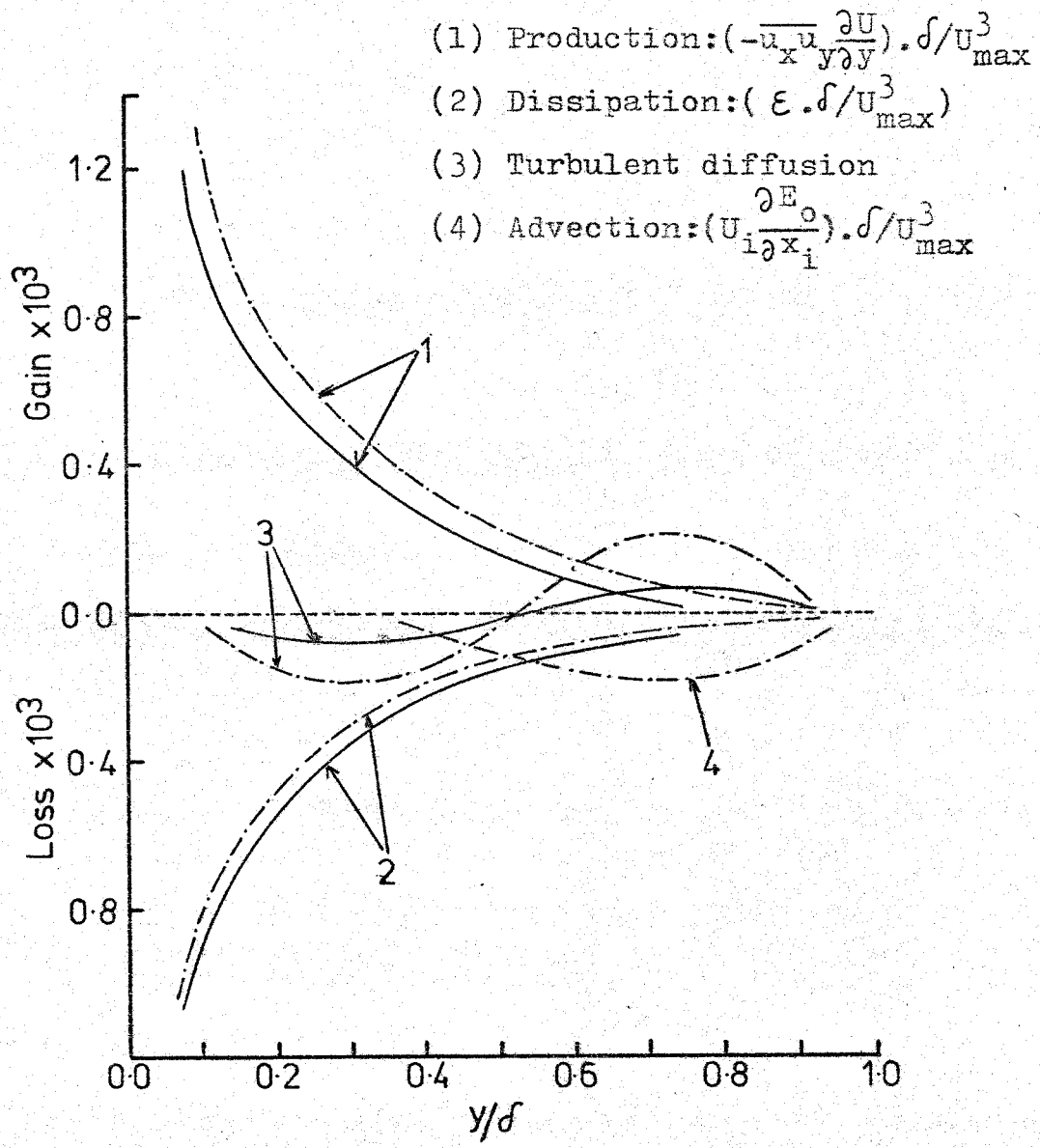

Fig. 4.23 Turbulence energy balance in a smooth flat-plate boundary layer. Pr=0.7 ; U_∞=40 m/s ; θ_{max}=30 °C .
—·— Experiment, Klebanoff (1955)
—— Predictions.

(1) Production: $(-\overline{u_y T'}\frac{\partial T}{\partial y}).\delta/(\theta^2_{max}.U_{max})$

(2) Dissipation: $(C_{TTl}\overline{\frac{1}{2}T'^2}\varepsilon/E_o).\delta/(\theta^2_{max}.U_{max})$

(3) Diffusion: $(\frac{\partial}{\partial y}(\gamma_{eff}\frac{\partial}{\partial y}\overline{\frac{1}{2}T'^2}).\delta/(\theta^2_{max}.U_{max})$

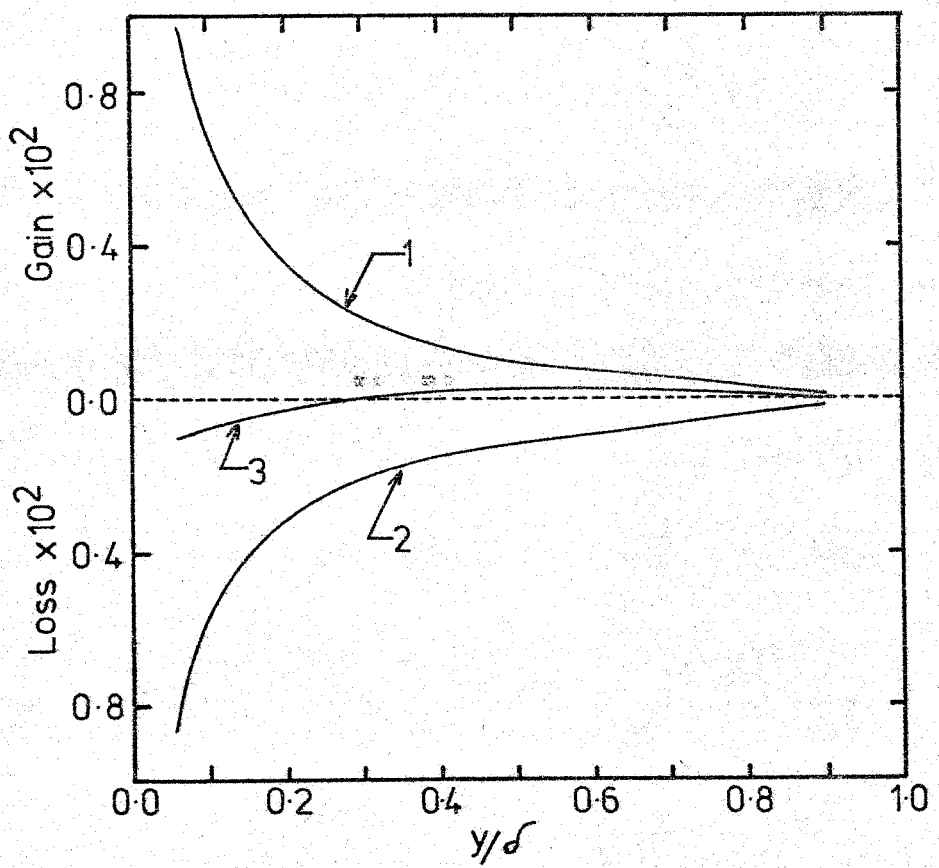

Fig. 4.24 Intensity of temperature fluctuation balance in a smooth flat-plate boundary layer. Pr=0.7; θ_{max}=30°C.
—— Predictions.

Velocity (U/U_{max}):

⊙ Experiment, Wignanski and Fiedler (1970)
⊡ Analitical solution by Tollmien (1945), from Patankar and Spalding (1970)
—— Predictions.

Temperature (θ/θ_{max}):

× Analitical solution by Tollmien (1945)
---- Predictions.

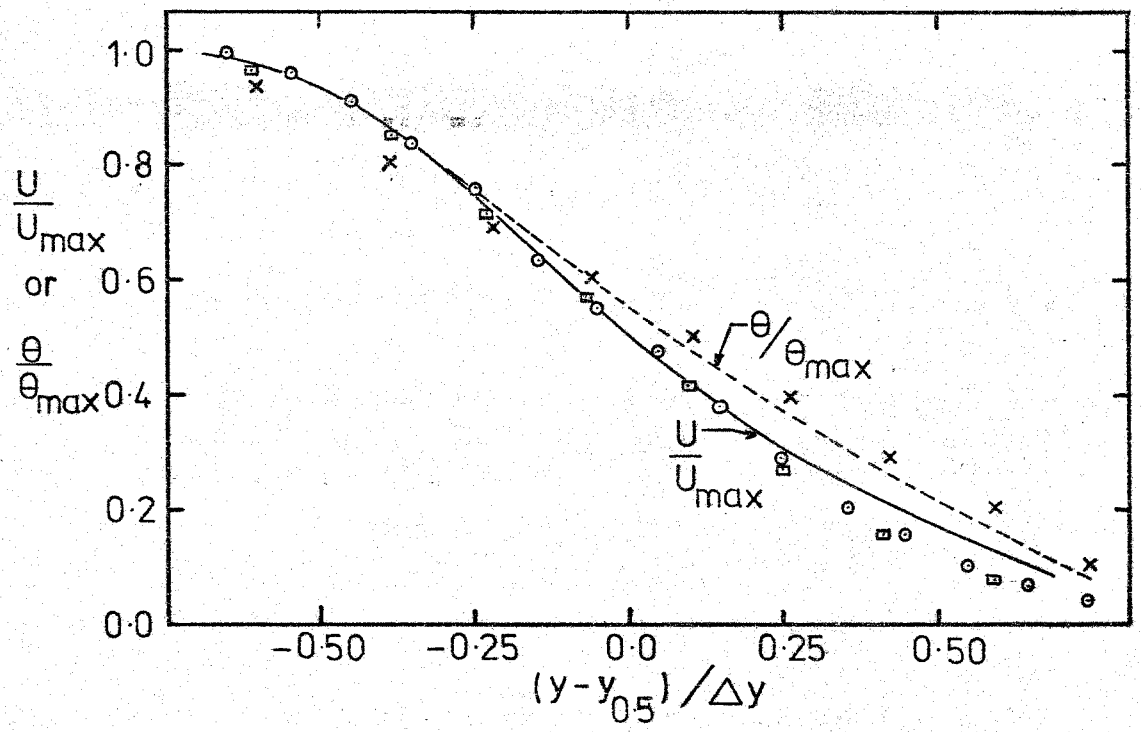

Fig. 4.25 Velocity and temperature profiles in a plane mixing layer, with zero velocity ratio. Pr=0.7 ; θ_{max}=30°C.

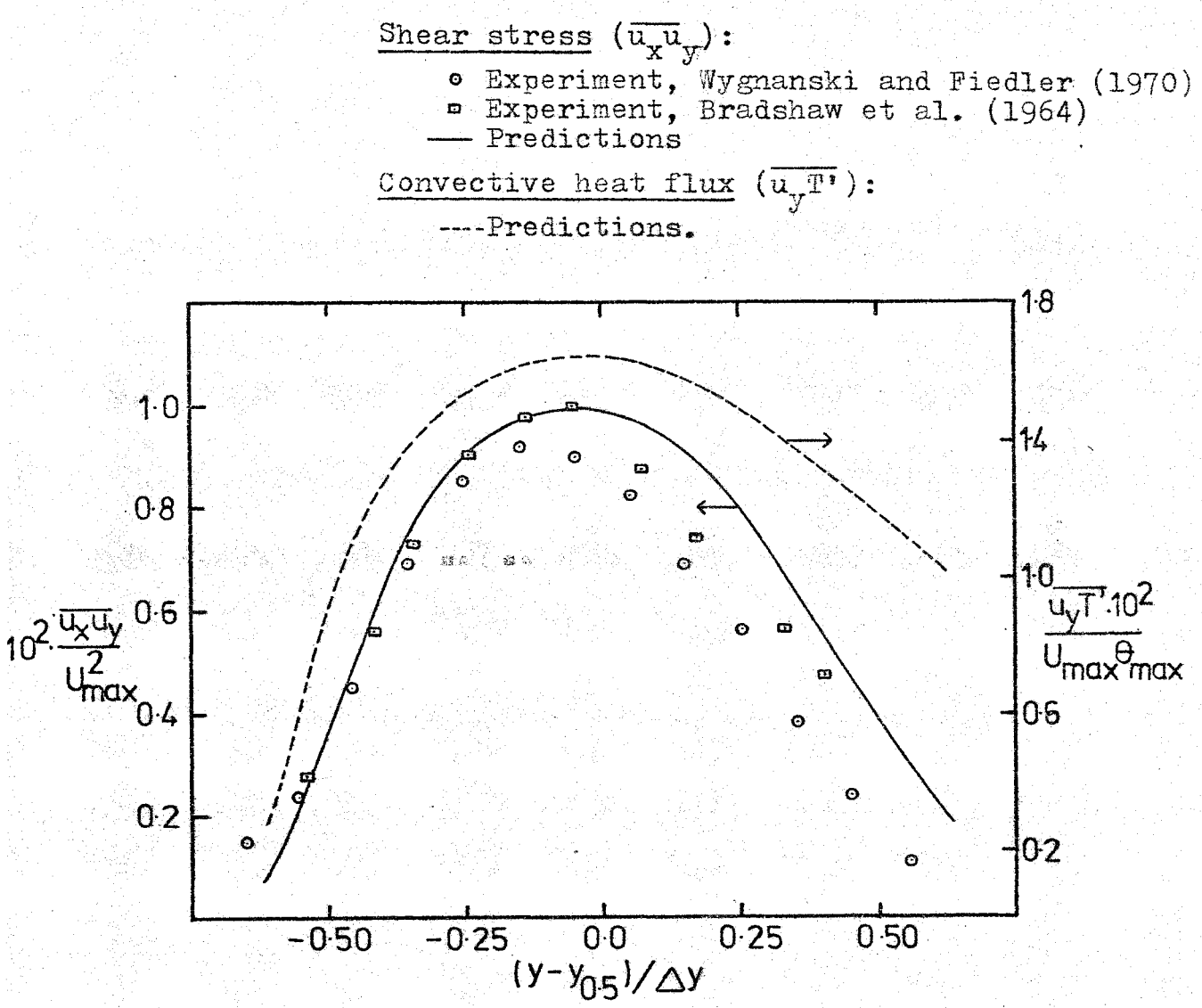

Fig. 4.26 Shear stress and convective heat flux profiles in a plane mixing layer, with zero velocity ratio. Pr=0.7 ; θ_{max}=30 °C .

Turbulence energy (E_o):

o Experiment, Wignanski and Fiedler (1970)

—— Predictions

Temperature intensity ($\overline{\frac{1}{2}T'^2}$):

----Predictions.

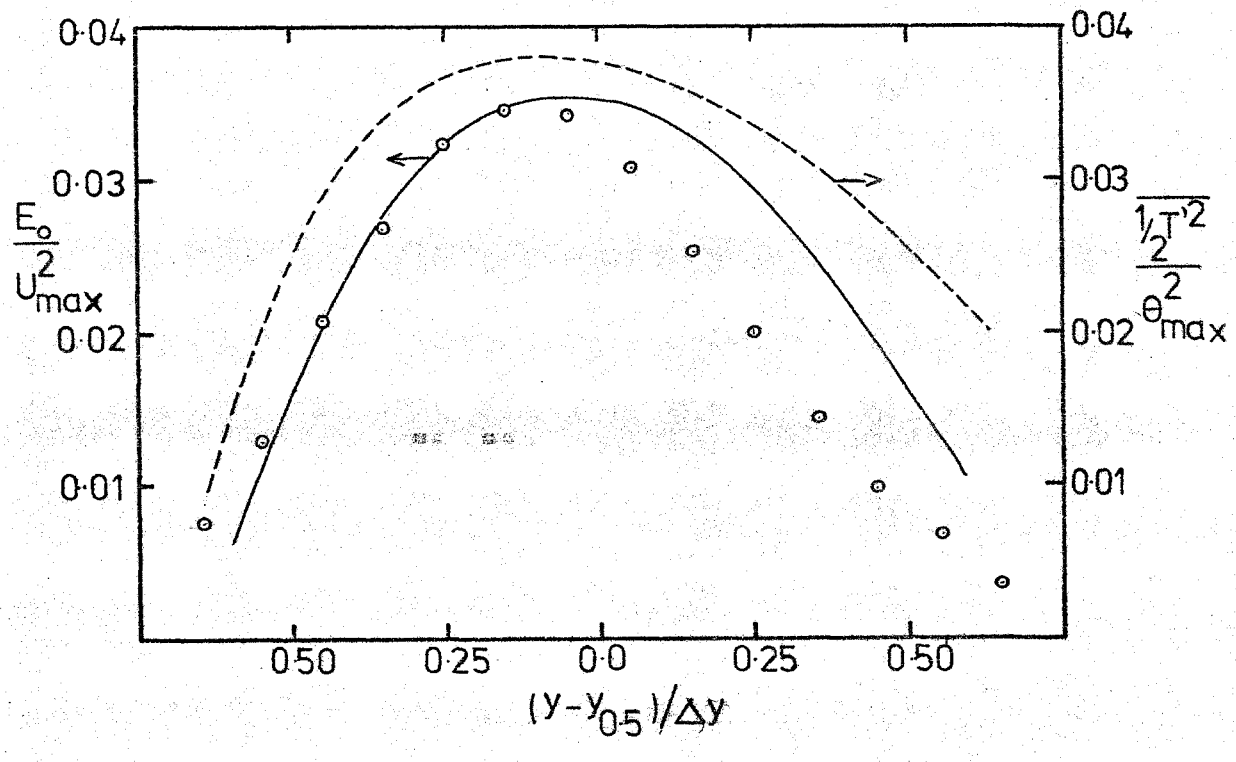

Fig. 4.27 Turbulence energy and temperature intensity fluctuation profiles in a mixing layer flow, with zero velocity ratio. Pr=0.7 ; θ_{max}=30 ^{o}C .

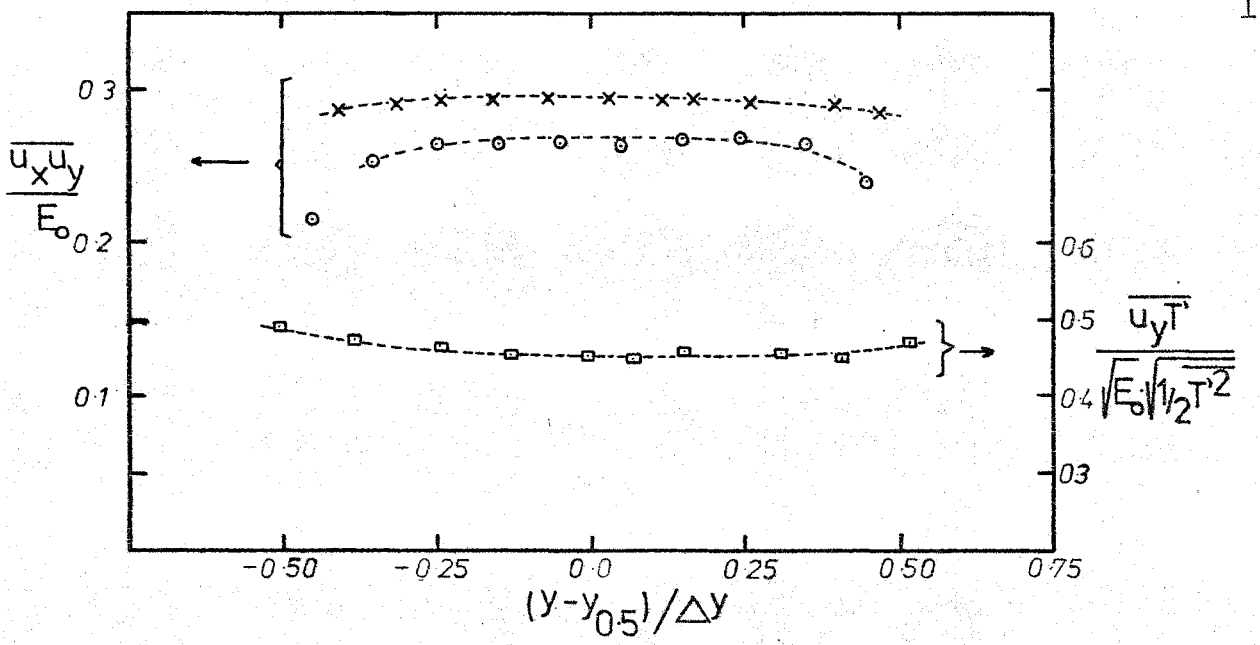

Fig. 4.28 Momentum and heat transfer flux correlations in a plane mixing layer, with zero velocity ratio.

Momentum ($\overline{u_x u_y}/E_o$):--o-- Experiment, Wygnanski and Fiedler (1970)

--x-- Predictions

Heat transfer:--□-- Predictions.

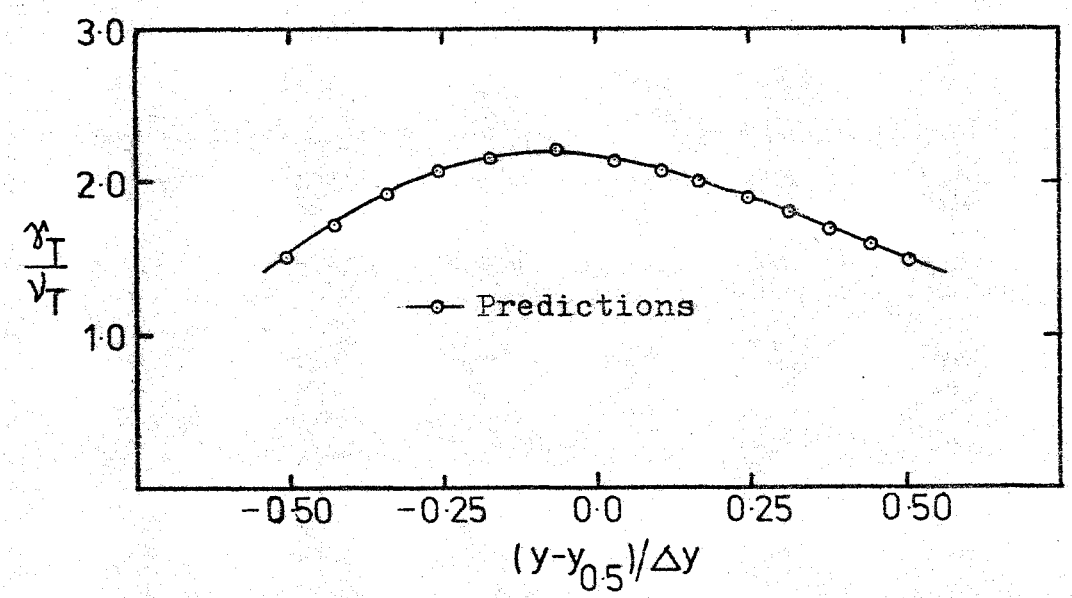

Fig. 4.29 Eddy diffusivity of heat and momentum ratio in a plane mixing layer flow, with zero velocity ratio. Pr=0.7 ; θ_{max}=30 °C .

Velocity (U/U_{max}):

⊙ Experiment, Bradbury (1965)

—— Predictions

Temperature (θ/θ_{max}):

▫ × Experiment, Jenkins and Goldschmidt (1973) at 2 stations, θ_{max}=20.7 °C

----Predictions.

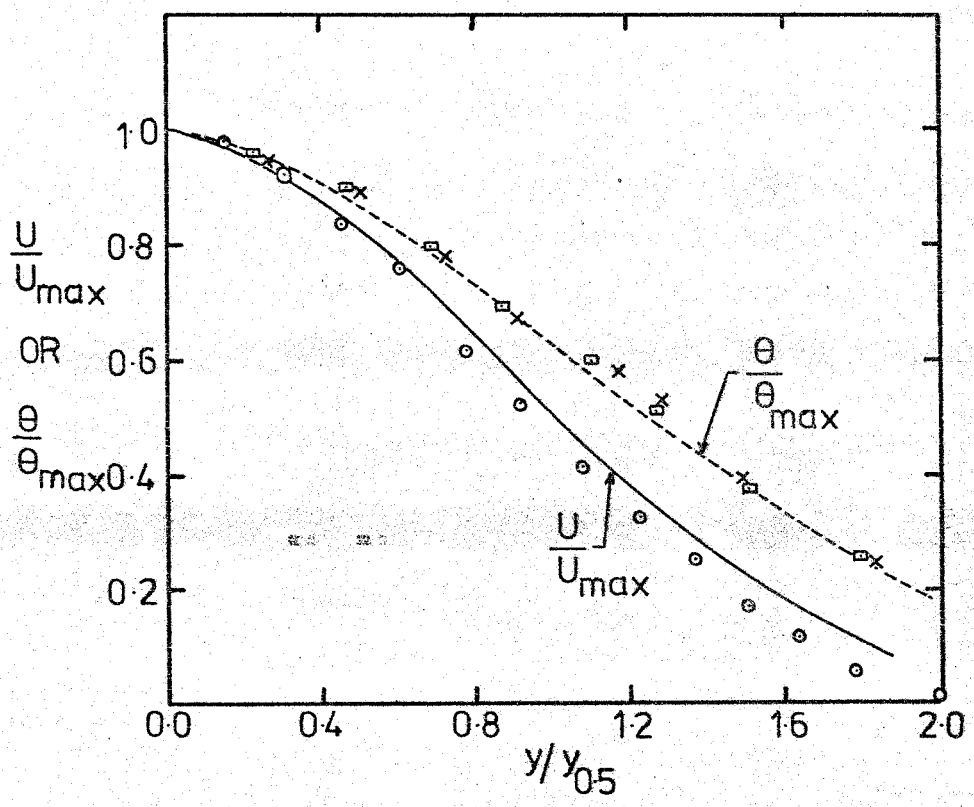

Fig. 4.30 Mean velocity and mean temperature profiles in a plane jet in stagnant surroundings. Pr=0.7 ; θ_{max}=30 °C .

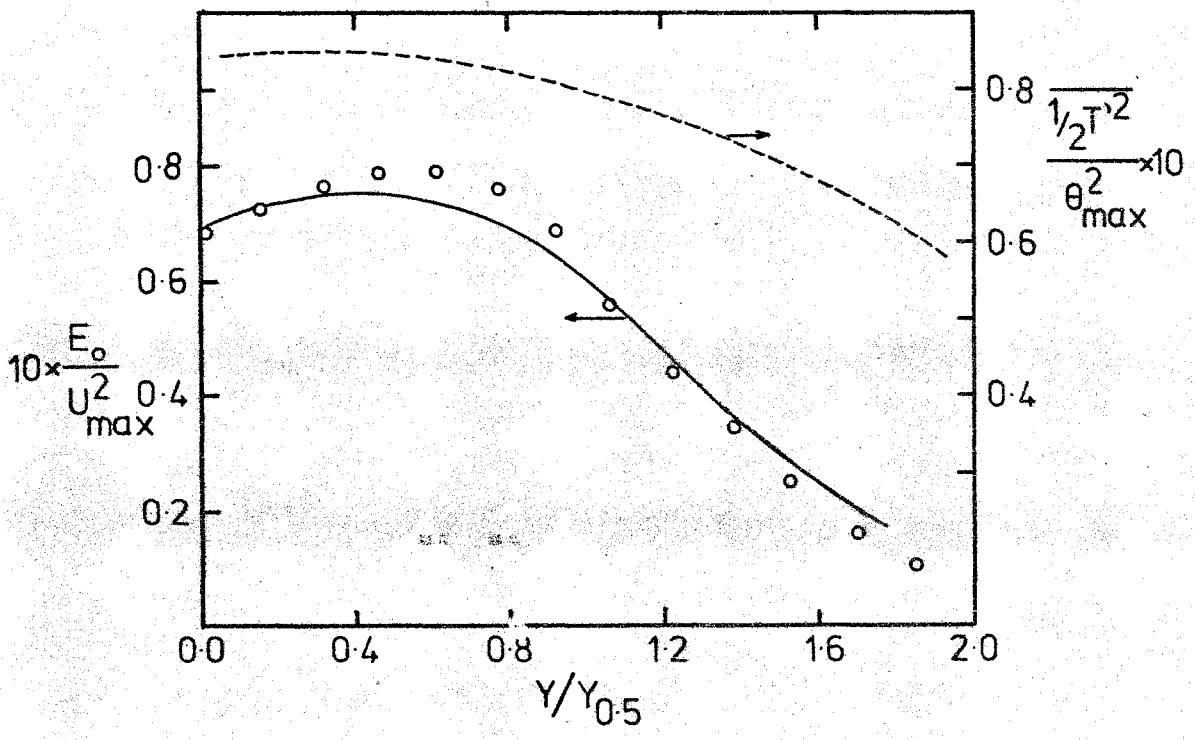

Fig. 4.31 Turbulence energy and intensity of temperature fluctuation profiles in a plane jet. Pr=0.7; $\theta_{max}=30^{o}C$
Turbulence energy (E_o): ⊙ Experiment, Bradbury (1965)
—Predictions
Intensity of temperature($1/2\overline{T'^2}$):----Predictions.

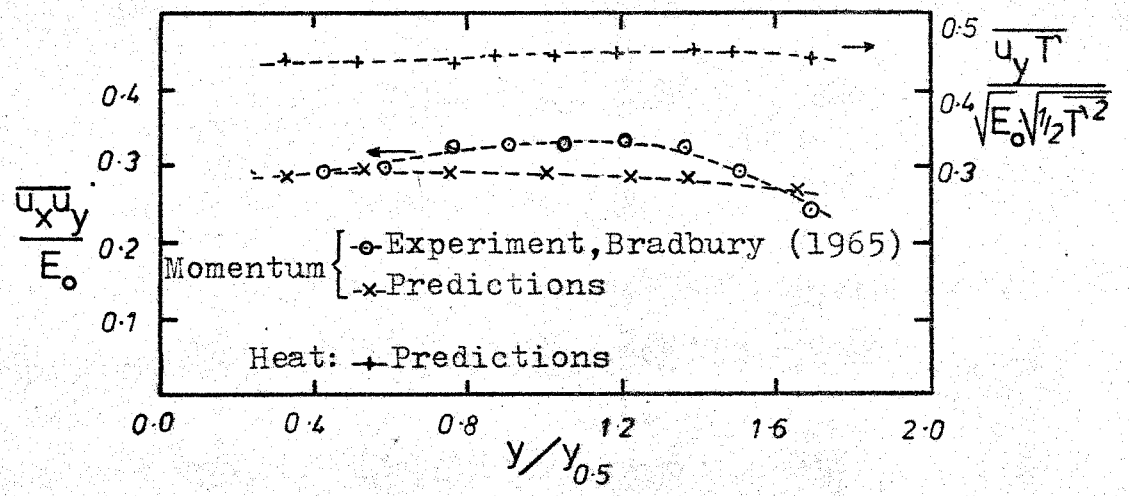

Fig. 4.32 Momentum and heat transfer flux correlations in a plane jet. Pr=0.7 ; θ_{max}=30 °C .

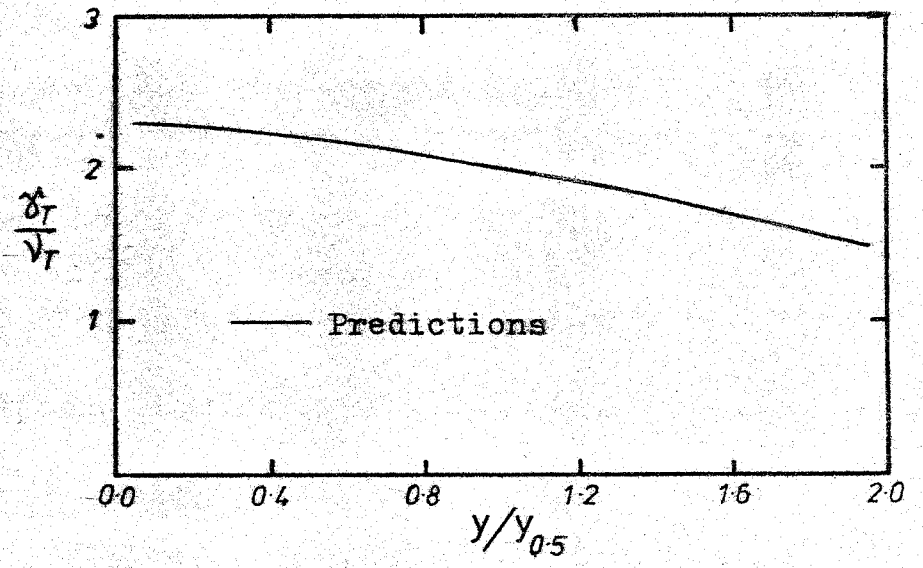

Fig. 4.33 Eddy diffusivity of heat and momentum ratio (γ_T/ν_T) in a plane jet. Pr=0.7 ; θ_{max}=30 °C .